

**Development of *Tupaia belangeri* as an animal model for viral infections**

**(ツパイウイルス感染動物モデルの開発)**

**The United Graduate School of Veterinary Science**

**Yamaguchi University**

**MOHAMMAD ENAMUL HOQUE KAYESH**

**March 2019**

## Contents

<b>Preface</b> .....	6
<b>Dedication</b> .....	7
<b>Acknowledgements</b> .....	8
<b>Summary</b> .....	9
<b>Summary in Japanese</b> .....	12
<b>List of Figures</b> .....	15
<b>List of Tables</b> .....	21
<b>Chapter I: General Introduction</b> .....	22
<b>Chapter II: Susceptibility and initial immune response of <i>Tupaia belangeri</i> cells to dengue virus infection</b> .....	24
Abstract .....	25
II.1. Introduction .....	26
II.2. Materials and Methods .....	28
II.2.1. Cell cultures .....	28
II.2.2. Virus stocks and titration .....	28
II.2.3. DENV infection of cells .....	29
II.2.4. DENV RNA quantification by quantitative reverse transcription PCR (qRT-PCR) .....	29
II.2.5. Immunofluorescence assay .....	30
II.2.6. Expression analysis of tupaia TLRs and cytokines .....	30
II.2.7. Silencing and detection of TLR8 .....	32
II.2.8. Statistical analysis .....	32
II.3. Results .....	33
II.3.1. DENV-1 replication in tupaia cells .....	33

II.3.2. Kinetic of DENV serotypes 2, 3, and 4 replication in tupaia cells .....	33
II.3.3. Phylogenetic analysis of tupaia TLRs .....	34
II.3.4. Tupaia TLR expression in response to DENV infection .....	34
II.3.5. Tupaia cytokine expression in response to DENV infection .....	34
II.4. Discussion .....	35
II.5. Conclusions .....	37
<b>Chapter III: Interferon-<math>\beta</math> response is impaired by hepatitis B virus infection in <i>Tupaia belangeri</i> .....</b>	<b>51</b>
Abstract .....	52
III.1. Introduction .....	54
III.2. Materials and Methods .....	55
III.2.1. Animals .....	55
III.2.2. Viruses .....	56
III.2.3. Infection .....	56
III.2.4. Measurement of ALT and viral load .....	57
III.2.5. Measurement of HBsAg .....	57
III.2.6. Gene expression analysis by quantitative reverse transcription-PCR (qRT-PCR) .....	58
III.2.7. Statistical analysis .....	58
III.3. Results .....	59
III.3.1. Infection of tupaia with HBV genotypes A2 and C .....	59
III.3.2. Chronic infection by HBV genotype A2 in tupaia .....	59
III.3.3. Effect of HBV genotype A2 in tupaia .....	59
III.3.4. Expression levels of cytokines and TLRs in liver tissues of HBV-A2-infected tupaia at 28 dpi .....	60

III.3.5. Expression levels of cytokines and TLRs in liver tissues of tupaia	
chronically infected with HBV-A2 at 31 wpi .....	60
III.3.6. Expression of cGAS in the liver tissues of HBV-A2-infected tupaia .....	61
III.3.7. Changes in the expression of NTCP in the liver tissues of	
HBV-A2-infected tupaia .....	61
III.4. Discussion .....	61
<b>Chapter IV: Oxidative stress and immune responses during hepatitis C</b>	
<b>virus infection in <i>Tupaia belangeri</i> .....</b>	<b>74</b>
Abstract .....	75
IV.1. Introduction .....	76
IV.2. Materials and Methods .....	78
IV.2.1. Animals .....	78
IV.2.2. Virus infection .....	78
IV.2.3. Measurement of ALT levels and viral load .....	79
IV.2.4. Gaussia luciferase immunoprecipitation system (GLIPS) assays .....	79
IV.2.5. Quantification of ROS levels .....	80
IV.2.6. Determination of 8-OHdG levels in genomic DNA from liver tissues .....	81
IV.2.7. Gene expression analysis by qRT-PCR .....	81
IV.2.8. Statistical analysis .....	82
IV.3. Results .....	82
IV.3.1. Alanine aminotransferase (ALT) levels and viral loads in	
HCV-infected tupaia sera .....	82
IV.3.2. Measurement of anti-core and anti-NS3 antibody titers .....	82
IV.3.3. Histological analysis of liver tissues from HCV-infected tupaia .....	83
IV.3.4. Measurement of ROS levels and anti-DHCR24 antibody titers .....	83

IV.3.5. Measurement of oxidative stress in the liver .....	84
IV.3.6. Changes in TLR, NTCP, and cytokine expression in liver tissues .....	84
IV.4. Discussion .....	85
<b>Chapter V: General Discussion .....</b>	<b>99</b>
<b>References .....</b>	<b>101</b>

## Preface

The current doctoral thesis is based on the following papers:

1. M.E.H. Kayesh, B. Kitab, T. Sanada, D. Hayasaka, K. Morita, M. Kohara and K. Tsukiyama-Kohara, 2017. Susceptibility and initial immune response of *Tupaia belangeri* cells to dengue virus infection. *Infection, Genetics and Evolution*, 51, 203–210.
2. M.E.H. Kayesh, S. Ezzikouri, H. Chi, T. Sanada, N. Yamamoto, B. Kitab, T. Haraguchi, R. Matsuyama, C. N. Nkogue, H. Hatai, N. Miyoshi, S. Murakami, Y. Tanaka, J-I. Takano, Y. Shiogama, Y. Yasutomi, M. Kohara, K. Tsukiyama-Kohara, 2017. Interferon-  $\beta$  response is impaired by hepatitis B virus infection in *Tupaia belangeri*. *Virus Research*, 237, 47–57.
3. M.E.H. Kayesh, S. Ezzikouri, T. Sanada, H. Chi, Y. Hayashi, K. Rebbani, B. Kitab, A. Matsuu, N. Miyoshi, T. Hishima, M. Kohara and K. Tsukiyama-Kohara, 2017. Oxidative stress and immune responses during hepatitis C virus infection in *Tupaia belangeri*. *Scientific Reports*, 7 (1), 9848.

## **Dedication**

To my beloved parents Late Jahanara Hoque and Md. Sirajul Hoque, and to my sweet daughter Ayesha Juwairia Hoque (Sairi), with all my love.

## **Acknowledgements**

It has been a long way to the achievement of this PhD. All praises are due to the almighty Allah, who enabled making the long awaited dream come true.

I would like to express my sincere gratitude to my supervisor Prof. Dr. Kyoko Tsukiyama-Kohara, for her unconditional support throughout the study period and guidance towards my research work and thesis write-up. I am also grateful to my co-supervisors Prof. Dr. Ken Maeda and Prof. Dr. Aya Matsuu for their suggestions and guidance. Also, I am greatly indebted to Prof. Dr. Michinori Kohara, for his scholastic suggestions and comments on my work.

I would like to thank all the faculty members in the Laboratory of Animal Hygiene, Kagoshima University, including Dr. Aya Matsuu, Dr. Makoto Ozawa, Dr. Tatsunari Masatani, Dr. Masayuki Horie (now moved to Kyoto University) for their constructive criticisms, valuable suggestions and cooperation to learn molecular techniques.

Brother Dr. Sayeh and my friends Dr. Bouchra and Dr. Chimene, contributions by you all towards my study are highly acknowledged. Also, I would like to acknowledge the contributions of Sanada-san, Khadiza-san, Yamaguchi-san, Kawabata-san, Matsuyama-san, Hirabayashi-san, Nadine-san, Nakagawa-san, Ueno-san, Nori-san, Okuya-san, Kanda-san, Handa-san, Haraguchi-san, Kato-san, and Matsui-kun towards my study.

Finally, I wish to express my appreciations and sincere indebtedness to my beloved family members, relatives, colleagues and friends for their heartiest blessings, affectionate feelings and all sorts of sacrifices to achieve my PhD.

Last but not least, I am grateful to the Patuakhali Science and Technology University, Bangladesh for allowing my study in Japan, and The Ministry of Education, Culture, Sports, Science and Technology, Japan, for providing a scholarship for my doctoral study and to The United Graduate School of Veterinary Science, Yamaguchi University for allowing me to achieve PhD.

## Summary

Suitable small animal model is an important tool for host-virus interactions and viral pathogenesis study. In this study I aimed to develop and expand the utility of tupaia (*Tupaia belangeri*) as an animal model for viral infections including dengue virus (DENV), hepatitis B virus (HBV), hepatitis C virus (HCV), and avian influenza virus. Dengue is an emerging disease of great public health significance worldwide. The lack of a suitable infection model has hampered DENV pathogenesis study. Here, I checked the susceptibility of tupaia fibroblast cells to DENV infection and characterised the innate immune response upon infections. I found that tupaia cells support replication of DENV serotypes 1-4 and showed a linear increase in viral load 24-96h post-infection in both cells and culture supernatants. DENV-2 showed the highest viral growth among all serotypes. To characterize the innate immune response I established an innate immune response measurement system by assessing the mRNA expression of Toll-like receptor (TLR) 1-9 and four cytokines in DENV-infected tupaia cells. All serotypes induced the upregulation of TLR8 mRNA expression in infected tupaia cells. Silencing of TLR8 led to an increase in viral replication, indicating the existence of antiviral response through TLR8 on DENV infection. This study demonstrates for the first time the susceptibility of tupaia cells to DENV infections and the role of TLR8 in the anti-viral response of tupaia cells to DENV. These findings demonstrate the potential utility of tupaia as a model for DENV research in the future.

To expand the use of tupaia in HBV and HCV infection, I infected tupaia with different subtypes of HBV and HCV. To date, chimpanzee has been used as the natural infection model for HBV and HCV. However, this model is very costly and difficult to use because of ethical and animal welfare issues. Developing suitable small animal models for HBV and HCV have been a long-standing challenge. Here, I have conducted the study to establish the tupaia as a

new animal model for HBV and HCV infection and characterized the immune response upon viral infections in each case.

In case of HBV infection, first, I compared the propagation of HBV genotypes A2 and C *in vivo* in tupaia hepatocytes. At 8–10 days post infection (dpi), the level of HBV-A2 propagation in the tupaia liver was found to be higher than that of HBV-C. Moreover, I found that HBV-A2 established chronic infection in some tupaia. I then aimed to characterize the intrahepatic innate immune response in tupaia model. At first, I infected six tupaia with HBV-A2 (strains JP1 and JP4). At 28 dpi, intrahepatic HBV-DNA and serum hepatitis B surface antigens (HBsAg) were detected in all tupaia. The levels of interferon (IFN)- $\beta$  were found to be significantly suppressed in the three tupaia infected with HBV A2\_JP4, while no significant change was observed in the three infected with HBV A2\_JP1. Next, I infected nine tupaia with HBV-A2 (JP1, JP2, and JP4), and characterized 31 weeks post-infection (wpi). Serum HBsAg levels were detected at 31 wpi and IFN- $\beta$  was found to be significantly suppressed in all tupaia. TLR3 was not induced, except in tupaia #93 and #96. Suppression of TLR9 was observed in all tupaia, except tupaia #93. Therefore, the tupaia infection model of HBV clearly indicated the suppression of IFN- $\beta$  at 31 wpi, which might have contributed to the establishment of chronic HBV infection.

HCV is a leading cause of chronic liver disease, cirrhosis, and hepatocellular carcinoma. To address the molecular basis of HCV pathogenesis using tupaia, I characterized host responses upon HCV infection. Adult tupaia were infected with four different HCV genotypes including 1a, 1b, 2a, or 4a. Viral RNA, alanine aminotransferase, anti-HCV core and anti-nonstructural protein NS3 antibody titers, reactive oxygen species (ROS), and anti-3 $\beta$ -hydroxysterol- $\Delta$ 24reductase (DHCR24) antibody levels were measured at 2-week intervals from 0 to 41 wpi. All HCV genotypes established infections and showed intermittent HCV propagation. Moreover, all tupaia produced anti-core and anti-NS3 antibodies. ROS levels in

sera and livers were significantly increased, resulting in induction of DHCR24 antibody production. Similarly, lymphocytic infiltration, disturbance of hepatic cords, and initiation of fibrosis were observed in livers from HCV-infected tupaia. Intrahepatic levels of Toll-like receptors 3, 7, and 8 were significantly increased in all HCV-infected tupaia. However, interferon- $\beta$  was only significantly upregulated in HCV1a- and HCV2a-infected tupaia. Therefore, the findings of this study showed that humoral and innate immune responses to HCV infection, ROS induction, and subsequent increases in DHCR24 auto-antibody production occurred in tupaia model, providing novel insights into understanding HCV pathogenesis.

In addition, I also contributed towards developing tupaia model for pathogenesis study of highly pathogenic avian influenza viruses (manuscript under revision in 'Virology').

Considering all the findings of the study, utilization of tupaia infection model in this study was an effective approach towards development of tupaia as an animal model for viral infections.

## Summary in Japanese (抄録)

最適な小動物モデルは宿主とウイルスの相互作用もしくはウイルス病原性を解析する研究において重要なツールである。本研究で私は、デング熱ウイルス(DENV), B型肝炎ウイルス(HBV), C型肝炎ウイルス(HCV)、鳥インフルエンザウイルスを含むウイルス感染の動物モデルをツパイ(*Tupaia belangeri*)を用いて開発した。デング熱は、世界中で大きな問題となる急性感染症である。適当な感染モデルを欠くことがデング熱病原性研究の進展を阻んでいる。

本研究では、ツパイの線維芽細胞の DENV に対する感染感受性と自然免疫の反応を解析した。ツパイ細胞は、DENV1~4 型に感染感受性であり、感染後 24-96 時間で直線的にウイルス量が増加した。この中で DENV-2 は最も高いウイルス増殖能を示した。自然免疫の反応は Toll-like receptor (TLR)1-9 と 4 つのサイトカインの mRNA 合成の DENV 感染による変化により解析した。全ての DENV 血清型で TLR8 mRNA の発現誘導が見られた。TLR8 を siRNA でノックダウンすると、ウイルス複製が増加し、TLR8 が抗ウイルス作用を持つ事が明らかとなった。本研究は、ツパイ細胞が DENV に感染感受性を持つ事を初めて明らかにし、TLR8 が抗ウイルス作用を持つ事を示した。これらの結果は、ツパイが DENV 研究において将来的に役立つ事を示している。

次に、ツパイに HBV, HCV を感染させ、解析を行った。これまでに、HBV と HCV の自然感染モデルはチンパンジーのみである。しかしながら、今日では、チンパンジーを用いるのは動物福祉の問題等で困難である。HBV や HCV のモデルを作り上げる事は長い間の挑戦であった。そこで、本研究でツパイを HBV や HCV の新たな感染動物モデルとして樹立し、その免疫反応を解析した。

HBV の感染では、最初に HBV 遺伝子型 A2 と C についてツパイの感染感受性を検討した。8-10 日後、肝臓における HBV-A2 の増殖は HBV-C よりも高い事が明らかとなった。HBV-

A2 感染後 8 日目で、肝細胞索の乱れが観察された。さらに、HBV-A2 はいくつかのツパイで慢性感染を樹立した。次にツパイの肝臓における自然免疫の反応を解析した。最初に、ツパイ 6 匹を HBV-A2(JP1 と JP2 株)で感染した。28 日後、肝臓内 HBV-DNA と血清中の HBs 抗原が全てのツパイで検出された。Interferon (IFN)- $\beta$  は HBV-A2\_JP4 で感染した全てのツパイで産生が抑制されていたが、HBV A2\_JP1 で感染した場合は変化がなかった。次に、9 匹のツパイを HBV-A2 (JP1, JP2, JP4 株)で感染し、31 週間後(wpi)に解析を行った。全てのツパイで血清中の HBs 抗原は検出されたが、IFN- $\beta$ は有意に抑制された。2 匹(#93, 96)を除く他のツパイで TLR3 が誘導されず、1 匹(#93)を除く全てのツパイで TLR9 の抑制が見られた。従って、感染後 31 週で見られる IFN- $\beta$ の抑制は HBV 慢性感染の成立に貢献したと考えられた。

HCV は慢性肝炎、肝硬変、肝がんを起こす。ツパイを用いて HCV 感染に伴う宿主の反応の解析を通じ、HCV の病原性の分子基盤を解析した。成獣のツパイを HCV の 4 つの遺伝子型の 1a, 1b, 2a, 4a で感染させた。ウイルス RNA, alanine aminotransferase (ALT), 抗 HCV コア抗体と非構造蛋白質 NS3 抗体、活性酸素(ROS)、と 3 $\beta$ -hydroxysterol- $\Delta$ 24reductase (DHCR24) 抗体を 2 週間間隔で 41 週間測定した。全ての HCV 遺伝子型は感染を成立させ、間歇的な HCV の増殖を示した。さらに、全てのツパイがコアや NS3 の抗体を産生した。血中や肝臓の ROS 産生は有意に上昇し、DHCR24 抗体産生を誘導した。同時に肝臓にはリンパ球浸潤や肝細胞索の乱れ、肝臓の繊維化が観察された。肝臓内の TLR3, 7, 8 は HCV 感染ツパイの肝臓で有意に上昇した。しかしながら、IFN- $\beta$ は HCV-1a と 2a が感染したツパイのみで上昇した。従って、本研究の結果、すなわち HCV 感染に対する液性免疫の反応や自然免疫の反応は、ROS を誘導し、その結果 DHCR24 自己抗体の産生をツパイモデルで誘導し、HCV 病原性の理解に新たな知見をもたらした。

これらに加えて、私は、高病原性鳥インフルエンザウイルスの病原性を解析するツパイモデルの研究も行った（論文投稿中）。

本研究のすべての知見を考慮すると、ツパイ感染モデルの利用はウイルス感染の動物モデルを開発するのに効果的なアプローチである。

## List of Figures

Figure 1.1. Kinetic of DENV-1 replication in (A) HuH-7 and (B) T-238 cells and culture supernatants. HuH-7 cells or T-238 cells were infected with DENV-1 at an MOI=1, and RNA was extracted at 24, 48, 72, and 96 h post-inoculation. Viral RNA copy numbers were quantified by one-step qRT-PCR, and DENV-1 RNA was normalized with corresponding *GAPDH* in cells.

Figure 1.2. Kinetic of DENV serotypes 1–4 replication in T-238 cells at 24, 48, 72, and 96 h post-infection (MOI = 0.1). Viral RNA was quantitated by qRT-PCR and normalized with tupaia *GAPDH* mRNA amount. Ratio to normalized viral RNA amount at 24 h was calculated at each time point and indicated. Vertical bars indicate SD.

Figure 1.3. Detection of DENV envelope protein in T-238 cells by immunofluorescence assay (400×). Cells were infected with DENV-1 strain Hue-525, DENV-2 strain Hue-397, DENV-3 strain Hue-397, or DENV-4 strain Hue-420 at an MOI = 0.1. At 72 h post-infection, cells were fixed and stained with anti-flavivirus group antibody (DI-4G2).

Figure 1.4. Phylogenetic tree of tupaia TLRs. A) TLR1 gene, B) TLR1 protein, C) TLR2 gene, D) TLR2 protein, E) TLR3 gene, F) TLR3 protein, G) TLR4 gene, H) TLR4 protein, I) TLR5 gene, J) TLR5 protein, K) TLR6 gene, L) TLR6 protein, M) TLR7 gene, N) TLR7 protein, O) TLR8 gene, P) TLR8 protein, Q) TLR9 gene, R) TLR9 protein. Trees were constructed with the neighbor-joining method using MEGA7. Numbers at nodes indicate percent bootstrap values of 1000 replicates; only values  $\geq 95$  are shown. Horizontal distances are proportional to genetic distances. Vertical distances are arbitrary. The scale bar at the bottom measures the nucleotide distance.

Figure 1.5. Expression of *TLR1–9* mRNA in tupaia cells infected with (A) DENV-1, (B) DENV-2, (C) DENV-3, and (D) DENV-4 at 72 h post-infection (MOI=1). RNA levels were

normalized with *GAPDH* mRNA, and the ratio to uninfected tupaia cells is indicated. \* $p < 0.05$ , \*\* $p < 0.01$  vs. mock control. Vertical bars indicate SD.

Figure 1.6. Effect of TLR8 in DENV infection. (A) TLR8 siRNA was transfected and incubated for 72 h. TLR8 protein was detected by western blotting using rabbit anti-tupaia TLR8 antibody in T-238 cells. (B) *TLR8* gene expression after *TLR8* siRNA treatment was measured by qRT-PCR. (C) Viral load in T-238 cells was calculated by quantification of viral copy number and normalized by *GAPDH* in cells (left). Viral load in supernatant was also measured (right). \*\* $p < 0.01$ , \*\*\* $p < 0.001$ . Vertical bars indicate SD.

Figure 1.7. mRNA expression levels of (A) *IFN- $\beta$* , (B) *IL-6*, (C) *TNF- $\alpha$* , and (D) *IL-8*. These levels were normalized with *GAPDH* or *Actin* mRNA, and the ratio to uninfected tupaia cells is indicated. Tupaia cells were infected with DENV serotypes 1–4 at an MOI=1. RNA was collected at 72 h post-infection. \* $p < 0.05$  vs. mock control. Vertical bars indicate SD.

Figure 2.1. HBV genotypes A2 and C infections. (A) Intrahepatic HBV-DNA levels in HBV-A2-infected tupaia or HBV-C-infected tupaia. (B) Histological analysis of tupaia liver infected with HBV-A2 at 8 dpi. Liver of an uninfected tupaia is also shown (left, 400 $\times$ ).

Figure 2.2. HBV-A2 infection in newborn tupaia #N48 and #N93. Serum HBV-DNA and alanine aminotransferase levels were measured serially in HBV genotype A (A2\_JP4)-infected tupaia #N48 and #N93.

Figure 2.3. HBV-A2 infection in adult tupaia. (A) Course of HBV-A2 infection in adult tupaia. (B) Intrahepatic and serum HBV-DNA levels and serum alanine aminotransferase levels and (C) Hepatitis B surface antigen levels in HBV-A2-infected tupaia at 28 days post infection. HBV genotype A (A2\_JP1 and A2\_JP4) isolated from hepatitis B patients was injected intraperitoneally into six adult tupaia (#17, #32, #36, #22, #43, and #48).

Figure 2.4. Changes in the expression of cytokine levels in HBV-A2-infected tupaia at 28 days post infection. Expression of (A) interferon- $\beta$ , (B) tumor necrosis factor- $\alpha$ , and (C) interleukin-

6 in the livers of HBV-A2-infected tupaia. Gene expression levels were determined using quantitative reverse transcription-polymerase chain reaction and was normalized against expression levels of GAPDH or actin mRNA. Data are presented as mean  $\pm$  SD (n = 3).

Figure 2.5. Changes in the expression of toll-like receptor mRNAs in HBV-A2-infected tupaia at 28 dpi. Expression of (A–I) TLR 1–9 mRNAs, measured by quantitative reverse transcription-polymerase chain reaction in the livers of HBV-A2-infected tupaia at 28 dpi. Gene expression levels were normalized against expression levels of GAPDH mRNA. Data are presented as mean  $\pm$  SD (n = 3).

Figure 2.6. HBV-A2 chronic infections in adult tupaia. (A) Course of HBV-A2 chronic infections in adult tupaia. (B) Serum hepatitis B surface antigen and serum alanine aminotransferase levels in HBV-A2-infected adult tupaia at 31 weeks post infection. HBV genotype A (A2\_JP1, A2\_JP2, and A2\_JP4) isolated from hepatitis B patients were used for infecting nine adult tupaia (#84, #85, #92, #93, #86, #94, #88, #96, and #97).

Figure 2.7. Changes in the expression of cytokine mRNAs in HBV-A2-infected tupaia at 31 weeks post infection. Expression of (A) interferon- $\beta$ , (B) tumor necrosis factor- $\alpha$ , and (C) interleukin-6 in the livers of HBV-infected tupaia. Gene expression was normalized against the expression levels of GAPDH or actin mRNA. Data are presented as mean  $\pm$  SD (n = 3).

Figure 2.8. Changes in the expression of toll-like receptor mRNAs in HBV-A2-infected tupaia at 31 wpi. Expression of (A–I) TLR 1–9 mRNA at 31 wpi in the livers of HBV-infected tupaia (#84, #85, #92, #93, #86, #94, #88, #96, and #97), measured by quantitative reverse transcription-polymerase chain reaction. Gene expression levels were normalized against the expression level of GAPDH mRNA. Data are presented as mean  $\pm$  SD (n = 3).

Figure 2.9. Changes in the level of cGAS mRNAs in hepatitis B virus (HBV)-A2-infected tupaia liver tissues. Expression of cGAS mRNA in HBV-A2-infected tupaia liver tissues at (A) 28 days post infection and (B) 31 weeks post infection, as measured by quantitative reverse

transcription-polymerase chain reaction. Gene expression levels were normalized against the expression level of GAPDH mRNA. Data are presented as mean  $\pm$  SD (n = 3).

Figure 2.10. Changes in the level of NTCP mRNAs in hepatitis B virus (HBV)-A2-infected tupaia liver tissues. Expression of NTCP mRNAs in the livers of HBV-A2-infected tupaia at (A) 28 days post infection and (B) 31 weeks post infection, as measured by quantitative reverse transcription-polymerase chain reaction. NTCP expression levels were normalized against the expression levels of GAPDH mRNA. Data are presented as mean  $\pm$  SD (n = 3).

Figure 3.1. Response of tupaia to HCV1a infection. (A) ALT levels and viral loads in sera from tupaia #21 collected at 2-week intervals from 0 to 41 weeks postinfection (wpi). (B) Anti-HCV core and anti-nonstructural protein NS3 antibody titers in tupaia #21 at 2-week intervals from 0 to 41 wpi. (C) Anti-DHCR24 antibody titers and ROS levels in tupaia #21 at 2-week intervals from 0 to 41 wpi. The empty vector was used as the negative control. \*  $p < 0.05$ , \*\*  $p < 0.01$ , \*\*\*  $p < 0.001$ , and \*\*\*\*  $p < 0.0001$  indicate significant differences in antibody titers or ROS levels, as appropriate, before infection and after infection at different weeks. Data are presented as means  $\pm$  SDs (n = 2).

Figure 3.2. Response of tupaia to HCV1b infection. (A) ALT levels and viral loads in sera from tupaia #22 collected at 2-week intervals from 0 to 41 weeks postinfection (wpi). (B) Anti-HCV core and anti-nonstructural protein NS3 antibody titers in tupaia #22 at 2-week intervals from 0 to 41 wpi. (C) Anti-DHCR24 antibody titers and ROS levels in tupaia #22 at 2-week intervals from 0 to 41 wpi. The empty vector was used as the negative control. \*  $p < 0.05$ , \*\*  $p < 0.01$ , \*\*\*  $p < 0.001$ , and \*\*\*\*  $p < 0.0001$  indicate significant differences in antibody titers or ROS levels, as appropriate, before infection and after infection at different weeks. Data are presented as means  $\pm$  SDs (n = 2).

Figure 3.3. Response of tupaia to HCV4a infection. (A) ALT levels and viral loads in sera from tupaia #23 collected at 2-week intervals from 0 to 41 weeks postinfection (wpi). (B) Anti-

HCV core and anti-nonstructural protein NS3 antibody titers in tupaia #23 at 2-week intervals from 0 to 41 wpi. (C) Anti-DHCR24 antibody titers and ROS levels in tupaia #23 at 2-week intervals from 0 to 41 wpi. The empty vector was used as the negative control. \*  $p < 0.05$ , \*\*  $p < 0.01$ , and \*\*\*  $p < 0.001$  indicate significant differences in antibody titers or ROS levels, as appropriate, before infection and after infection at different weeks. Data are presented as means  $\pm$  SDs (n = 2).

Figure 3.4. Response of tupaia #24 to HCV2a infection. (A) ALT levels and viral loads in sera from tupaia #24 collected at 2-week intervals from 0 to 41 weeks postinfection (wpi). (B) Anti-HCV core and anti-nonstructural protein NS3 antibody titers in tupaia #24 at 2-week intervals from 0 to 41 wpi. (C) Anti-DHCR24 antibody titers and ROS levels in tupaia #24 at 2-week intervals from 0 to 41 wpi. The empty vector was used as the negative control. \*  $p < 0.05$ , \*\*  $p < 0.01$ , \*\*\*  $p < 0.001$ , and \*\*\*\*  $p < 0.0001$  indicate significant differences in antibody titers or ROS levels, as appropriate, before infection and after infection at different weeks. Data are presented as means  $\pm$  SDs (n = 2).

Figure 3.5. Histopathological analysis of liver tissues from normal and HCV-infected tupaia #24 at 41 wpi. Histopathological analysis was performed with H&E or silver staining. H&E staining images (upper panel) and silver staining images (lower panel) of liver tissues from (A) Normal tupaia #5, (B) Normal tupaia #38, (C) HCV genotype 1a-infected tupaia #21, (D) HCV genotype 1b-infected tupaia #22, (E) HCV genotype 4a -infected tupaia #23, and (F) HCV genotype 2a -infected tupaia #24 have been shown. Black bars indicate 100  $\mu$ m.

Figure 3.6. Intrahepatic ROS and 8-OHdG levels in normal and HCV-infected tupaia #24 at 41 wpi. (A) ROS in liver lysates and (B) 8-OHdG levels in genomic DNA from HCV-infected tupaia #24 were compared to those of normal controls. Horizontal bars in (A) indicate the mean value. \*\*  $p < 0.01$  indicates significant differences compared to normal controls.

Figure 3.7. Changes in the expression of *TLR* mRNAs in HCV-infected tupaia at 41 wpi. (A) *TLR3*, (B) *TLR7*, and (C) *TLR8* mRNA expression in livers of HCV-infected tupaia was measured by one-step qRT-PCR. Gene expression levels were normalized to the expression level of *GAPDH* mRNA. \*  $p < 0.05$ , \*\*  $p < 0.01$ , \*\*\*  $p < 0.001$ , and \*\*\*\*  $p < 0.0001$  indicate significant differences compared to normal controls. Data are presented as means  $\pm$  SDs (n = 3).

Figure 3.8. Changes in the expression of *NTCP* and cytokine mRNAs in HCV-infected tupaia at 41 wpi. (A) *NTCP*, (B) *IFN- $\beta$* , and (C) *IL-6* mRNA expression in livers of HCV-infected tupaia was measured by one-step qRT-PCR. Gene expression levels were normalized to the expression level of *GAPDH* mRNA. \*  $p < 0.05$ , \*\*  $p < 0.01$ , \*\*\*  $p < 0.001$ , and \*\*\*\*  $p < 0.0001$  indicate significant differences compared to normal controls. Data are presented as means  $\pm$  SDs (n = 3).

## **List of Tables**

Table 1.1. GenBank accession numbers of TLR gene sequences of different species used for phylogenetic tree construction

Table 1.2. List of primers sequences used for qRT-PCR

Table 2.1. Quantitative reverse transcription-polymerase chain reaction primers sequences

## Chapter I

### General Introduction

Tupaia or tree shrew (*Tupaia belangeri*) is a small mammal belonging to the Tupaiidae family, which consists of four genera and 19 extant species. Tupaia is similar to squirrel in appearance, and its body weight ranges between 120-200g (Tsukiyama-Kohara and Kohara, 2014). The natural habitat of tupaia consists of the tropical rainforests in South East Asia, where they feed on fruits, insects, and small vertebrates (Eliot, 1971). The evolutionary characterization of 7S RNA-derived short interspersed elements (SINEs) showed that tupaia possess specific chimeric Tu-type II SINEs, and thus it can be grouped with primates (Kriegs et al., 2007). Genomic analysis has revealed that tupaia is much more closely related to humans than it is to rodents (Fan et al., 2013).

Tupaia have been used in viral infection studies, especially with hepatitis B virus (Sanada et al., 2016; Yang et al., 2015; Walter et al., 1996), and hepatitis C virus (Amako et al., 2010; Xu et al., 2007). So far, chimpanzee is the only existing naturally occurring animal model for studies on human infections with these viruses. However, ethical concerns and stringent animal welfare regulations and very high expenses limit its experimental use, and development of an alternate natural infection model is crucial for the development of vaccine and therapeutic strategies. HCV can successfully establish infection in the humanized chimeric mice liver (Mercer et al., 2001), but these liver cells lack immune response; therefore, the pathogenicity of HCV could not be characterized using humanized chimeric mice liver cells. In addition, tupaia has also been reported to be susceptible to hepatitis E virus (Yu et al., 2016a), herpes simplex virus (Li et al., 2016), Newcastle disease virus and Sendai virus (Xu et al., 2015, Xu et al., 2016). Therefore, tupaia could be a promising candidate as a small animal model for viral infection study.

In this study, I aimed to expand the potentiality of the tupaia animal model for other viruses and I showed the susceptibility of tupaia cells to dengue virus (DENV) infection by four different DENV serotypes- 1, 2, 3 and 4. In addition, I characterized tupaia infected with different subtypes of hepatitis B virus and hepatitis C virus. Taken together, the tupaia shows high potential as an animal model, and in this study I have further expanded the potentiality of this tupaia model for viral infections and immune response characterization, which is expected to contribute towards the development of a tupaia animal model.

**Chapter II: Susceptibility and initial immune response of *Tupaia belangeri* cells to dengue virus infection**

## Abstract

Dengue is an emerging disease of great public health significance worldwide. The lack of a suitable infection model has hampered dengue virus (DENV) pathogenesis study, and developing a suitable small animal model has been a long-standing challenge. The aim of this study was to develop a feasible experimental model of DENV infection using *Tupaia belangeri*. The susceptibility of tupaia to DENV infection and characteristics of its innate immune response were examined in vitro. I found that tupaia fibroblast cells support replication of DENV serotypes 1–4 with a linear increase in viral load 24–96 h post-infection in both cells and culture supernatants. DENV-2 resulted in the highest viral growth among all serotypes. To characterize the innate immune response in tupaia cells during the early phase of DENV infection, I first evaluated the evolutionary relationship between tupaia Toll-like receptors (TLR1–9) and those of other mammalian species. Phylogenetic analysis showed that tupaia TLRs are evolutionarily much closer to human than they are to rodent. I next established an innate immune response measurement system by assessing the mRNA expression of TLR1–9 and four cytokines in DENV-infected tupaia cells. All serotypes induced the upregulation of TLR8 mRNA expression in infected tupaia cells. Silencing of TLR8 led to an increase in viral replication, indicating the existence of antiviral response through TLR8 on DENV infection. Although upregulation of IFN- $\beta$  and IL-6 expression was only observed in DENV-1 infected cells and a significant suppression of TNF- $\alpha$  was observed in DENV-2 infected cells alone, IL-8 was upregulated in all DENV-1–4. Thus, this study demonstrates for the first time the susceptibility of tupaia cells to DENV infections and the role of TLR8 in the anti-viral response of tupaia cells to DENV. These findings demonstrate the potential utility of tupaia as a model for DENV research in the future.

## II.1. Introduction

Dengue is the most prevalent and rapidly spreading mosquito-borne viral disease affecting humans. It is caused by dengue virus (DENV), which is transmitted through the bites of infected *Aedes aegypti* and *Aedes albopictus* mosquitos. Recent estimates revealed that 3.9 billion people are at risk of acquiring DENV infection, and approximately 390 million DENV infections occur each year worldwide (Bhatt et al., 2013). DENV is a positive-strand RNA virus belonging to the Flaviviridae family. It circulates as four distinct but closely related serotypes (DENV-1, DENV-2, DENV-3, and DENV-4), and infection with any of the four serotypes can cause dengue (Simmons et al., 2012). Though DENV infection in humans is often asymptomatic, it may lead to several clinical manifestations ranging from self-limited dengue fever to the potentially life-threatening dengue hemorrhagic fever and dengue shock syndrome (Simmons et al., 2012). The mechanisms underlying dengue-related diseases are still not completely understood. However, it is clear that a complex interplay of virus and host immune responses are likely to determine the outcome of DENV infection (Costa et al., 2013, Yacoub et al., 2013). In addition, evidence suggests a pivotal role of innate immunity during early DENV infection stages in priming both protection and disease induction (Costa et al., 2013).

DENV can infect various cell types, including dendritic cells, peripheral leukocytes, epithelial and endothelial cells, hepatocytes, and fibroblasts (Balsitis et al., 2009, Bonner and O'Sullivan, 1998, Diamond et al., 2000, Kurane et al., 1990, Kurane et al., 1992, Marianneau et al., 1996, Suksanpaisan et al., 2007). Innate immune responses represent the first line of defense and are promptly activated after DENV recognition by specific receptors named pattern-recognition receptors (PRRs), which leads to the activation of intracellular signaling pathways that induce the release of proinflammatory cytokines and type I interferons (IFNs) (Akira et al., 2006). An important class of PRRs, the Toll-like receptors (TLRs), has been shown to play a pivotal role

during DENV infection. TLRs are evolutionarily conserved innate receptors expressed in various immune cells including dendritic cells, macrophages, B and T cells, and non-immune cells such as epithelial cells and fibroblasts. To date, 10 functional members of the TLR family have been identified in humans (Blasius and Beutler, 2010). TLR3 has been found to participate actively in early DENV infection stages and initiates strong IL-8 and IFN- $\alpha/\beta$  responses in vitro (Liang et al., 2011, Tsai et al., 2009). TLR7 and TLR8 were also found to promote antiviral mechanisms against DENV, leading to decreased viral replication in vitro and in vivo (Sariol et al., 2011, Sun et al., 2009).

There are currently no worldwide available vaccines or antiviral treatments for the prevention and control of DENV infection. A major obstacle complicating the progress of therapeutic and preventive interventions, as well as advancements in understanding DENV pathogenesis, is the lack of a suitable animal model that mimics dengue diseases in humans (Chan et al., 2015). Humans and mosquitoes are so far the only known natural hosts for circulating DENV serotypes. While many animal models, including different types of mouse models, and non-human primates like rhesus monkeys, chimpanzees, and marmosets have been investigated for use in DENV infection studies, the ability to recapitulate the complete disease remains a challenge (Chan et al., 2015).

With a view to developing *Tupaia belangeri* (or tree shrew) as an animal model for DENV infection, the present study aimed to investigate the susceptibility of tupaia to DENV infection in vitro, using a tupaia fibroblast cell (T-238). Tupaia is a small mammal belonging to the Tupaiidae family, similar to a squirrel in appearance. Genomic analysis has revealed that tupaia is much more closely related to humans than it is to rodents (Fan et al., 2013, Tsukiyama-Kohara and Kohara, 2014). In addition, tupaia has been reported to be susceptible to several pathogenic viruses infecting humans, including hepatitis B virus (Sanada et al., 2016, Yang et al., 2015), hepatitis C virus (Amako et al., 2010, Xu et al., 2007), hepatitis E virus (Yu et al.,

2016a), herpes simplex virus (Li et al., 2016), Newcastle disease virus and Sendai virus (Xu et al., 2015, Xu et al., 2016), until now there is no report of dengue virus susceptibility of tupaia cells. Also, the major limitation of using the tupaia as an animal model was the lack of tools for its characterization previously, therefore I have performed genome analysis to develop specific antibodies and cDNAs (Tsukiyama-Kohara and Kohara, 2014).

In the present study, I characterized the genomic sequence and transcript expression of the tupaia TLR genes and evaluated the susceptibility of tupaia cells to all DENV serotypes. I also characterize the innate immune response in tupaia cells upon DENV infection by assessing TLRs and cytokines expression.

## **II.2. Materials and Methods**

### **II.2.1. Cell cultures**

Tupaia fibroblast cell line T-23 clone 8 (T-238) was established from a lung of a new-born male Tupaia as described previously (Taketomi et al., 1986) and provided from the Japanese Collection of Research Bioresources Cell Bank (JCRB Cell Bank, Osaka, Japan). Human hepatoma cells (HuH-7), highly susceptible to DENV infection, were used as positive control. T-238 and HuH-7 cells were cultured at 37 °C in a 5% CO<sub>2</sub> incubator in Dulbecco's modified Eagle's medium (DMEM) with high glucose and low glucose, respectively, supplemented with 10% fetal bovine serum (FBS), 1% l-glutamine, and 0.2% sodium bicarbonate.

### **II.2.2. Virus stocks and titration**

The low-passage DENV strains used in this study, including DENV-1 strain Hue-525, DENV-2 strain Hue-397, DENV-3 strain Hue-453, and DENV-4 strain Hue-420, were isolated during a dengue outbreak that occurred in Hue, Vietnam in 2013. To generate working stocks, the viruses were propagated in C6/36 (E2) cells, as described previously (Aoki et al., 2006). The virus titer was determined by fluorescent focus assay (FFA) using C6/36 (E2) cells, as

described previously (Payne et al., 2006), and expressed as fluorescent focus units (FFU) per ml.

### **II.2.3. DENV infection of cells**

T-238 and HuH-7 cells were seeded into 60 mm cell culture plates at a density of  $5 \times 10^5$  cells and maintained at 37 °C in a 5% CO<sub>2</sub> incubator. After 24 h, growth medium was removed, and cells were infected with DENV-1 strain Hue-525 at an multiplicity of infection (MOI) = 1. Cells were incubated for 1 h at 37 °C with gentle agitation every 10 min. Next, the inoculum was removed, and fresh culture medium was added. All cells were incubated at 37 °C with 5% CO<sub>2</sub>. At 24, 48, 72, and 96 h post-infection, cells and culture supernatants were collected for DENV RNA quantification. T-238 cells were similarly infected with DENV-1 strain Hue-525, DENV-2 strain Hue-397, DENV-3 strain Hue-453, or DENV-4 strain Hue-420 at an MOI = 0.1 and incubated at 37 °C with 5% CO<sub>2</sub>. At 24, 48, 72, and 96 h post-infection, cells and culture supernatants were collected for DENV RNA quantification.

### **II.2.4. DENV RNA quantification by quantitative reverse transcription PCR (qRT-PCR)**

Viral RNA was extracted from culture supernatants using an ISOGEN-LS Kit (Nippon Gene, Japan) according to the manufacturer's instructions and eluted in 20 µl nuclease-free water. Total RNA was extracted from infected tupaia cells and HuH-7 cells using an ISOGEN Kit (Nippon Gene) according to the manufacturer's instructions and eluted in 50 µl nuclease-free water. The concentration and purity of each extracted RNA sample were determined using a Nanodrop Spectrophotometer ND-1000 (NanoDrop Technologies, Inc., USA). All RNA samples were stored at – 80 °C for further use.

Viral RNA copy numbers were quantified in culture supernatants and cells using Brilliant IV Ultra-Fast SYBR® Green qRT-PCR Master Mix (Agilent Technologies, USA). Primers targeted a region of the nonstructural protein 1 (NS1) gene that was highly conserved among the four DENV serotypes and consisted of a forward primer (5'-GTB CAC ACH TGG ACA

GA-3') as previously reported (Suwanwong et al., 2010) and a reverse primer (5'-KGG TAT TTG YTT CCA CA-3'). All reactions were performed in 96 micro-well plates using the CFX Connect™ Real-Time PCR Detection System (Bio-Rad, USA). Each 20- $\mu$ l reaction was performed in triplicate. The cycling conditions comprised reverse transcription at 50 °C for 10 min, initial denaturation at 95 °C for 3 min, and 35 cycles at 95 °C for 5 s and 45 °C for 10 s. The standard curve was generated using serial 10-fold dilutions of the full-length DENV serotype 1 NS1 gene (strain Hue-525). Tupaia and human GAPDH were used as endogenous controls for normalization of DENV quantification. Primers used for quantification of tupaia GAPDH mRNA are provided in Table S2. To quantify human GAPDH mRNA, TaqMan Human GAPDH Control Reagents including primer sets (Applied Biosystems) were used.

#### **II.2.5. Immunofluorescence assay**

T-238 cells were seeded in 24-well culture plates containing glass coverslips at  $5 \times 10^4$  cells per well and maintained at 37 °C in a 5% CO<sub>2</sub> incubator. After 24 h, growth medium was removed, and cells were infected with DENV-1 strain Hue-525, DENV-2 strain Hue-397, DENV-3 strain Hue-453, or DENV-4 strain Hue-420 at an MOI = 0.1, as described above. Mock-infected cells were used as controls. At 72 h post-infection, cells were fixed with cold acetone-methanol (1:1) and stained with anti-flavivirus group antibody (clone D1-4G2) (Merck Millipore Co., Germany) and anti-mouse Alexa488 (Thermo Fisher Scientific Co., USA), and observed with BZ-X700 (Keyence Co., Japan).

#### **II.2.6. Expression analysis of tupaia TLRs and cytokines**

Tupaia TLR1–9, IFN- $\beta$ , IL-6, TNF- $\alpha$  and IL-8 gene sequences were determined from genome sequence and cDNA sequence which I originally determined from tupaia genome and mRNA, and submitted to GenBank (KX438361-KX438372, LC218169, Table 1.1 and 1.2). To assess the genetic relationship between the TLRs of tupaia (TLR1–9) and those of other mammals, including human, gorilla, chimpanzee, orangutan, macaque, marmoset, cow, horse, dog, ferret,

bat, rat, and mouse, a phylogenetic analysis was performed using both nucleotide and protein sequences (Table 1.1). Nucleotide and protein sequences of TLR from other than tupaia used in the phylogenetic analysis were derived from the GenBank database. Phylogenetic trees were constructed using the neighbor-joining method (Saitou and Nei, 1987), and evolutionary distances were computed using the p-distance method (Nei and Kumar, 2000). Evolutionary analyses were conducted in MEGA7 (Kumar et al., 2016). Frog TLR nucleotide and amino acid sequences were used as outgroups. The reliability of the trees was assessed using bootstrap analysis with 1000 replicates.

To evaluate the expression of tupaia TLR genes during DENV infection, T-238 cells were seeded into 60 mm cell culture plates and infected with DENV-1 strain Hue-525, DENV-2 strain Hue-397, DENV-3 strain Hue-453, or DENV-4 strain Hue-420, as described above. Uninfected T-238 cells (medium alone) were used as controls. At 72 h post-infection, uninfected and DENV-infected cells were collected for total RNA extraction using an ISOGEN Kit (Nippon Gene) according to the manufacturer's instructions. RNA was resuspended in 50  $\mu$ l of RNase-free distilled water and stored at  $-80^{\circ}\text{C}$ .

Expression levels of tupaia TLRs were quantified using one-step qRT-PCR with Brilliant IV Ultra-Fast SYBR® Green qRT-PCR Master Mix (Agilent Technologies) supplemented with specific primers for tupaia TLR genes. Primers used for amplification of the genes of interest and reference genes were designed using Primer-Blast (<http://www.ncbi.nlm.nih.gov/tools/primer-blast/>) based on target sequences available in GenBank (Table 1.2). All reactions were performed in 96 micro-well plates using the CFX Connect™ Real-Time PCR Detection System (Bio-Rad). Each 20- $\mu$ l reaction was performed in triplicate. The cycling conditions included reverse transcription at  $50^{\circ}\text{C}$  for 10 min, initial denaturation at  $95^{\circ}\text{C}$  for 3 min, and 40 cycles of  $95^{\circ}\text{C}$  for 5 s and  $60^{\circ}\text{C}$  for 10 s for all genes except TLR8, IL-8, and TNF- $\alpha$ . Annealing and extension temperature was  $55^{\circ}\text{C}$  for TLR8 and

65 °C for IL-8 and TNF- $\alpha$ . PCR reaction specificity was confirmed by melting curve analysis and gel electrophoresis of the amplified product. After each run, a melt curve was performed between 65 and 95 °C with a heat increment of 0.1 °C per second and continuous fluorescence measurement. Each experiment included a no-template control and a standard curve for each gene. Standards were generated from prequantified plasmids containing each target gene sequence. Tupaia GAPDH or actin was used as an endogenous control for normalization of the results. For fold-change calculation of gene copy numbers, I first calculated the normalized ratio in uninfected (control) and infected groups by dividing the target gene copy number by the reference gene copy number in uninfected and infected groups, respectively. Then, I divided the normalized ratio obtained in the infected group by the normalized ratio obtained in the uninfected group, yielding the fold-change value of gene expression.

#### **II.2.7. Silencing and detection of TLR8**

Silencing of TLR8 was performed using stealth siRNA (Invitrogen, USA; 1793) AAUAGUGGGCGUUAUAGCUGAGAUC and RNAi Max (Invitrogen). TLR8 protein was detected by rabbit polyclonal anti-TLR8 antibody, which was made through immunization of three synthetic peptides, SFQSHTLKTRSADTNFDC, EFFTERNYFRSYPC, and NRLDFDDDKTLQDLPYLC and purified by MBL Co. (USA).

#### **II.2.8. Statistical analysis**

Values are expressed as mean  $\pm$  standard deviation (SD). To analyze the statistical significance of viral load results obtained in HuH-7 and tupaia cells, unpaired t-test was used. For analysis of the statistical significance of TLR gene expression results obtained in control and infected tupaia cells, paired t-test was used. All statistical analyses were performed using GraphPad software (<http://graphpad.com/quickcalcs/ttest1/>). P-values  $< 0.05$  were considered significant.

## **II.3. Results**

### **II.3.1. DENV-1 replication in tupaia cells**

To examine the susceptibility of tupaia cells to DENV infection in vitro, I used tupaia fibroblast cells (T-238) as well as human hepatoma HuH-7 cells as positive control, previously reported to be highly susceptible to DENV infection. The cells were inoculated with low-passage DENV-1 strain Hue-525 at an MOI = 1, and levels of DENV RNA were determined in cells and culture supernatants by qRT-PCR at various time points. As shown in Figure 1.1, a linear increase in viral load was observed in tupaia and HuH-7 cells and culture supernatants from 24 to 96 h post-infection. This indicates that tupaia cells are permissive to DENV infection. Of note, kinetic of viral replication of DENV-1 in tupaia cells was slower than that in HuH-7 cells. Levels of intracellular DENV RNA in tupaia and HuH-7 cells reached 9 and 35 copies/ $\mu\text{g}$  of total RNA ( $p = 0.0001$ ), respectively, at 96 h post infection. Viral loads in the culture supernatants of tupaia and HuH-7 cells reached  $8.6 \times 10^8$  and  $1.6 \times 10^9$  copies/ml ( $p = 0.0009$ ), respectively, at 96 h post-infection.

### **II.3.2. Kinetic of DENV serotypes 2, 3, and 4 replication in tupaia cells**

The kinetic of DENV-2 strain Hue-397, DENV-3 strain Hue-453, and DENV-4 strain Hue-420 replication was compared to those of DENV-1 strain Hue-525 in tupaia cells. Cells were inoculated with each DENV serotype at an MOI = 0.1, and intracellular DENV RNA levels were determined by qRT-PCR at various time points post-infection. As shown in Figure 1.2, DENV-1, DENV-2, and DENV-3 strains grew linearly in tupaia cells. A slow viral replication rate was observed for DENV-4. DENV-2 exhibited more efficient growth than other serotypes. Next, tupaia cells were tested for the expression of DENV antigens by immunofluorescence assay using a mouse monoclonal antibody against the viral envelope (E) protein. For all DENV serotypes, positive staining of DENV antigen was specifically detected in infected tupaia cells (Figure 1.3). No E protein expression was detected in mock-infected cells.

### **II.3.3. Phylogenetic analysis of tupaia TLRs**

To further characterize the antiviral innate immune responses of tupaia cells to DENV infection, I sought to determine the genetic relationship between the tupaia and other mammals by performing a phylogenetic analysis of determined tupaia TLR nucleotide and predicted amino acid sequences (TLR1–9) with corresponding TLR sequences from 13 mammalian species. Tupaia TLR10, recently described as a pseudogene (Yu et al., 2016b), was excluded from this analysis. Frog TLR sequences were used as an outgroup. The short, partial sequence of frog TLR4 (GenBank accession: AB280751) was excluded from analysis.

The constructed neighbor-joining trees based on both nucleotide and amino acid sequences of nine mammalian TLR genes (Figure 1.4) revealed that all tupaia TLRs (TLR1–9) are more closely related to human TLRs than to rodent TLRs, with the exception of tupaia TLR2, which appears closer to rodents in the nucleotide tree. In particular, tupaia TLR4, TLR5, and TLR8 are more similar to their human and non-human primate counterparts than to those of any other species in both the nucleotide and amino acid trees.

### **II.3.4. Tupaia TLR expression in response to DENV infection**

The expression levels of tupaia TLR1–9 in response to DENV infection was measured using qRT-PCR (Figure 1.5). In all DENV infections, an increase in the tupaia TLR8 mRNA levels was observed. Therefore, I further assessed the effect of TLR8 on DENV infection in tupaia cells through siRNA treatment. Treatment with TLR8 siRNA knocked down TLR8 mRNA and protein expression (Figure 1.6A, B). Knockdown of TLR8 expression led to a significant increase in DENV-1 viral load, both in tupaia cells and corresponding culture supernatants (Figure 1.6C). Thus, tupaia TLR8 possesses a suppressive role in DENV replication in vitro.

### **II.3.5. Tupaia cytokine expression in response to DENV infection**

I also evaluated the expressions of IFN- $\beta$ , IL-6, IL-8, and TNF- $\alpha$  mRNA in DENV-infected tupaia cells and observed changes in cytokine expression in response to DENV infection.

Significantly elevated levels of IFN- $\beta$  mRNA were only observed following DENV-1 infection (Figure 1.7A). For IL-6 mRNA, there was no significant change in expression between mock- and DENV-infected cells (Figure 1.7B). Infection with DENV-2 caused a significant decrease in TNF- $\alpha$  mRNA expression in tupaia cells (Figure 1.7C). Finally, a significant increase with DENV-1 and -2 infection and increase with DENV-3 and 4 infection in IL-8 mRNA expression was observed (Figure 1.7D).

#### **II.4. Discussion**

The lack of a reliable animal model is a major obstacle for investigations into DENV pathogenesis and development of effective therapeutic and preventive interventions. In the present study, I aimed to develop an experimental model of DENV infection using the tree shrew (or tupaia), a small squirrel-like mammal that is more closely related to primates than to rodents. Therefore, I assessed the ability of tupaia cells to support DENV infection *in vitro*. A tupaia fibroblast cell line (T-238) was used as it is widely known that human fibroblasts are permissive for DENV replication both *in vitro* and *in vivo* (Bustos-Arriaga et al., 2011, Diamond et al., 2000). I found that tupaia cells can support DENV-1 replication, yielding a linear increase in viral load 24–96 h post-infection in both cells and culture supernatants. This may be consistent with the previous observation that tupaia cells have functional MAVS (Xu et al., 2015) and MDA5 (Xu et al., 2016) that can compensate the lack of RIG-I (Xu et al., 2016). Serotypes DENV-2, DENV-3, and DENV-4 were also able to infect and replicate in tupaia cells. Higher replication efficiency was observed for DENV-2 than for the other serotypes, suggesting a higher pathogenicity of DENV-2 in tupaia cells. Several *in vitro* and clinical studies have similarly reported differences in virological characteristics between DENV serotypes (Vicente et al., 2016, Yohan et al., 2014). In addition, one previous study

(Vaughn et al., 2000) reported higher viral replication rates for DENV-2 in primed hosts, which confer enhanced pathogenicity, compared with those of other serotypes.

Based on kinetic of viral replication, I characterized innate immune responses in tupaia cells during the early phase of DENV infection in vitro. Central to innate immunity are TLRs, which stimulate the production of anti-viral components and co-stimulatory molecules via TLR signaling pathways and serve as a link between innate and acquired immunity (Akira et al., 2006). TLRs are important initiators of cytokine production, and TLR signaling cascades are mainly controlled by the MyD88-dependent and TRIF-dependent pathways, both of which lead to activation of NF- $\kappa$ B and mitogen-activated protein kinases (MAPKs) (Brown et al., 2011, Kawai and Akira, 2010). Both NF- $\kappa$ B and MAPKs have been found to play crucial roles in cytokine induction (Barnes and Karin, 1997, Carter et al., 1999).

I conducted a phylogenetic analysis to assess the genetic relationships between tupaia TLRs and those of other mammalian species. Although the evolutionary distances between tupaia and other mammals exhibited some variation, all tupaia TLRs were evolutionarily more similar to human or primate TLRs than to rodent TLRs. A previous genomic analysis also suggested that tupaia is more closely related to human than it is to rodents (Fan et al., 2013, Kriegs et al., 2007). In addition, the evolutionary characterization of 7SL RNA-derived short interspersed elements (SINEs) showed that tupaia possesses specific, chimeric Tu-type II SINEs and can be grouped with primates (Kriegs et al., 2007).

Analysis of tupaia TLR1–9 mRNA levels revealed upregulation of TLR8 following infection with all DENV serotypes. Interestingly, silencing of TLR8 induced an increase in viral replication, suggesting some antiviral activity of TLR8 in DENV-infected tupaia cells. TLR8 recognizes single-stranded viral RNA and is involved in protection against viruses (Akira et al., 2006). Increase of TLR8, IL-8 and other cytokine gene expression was also observed in DENV infected HepG2 cells (Conceição et al., 2010). Activation of TLR8 induces production

of the proinflammatory cytokines TNF- $\alpha$  and type I IFNs (Akira et al., 2006). In line with these data, significant induction of TLR8 and IFN- $\beta$  were observed in DENV-1-infected tupaia cells. In DENV-2 infection, TLR8 expression increased but not significantly. In addition, significant suppression of TNF- $\alpha$  expression and an absence of IFN- $\beta$  induction were observed. Inhibitory effects of IFN- $\beta$  (Liang et al., 2011, Tsai et al., 2009) and TNF- $\alpha$  (Shi et al., 2006) have been reported for DENV infection. DENV-2 exhibited the highest viral replication activity in tupaia cells among the serotypes; therefore, I suggest that its inhibitory effect on IFN- $\beta$  and/or TNF- $\alpha$  expression contributes to its high efficiency of replication in tupaia cells. Further studies are needed to elucidate the detailed mechanism of suppression of IFN- $\beta$  and TNF- $\alpha$  in DENV-2 infection.

## **II. Conclusions**

To my knowledge, this is the first study showing the susceptibility of tupaia fibroblast cells to DENV infection. Differences in viral replication kinetic and TLR/cytokine expression profiles in tupaia cells were observed among DENV serotypes. Tupaia TLR8 was highly induced during DENV infection, inhibiting viral replication. Although further research is required to validate tupaia as an animal model for DENV research, this study lays the groundwork for the use of tupaia cells as a DENV cell infection model. Modulation of the innate immune response following infection implies an active interaction between cells and virus. The characterization of immune responses established in this study contributes to the establishment of a tupaia animal model, which may aid in the development of effective antiviral drugs and vaccines against DENV.

**Table 1.1.** GenBank accession numbers of TLR gene sequences of different species used for phylogenetic tree construction

Name (Species)	TLR1	TLR2	TLR3	TLR4	TLR5	TLR6	TLR7	TLR8	TLR9
<b>Tupaia</b> ( <i>Tupaia belangeri</i> )	KX43836 1	KX43836 2	KX43836 3	KX43836 4	KX43836 5	KX43836 6	KX43836 7	KX43836 8	KX43836 9
<b>Human</b> ( <i>Homo Sapiens</i> )	NM_0032 63	U88878	NM_0032 65	NM_1385 54	AB06069 5	AB02080 7	AB44565 9	NM_0166 10	AY35908 5
<b>Chimpanzee</b> ( <i>Pan troglodytes</i> )	XM_0094 47484	KF31974 8	NM_0011 30470	NM_0011 44863	KF32081 9	NM_0011 30468	NM_0011 30133	NM_0011 30472	NM_0011 44866
<b>Marmoset</b> ( <i>Callithrix jacchus</i> )	XM_0089 93481	XM_0027 45381	XM_0089 92313	XM_0090 02532	XM_0027 60480	XM_0027 45913	XM_0027 62618	XM_0089 88948	XM_0027 58237
<b>Macaque</b> ( <i>Macaca fascicularis</i> )	XM_0055 54676	AY04557 3	NM_0010 36685	AB44564 3	AB44565 0	NM_0011 30430	NM_0011 30426	AB445671	EU20494 7
<b>Gorilla</b> ( <i>Gorilla gorilla</i> )	KF31950 7	KF31971 5	NM_0012 79752	NM_0012 79583	KF32075 7	NM_0012 79638	XM_0040 63793	AB445669	XM_0040 34272
<b>Orangutan</b> ( <i>Pongo pygmaeus</i> )	AB44562 1	AB44562 8	XM_0092 40513	AB44564 2	AB44564 9	AB44565 6	AB44566 3	AB445670	XM_0092 38945
<b>Cow</b> ( <i>Bos taurus</i> )	NM_0010 46504	NM_1741 97	NM_0010 08664	NM_1741 98	NM_0010 40501	NM_0010 01159	NM_0010 33761	NM_0010 33937	NM_1830 81
<b>Horse</b> ( <i>Equus caballus</i> )	NM_0012 56899	NM_0010 81796	NM_0010 81798	AY00580 8	XM_0085 33398	XM_0056 08583	NM_0010 81771	NM_0011 11301	DQ39054 1
<b>Dog</b> ( <i>Canis lupus familiaris</i> )	XM_0141 12328	NM_0010 05264	XM_0056 29968	AB08036 3	NM_0011 97176	EU55114 7	NM_0010 48124	XM_0034 35448	NM_0010 02998
<b>Ferret</b> ( <i>Mustela putorius furo</i> )	XM_0130 62225	XM_0047 72000	XM_0130 59017	XM_0047 74068	XM_0130 50637	XM_0130 62215	XR_0011 80586	JP019628	JP019629
<b>Bat</b> ( <i>Myotis lucifugus</i> )	XM_0144 55635	XM_0145 43903	XM_0058 63095	XM_0060 91085	XM_0145 39935	XM_0058 77436	XM_0058 80946	XM_0145 28933	XM_0144 48429
<b>Rat</b> ( <i>Rattus norvegicus</i> )	NM_0011 72120	NM_1987 69	NM_1987 91	NM_0191 78	NM_0011 45828	NM_2076 04	NM_0010 97582	NM_0011 01009	NM_1981 31
<b>Mouse</b> ( <i>Mus musculus</i> )	XM_0065 03852	NM_0119 05	AF35515 2	NM_0212 97	NM_0169 28	NM_0116 04	NM_1332 11	NM_1332 12	NM_0311 78
<b>Frog</b> ( <i>Xenopus tropicalis</i> )	XM_0029 38656	XM_0029 33492	XM_0029 34402	-	NM_0010 78891	XM_0180 95357	NM_0011 27411	XM_0029 33813	XM_0180 93220

**Table 1.2. List of primers sequences used for qRT-PCR**

Gene	Primer sequences (5'-3' ) Forward (F), Reverse (R)	GenBank Accession number	Product length (bp)
tGAPDH	F: AATTTGGCTACAGCAACAGG R: ATTGATGGTTCGTGACAAGG	KC215182	234
tActin	F: GAGCATCCCTAGAGTTCTGCAA R: TCCTGTAACAATGCGTCTCACA	AF110103	102
tTLR1	F: TGCTGACTGTGACCATGACC R: GCAAGTTCCTTGCTCTGCG	KX438361	105
tTLR2	F: AGCTGCTGTTTTACGCTT R: AGGTAAAACCTGGGGATGTG	KX438362	160
tTLR3	F: AGCCTTCAACGACTGATGCT R: GTTGAGGACGTGGAGGTGAT	KX438363	264
tTLR4	F: TACAGAAGCTGGTGGCTGTG R: CTCCAGGTTGGGCAGGTTAG	KX438364	152
tTLR5	F: GCTGGTCAGTGGACATCACA R: CCAGGCCAGCAAATGTGTTC	KX438365	147
tTLR6	F: GTGGAGGACTGGCCTGATTC R: GATGCAGAGGAGGGTCATGG	KX438366	168
tTLR7	F: AGATGTCCCCACTGTTTTGC R: TAACAACGAGGGCAGTTTCC	KX438367	141
tTLR8	F: AAACCTCTCTAGCACTTC R: CAAGTGTTTCTAAGTAGTCC	KX438368	152
tTLR9	F: TATAACTGCATCGCGCAGAC R: CGGCTGTGGATATTGTTGTG	KX438369	257
tIFN- $\beta$	F: GCAGCAGTTTGGCGTGTAAG R: TTCTGGAACCTGCTGTGGTCG	KX438370	121
tIL-6	F: ATACCAGAACCCACCTCCAC R: GTGCAACCCTGCACTTGTA	KX438371	115
tTNF- $\alpha$	F: GCCTAGTCAACCCTCTGACC R: CCCTTGTTTTGGGGGTTTTGC	KX438372	100
tIL-8	F: TATTGCTCTGTTGGCAGCCT R: TGAAAAGGCGTCGAGTGTGT	LC218169	117

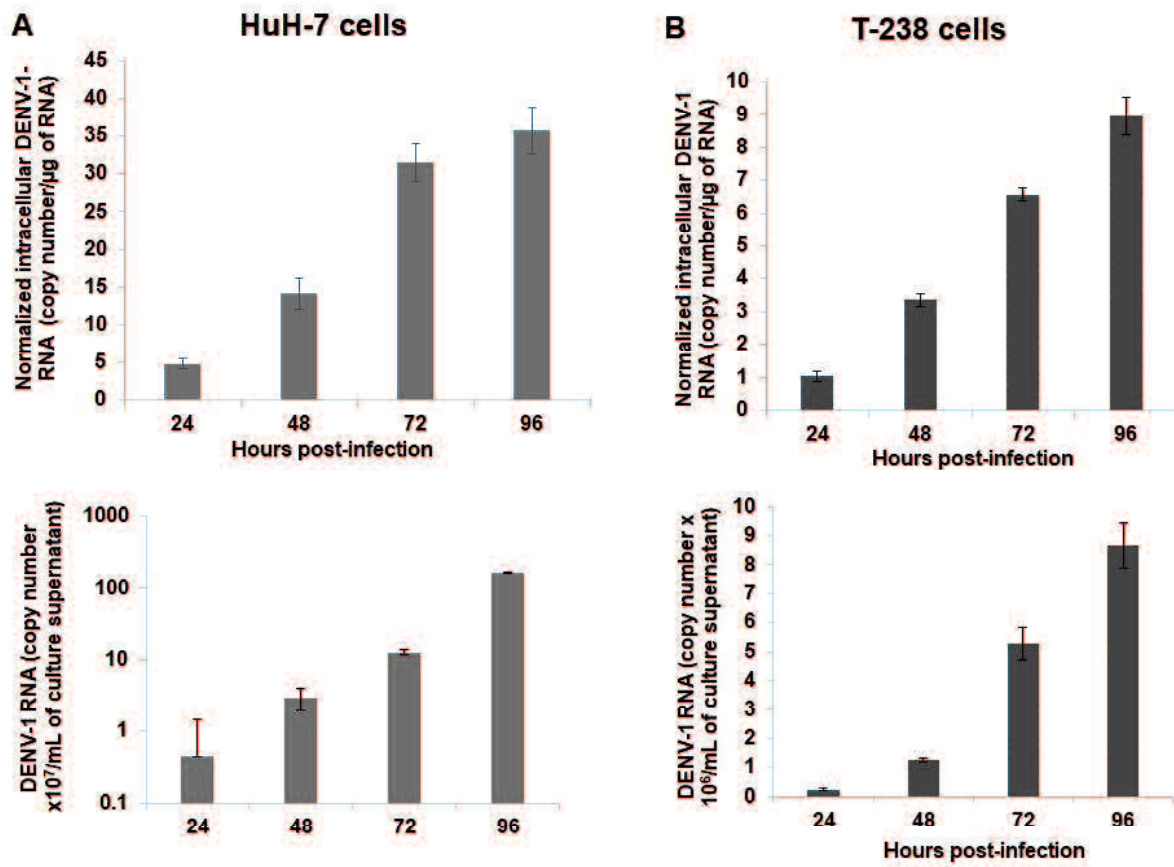


Figure 1.1. Kinetic of DENV-1 replication in (A) HuH-7 and (B) T-238 cells and culture supernatants.

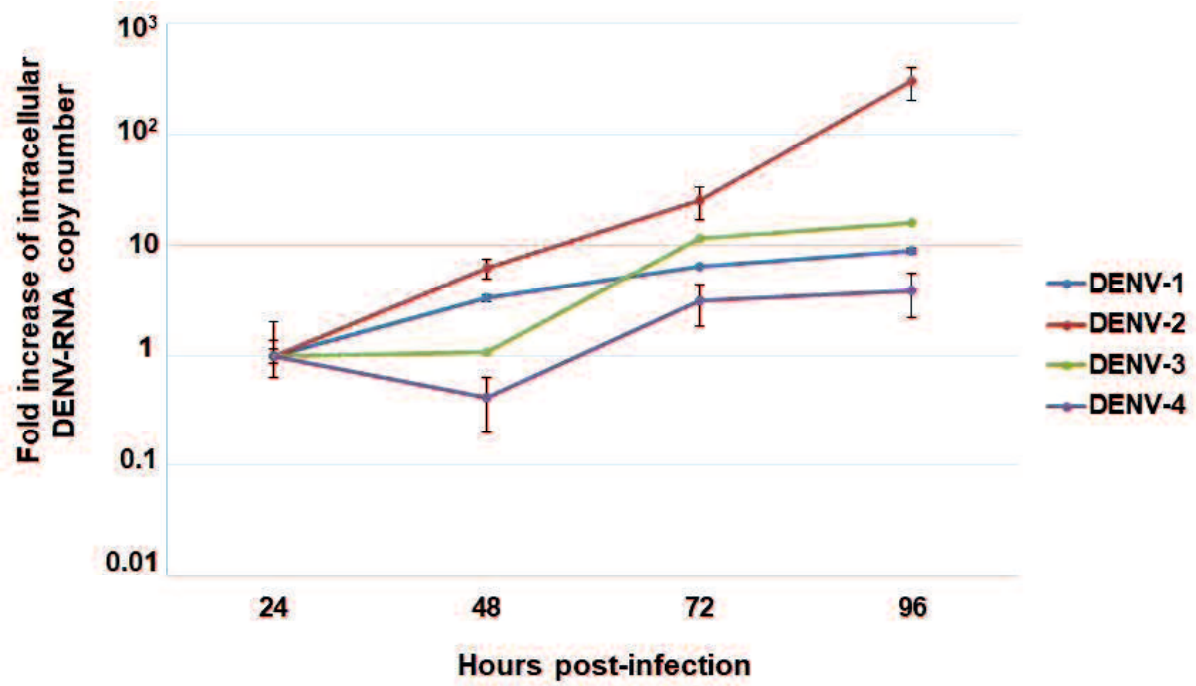
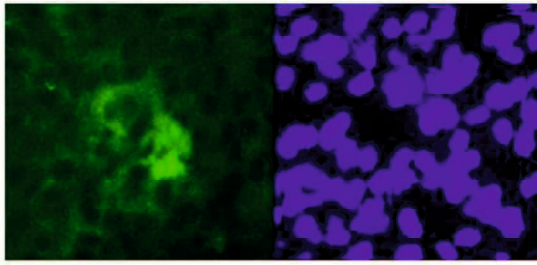
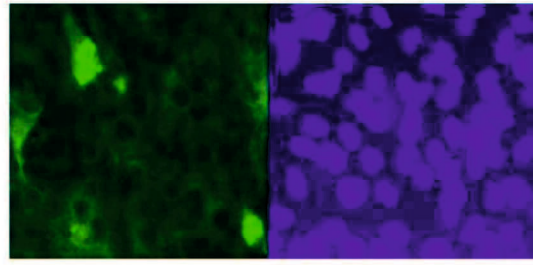


Figure 1.2. Kinetic of DENV serotypes 1–4 replication in T-238 cells at 24, 48, 72, and 96 h post-infection (MOI = 0.1).

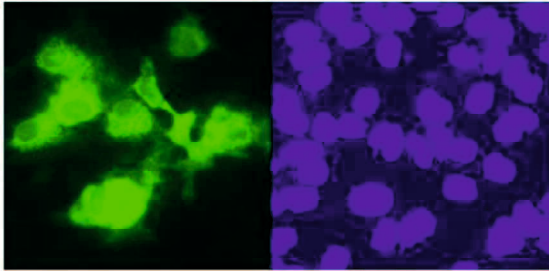
**DENV-1**



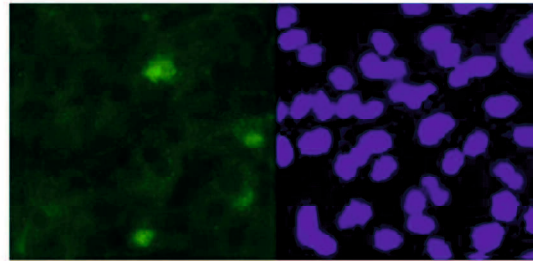
**DENV-3**



**DENV-2**



**DENV-4**



**Mock**

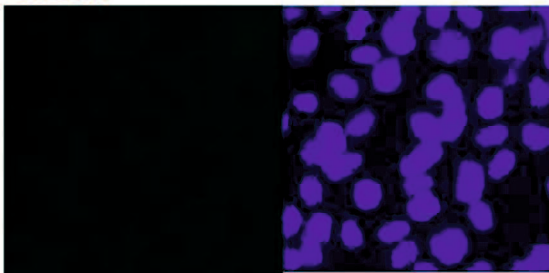
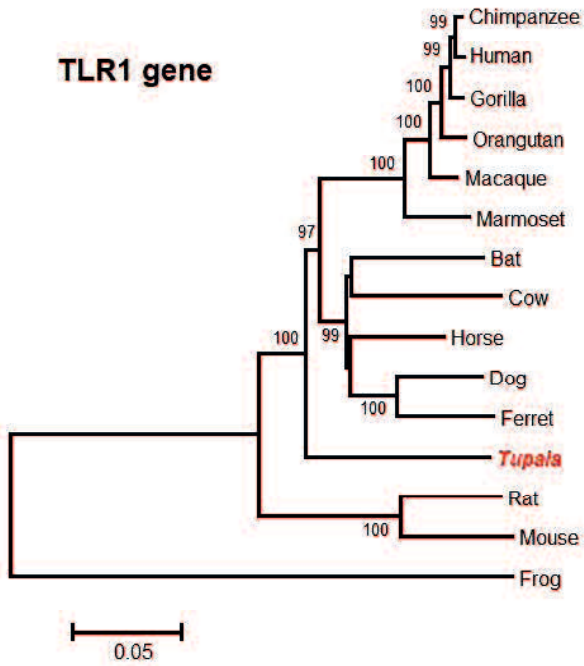


Figure 1.3. Detection of DENV envelope protein in T-238 cells by immunofluorescence assay (400×).

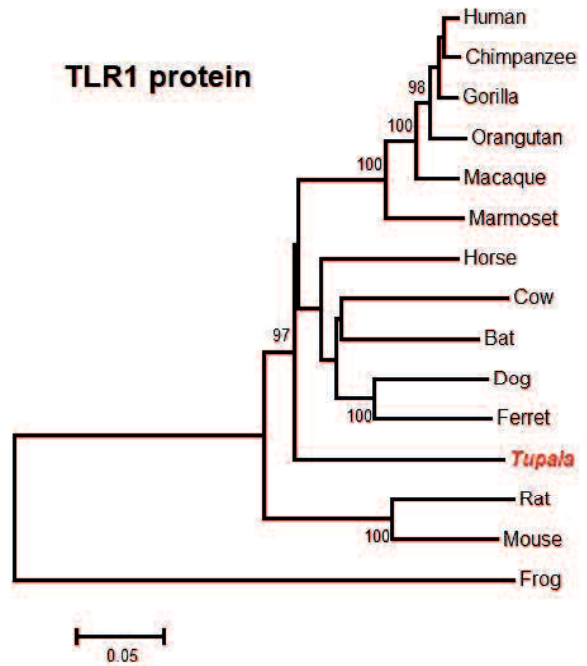
**A**

**TLR1 gene**



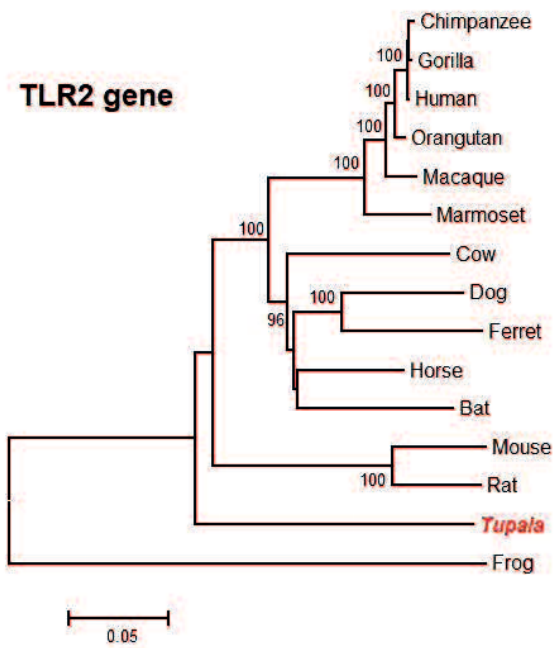
**B**

**TLR1 protein**



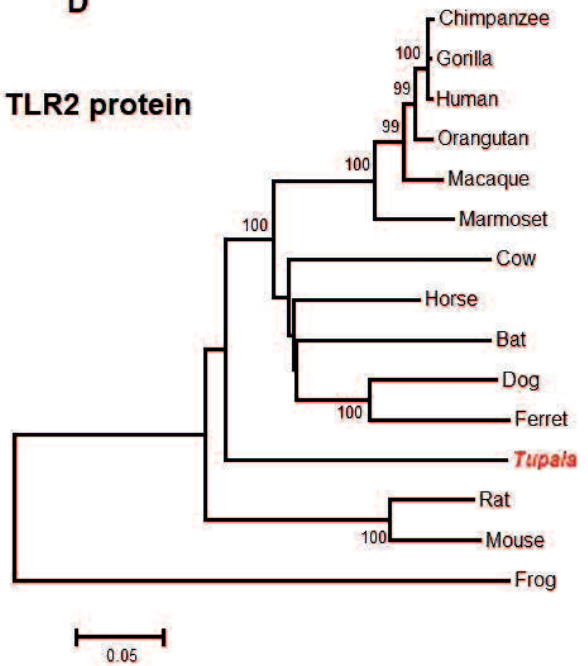
**C**

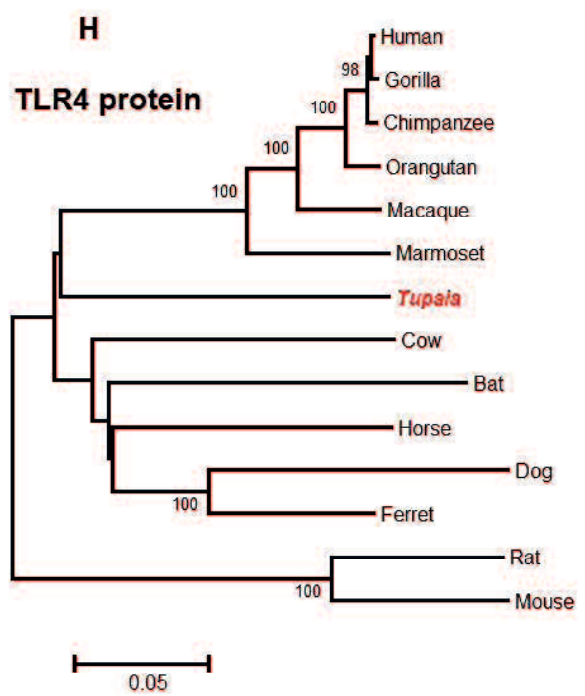
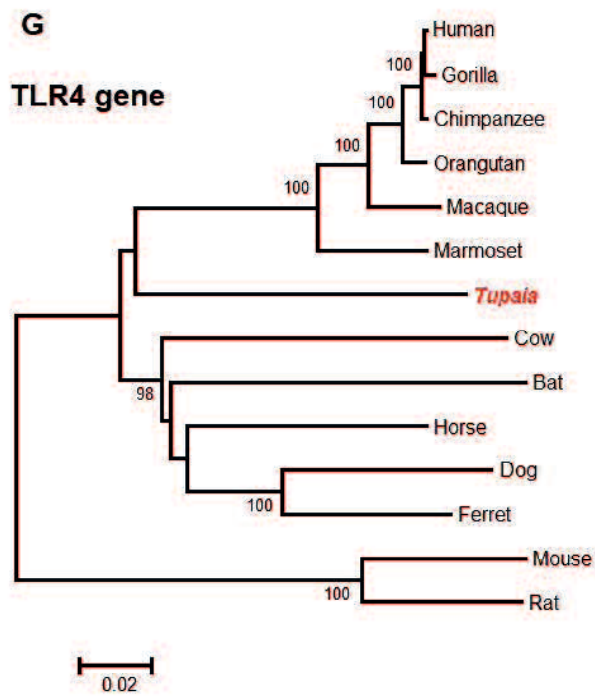
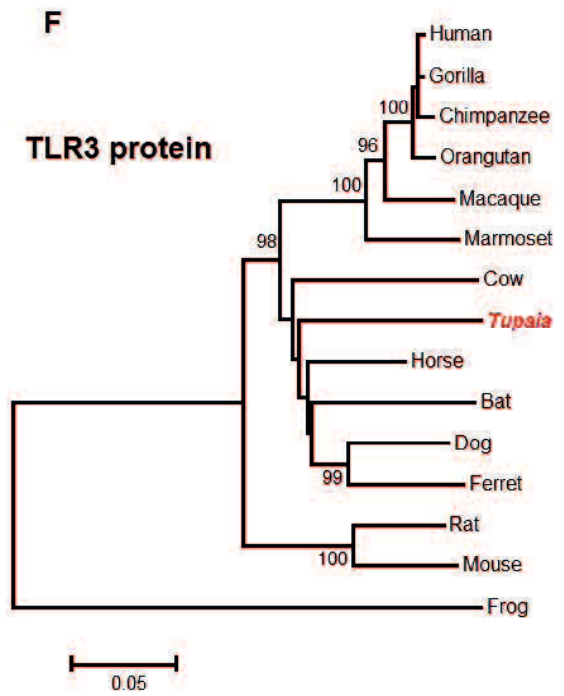
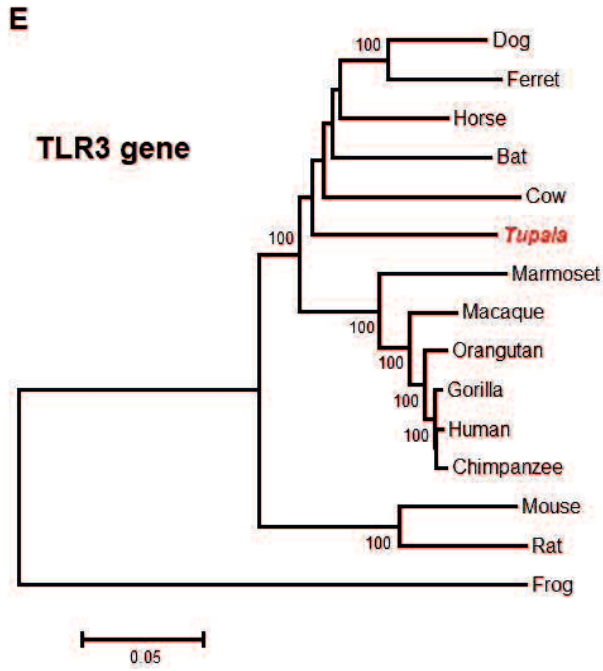
**TLR2 gene**

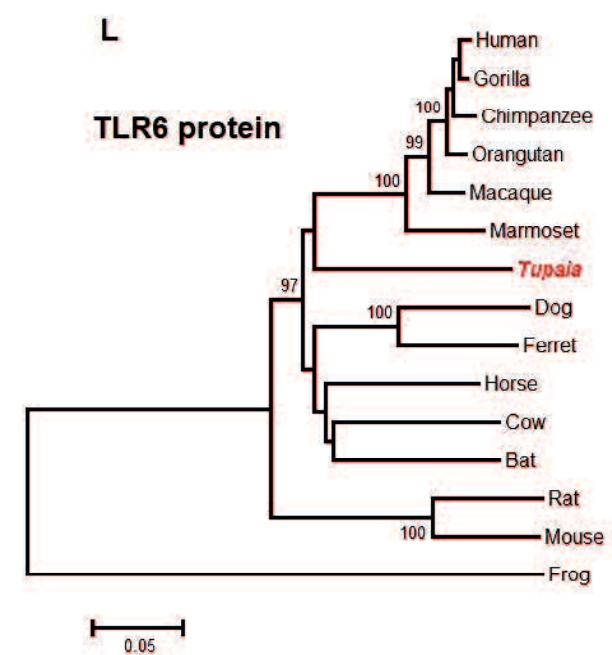
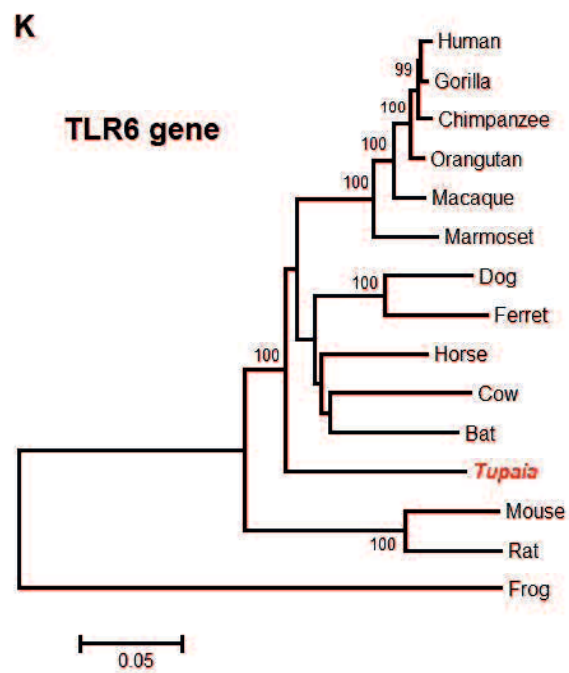
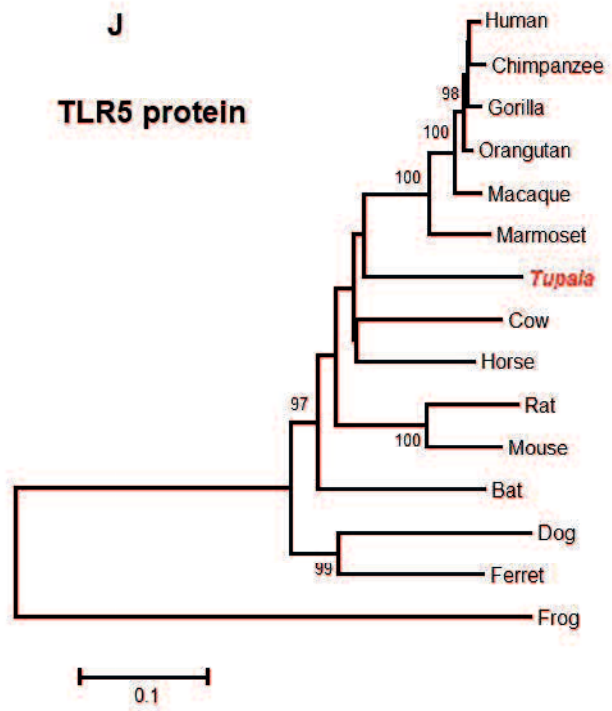
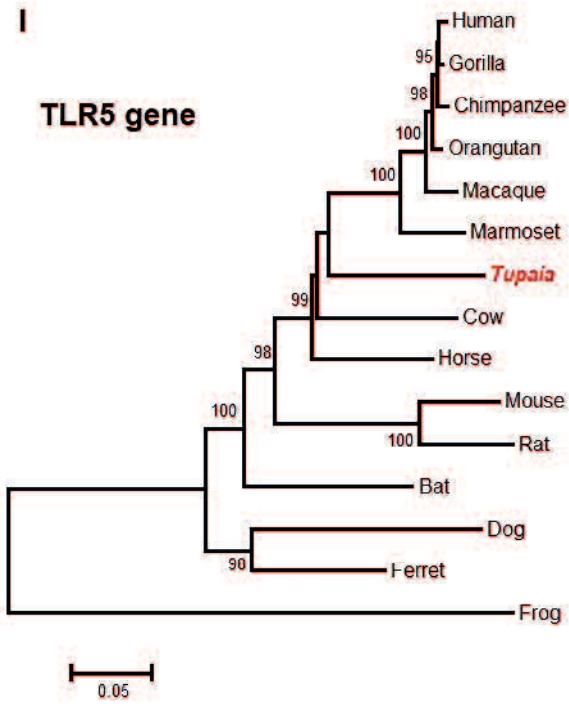


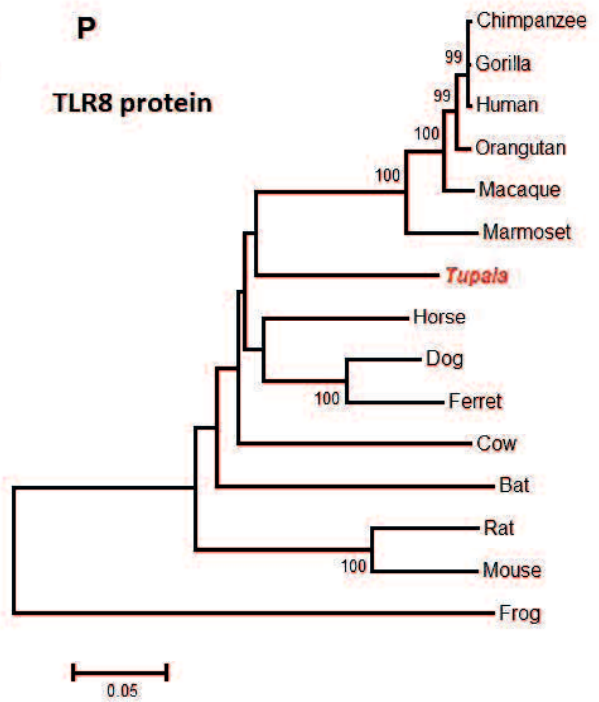
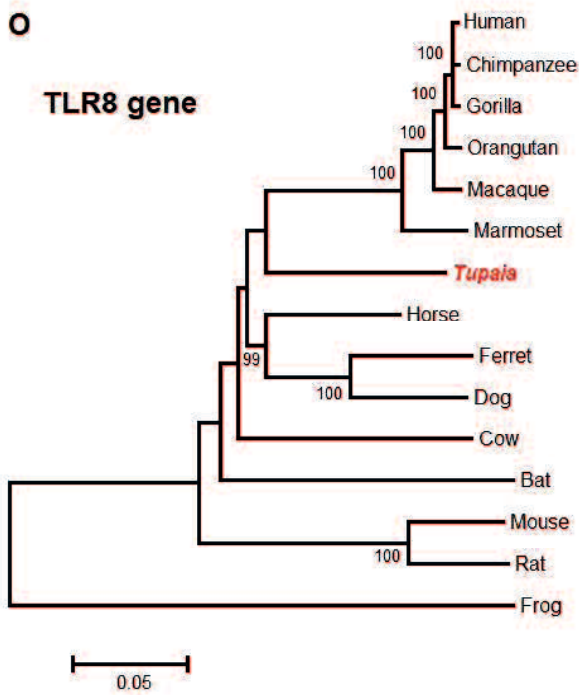
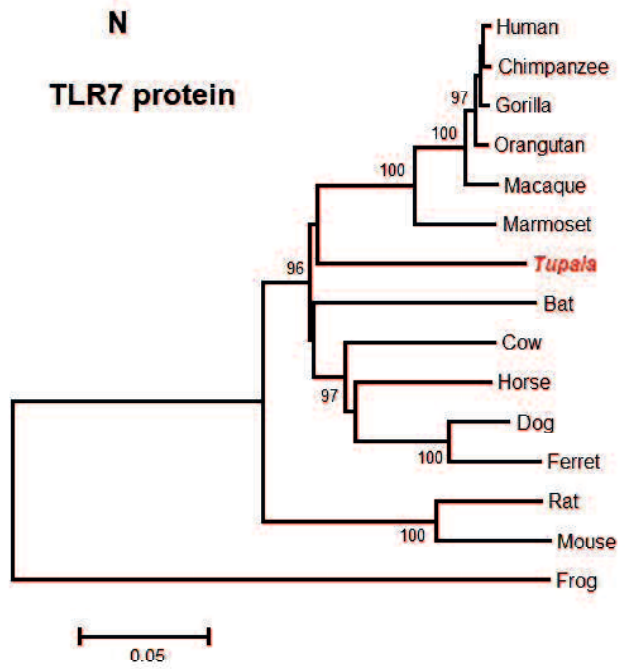
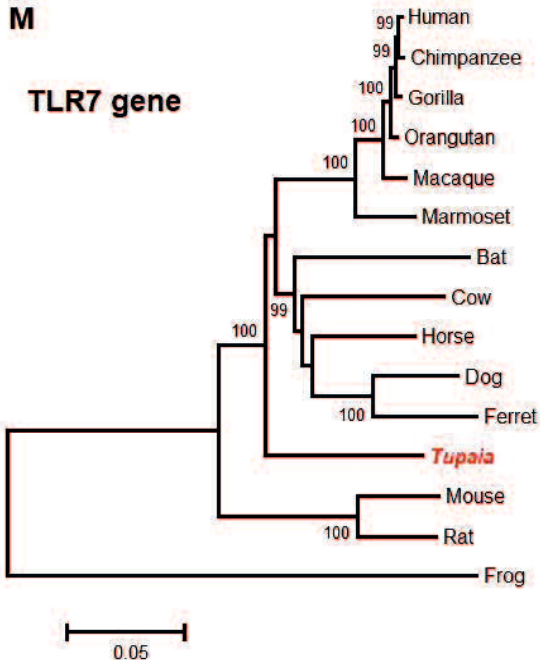
**D**

**TLR2 protein**









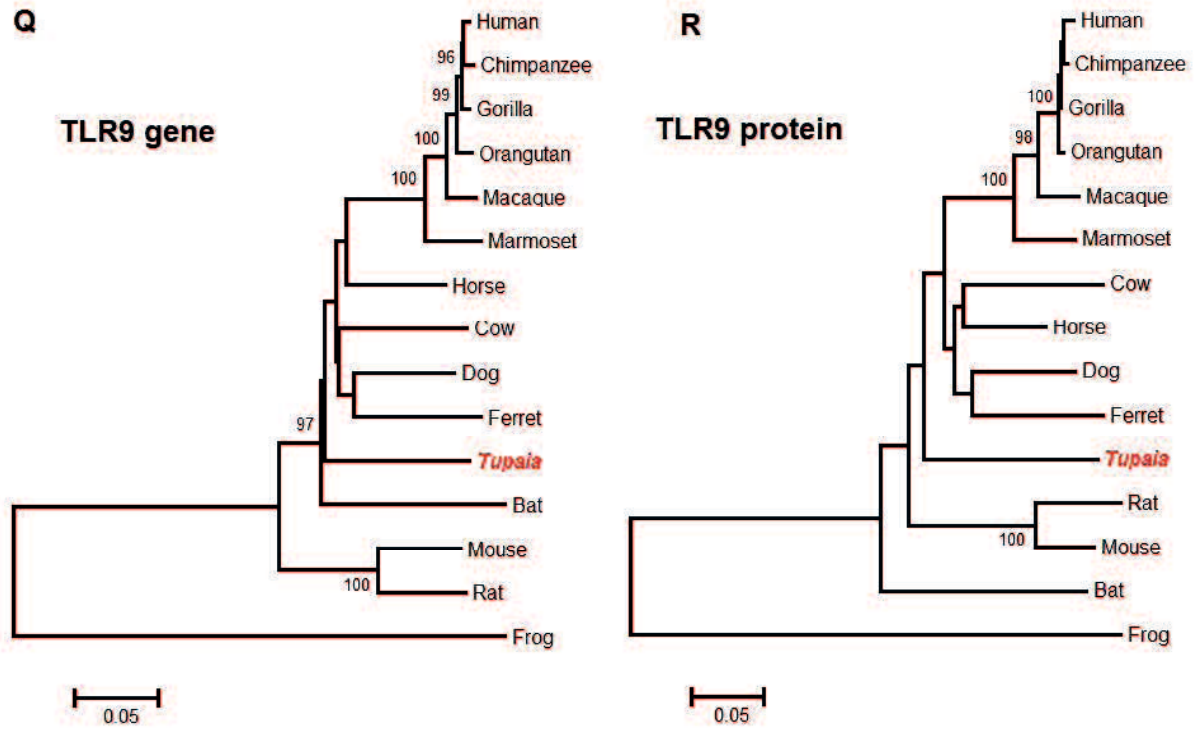


Figure 1.4. Phylogenetic tree of tupaia TLRs.

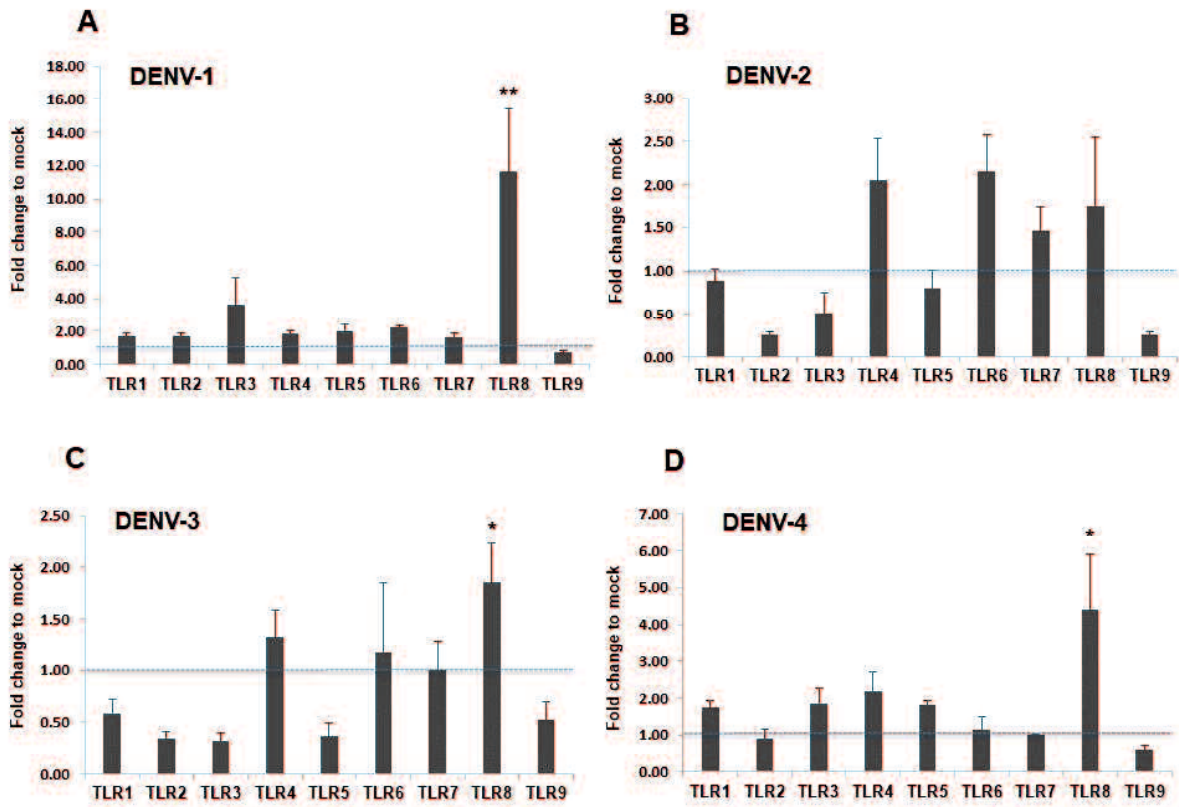


Figure 1.5. Expression of *TLR1–9* mRNA in tupaia cells infected with (A) DENV-1, (B) DENV-2, (C) DENV-3, and (D) DENV-4 at 72 h post-infection (MOI=1).

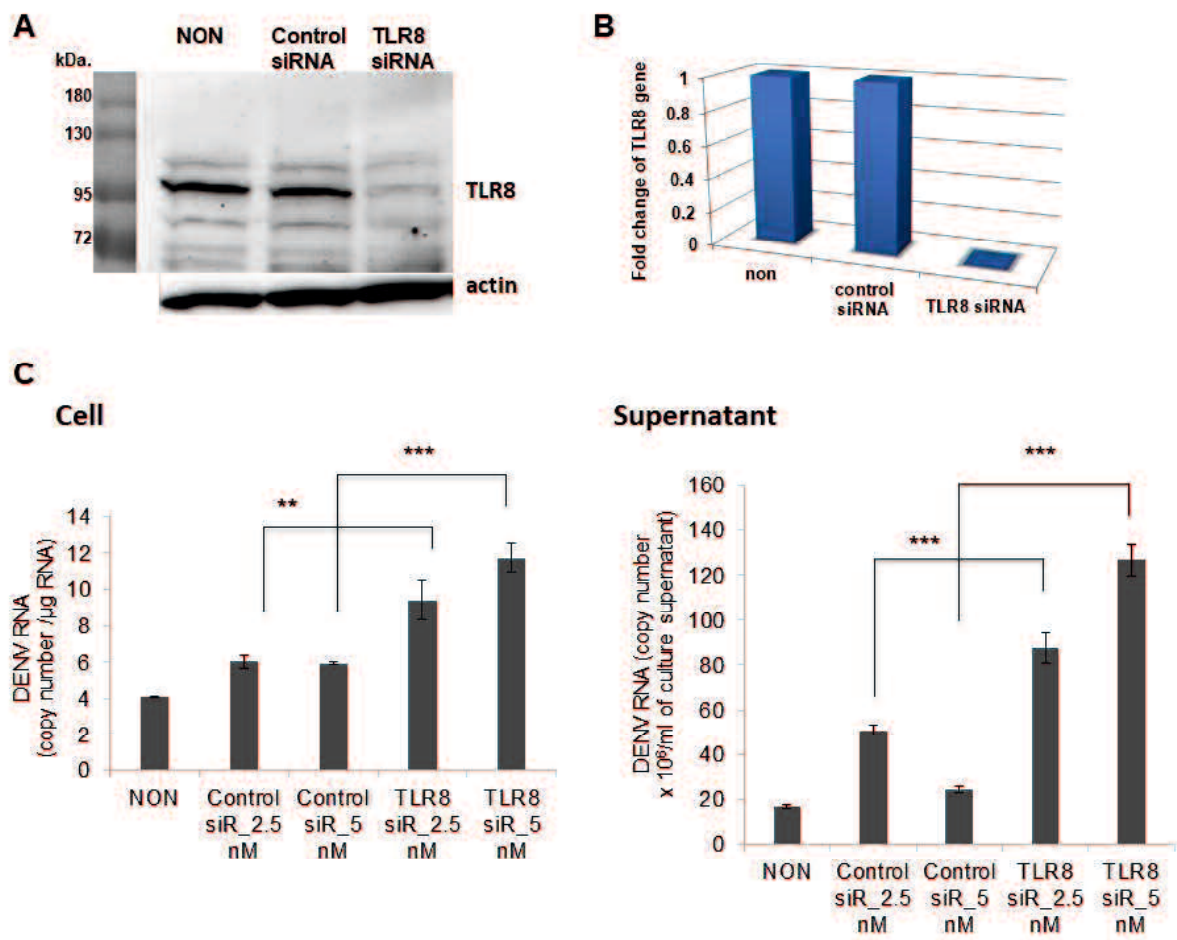


Figure 1.6. Effect of TLR8 in DENV infection.

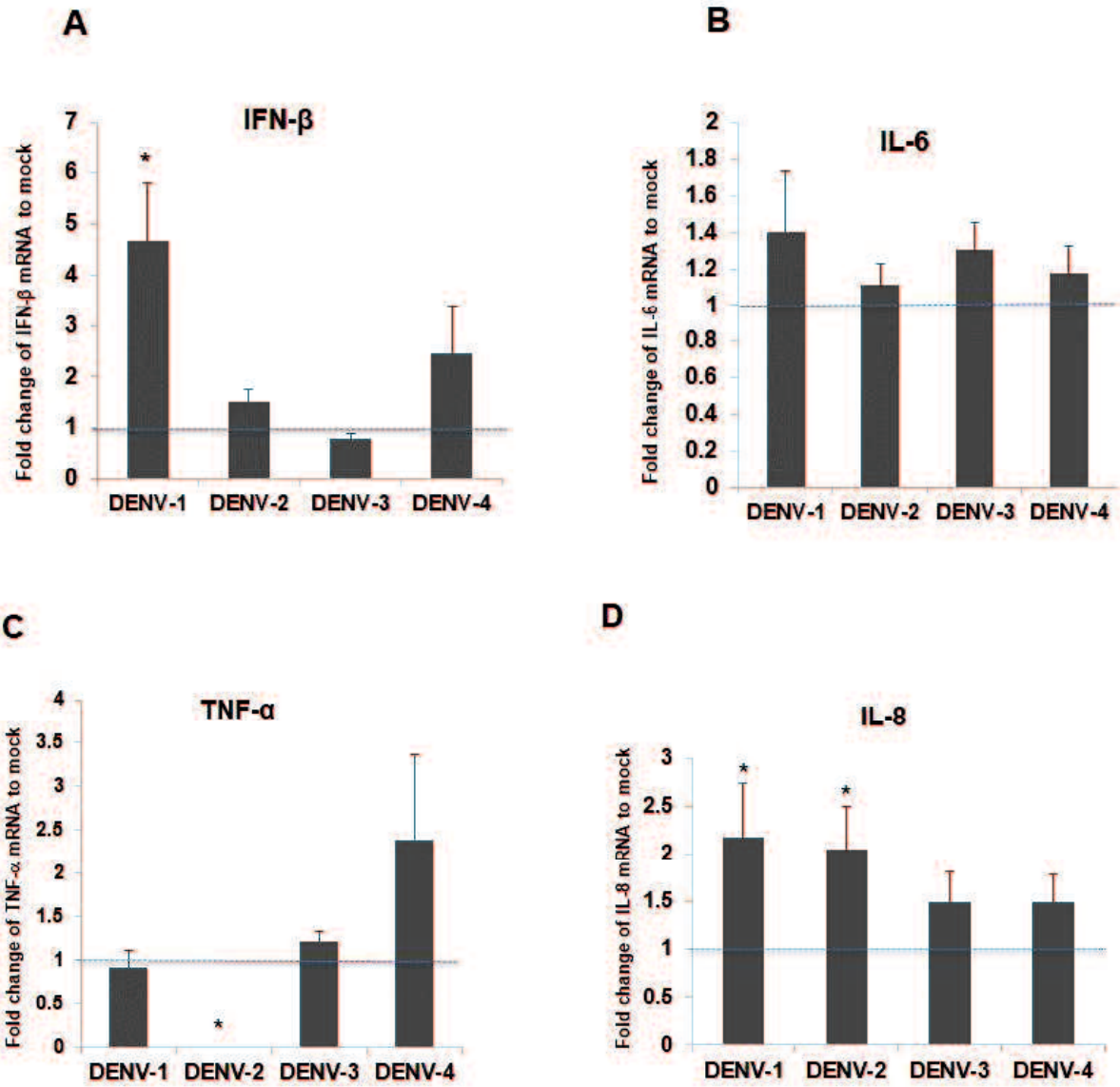


Figure 1.7. mRNA expression levels of (A) *IFN- $\beta$* , (B) *IL-6*, (C) *TNF- $\alpha$* , and (D) *IL-8*.

**Chapter III: Interferon- $\beta$  response is impaired by hepatitis B virus infection in *Tupaia belangeri***

## Abstract

To date, the chimpanzee has been used as the natural infection model for hepatitis B virus (HBV). However, as this model is very costly and difficult to use because of ethical and animal welfare issues, I aimed to establish the tupaia (*Tupaia belangeri*) as a new model for HBV infection and characterized its intrahepatic innate immune response upon HBV infection. First, I compared the propagation of HBV genotypes A2 and C *in vivo* in tupaia hepatocytes. At 8-10 days post infection (dpi), the level of HBV-A2 propagation in the tupaia liver was found to be higher than that of HBV-C. Abnormal architecture of liver cell cords and mitotic figures were also observed at 8 dpi with HBV-A2. Moreover, I found that HBV-A2 established chronic infection in some tupaia. I then aimed to characterize the intrahepatic innate immune response in this model. First, I infected six tupaia with HBV-A2 (strains JP1 and JP4). At 28 dpi, intrahepatic HBV-DNA and serum hepatitis B surface antigens (HBsAg) were detected in all tupaia. The levels of interferon (IFN)- $\beta$  were found to be significantly suppressed in the three tupaia infected with HBV A2\_JP4, while no significant change was observed in the three infected with HBV A2\_JP1. Expression of toll-like receptor (TLR) 1 was suppressed, while that of TLR3 and TLR9 were induced, in HBV A2\_JP1-infected tupaia. Expression of TLR8 was induced in all tupaia. Next, I infected nine tupaia with HBV-A2 (JP1, JP2, and JP4), and characterized the infected animals after 31 weeks. Serum HBsAg levels were detected at 31 weeks post-infection (wpi) and IFN- $\beta$  was found to be significantly suppressed in all tupaia. TLR3 was not induced, except in tupaia #93 and #96. Suppression of TLR9 was observed in all tupaia, except tupaia #93. Also, I investigated the expression levels of cyclic GMP-AMP synthase, which was found to be induced in all tupaia at 28 dpi and in four tupaia at 31 wpi. Additionally, I evaluated the expression levels of sodium-taurocholate cotransporting polypeptide, which was found to be suppressed during chronic HBV infection. Thus, the tupaia

infection model of HBV clearly indicated the suppression of IFN- $\beta$  at 31 wpi, which might have contributed to the establishment of chronic HBV infection.

### **III.1. Introduction**

The innate immune response is considered the first line of immune defense that halts many viral infections (Zuniga et al., 2015). Viral nucleic acids and proteins are recognized by different pattern recognition receptors (PRRs), such as toll-like receptors (TLRs), RIG-I-like receptors, and NOD-like receptors (Kawai and Akira, 2011). TLRs, one of the important components of innate immunity, play a crucial role in sensing invaders and initiating innate immune response, thus limiting the spread of infections and modulating efficient adaptive immune responses (Takeuchi and Akira, 2010). Recently discovered Cyclic GMP-AMP (cGAMP) synthase (cGAS), a cytosolic DNA sensor is an important element in the induction of innate immune response (Civril et al., 2013, Gao et al., 2013). NTCP has been found to be involved in Hepatitis B virus (HBV) infection (Yan et al., 2012).

HBV is major causative agent of chronic hepatitis, liver cirrhosis, and/or hepatocellular carcinoma. HBV, a member of the Hepadnaviridae family, is an enveloped, circular, and partially double-stranded DNA virus (Lee, 1997). More than 248 million people worldwide, i.e., approximately 5% of the world's population, are chronically infected with HBV (Ganem and Prince, 2004, Schweitzer et al., 2015). Based on phylogenetic studies and sequence analyses, HBV strains have been classified into 10 genotypes (A–J) (Lin and Kao, 2015). These different genotypes have not all been characterized, and HBV-induced immunopathogenesis is poorly understood because of the lack of an appropriate animal infection model. Animal infection models are also essential for the development of new drugs and vaccines (Keating and Noble, 2003). Although the role of adaptive immunity in the control of HBV infection is well documented, the effects of innate immunity in this regard are yet to be explored.

So far, chimpanzees have been used as infection models for HBV; however, owing to economic and ethical reasons, it is now difficult to use chimpanzees for experimental infection. Recently, humanized chimeric mice were developed (Mercer et al., 2001), and HBV have been reported

to efficiently infect these mice (Nakagawa et al., 2013). However, the use of mice also possess some disadvantages, including high cost, immunocompromised animal status, and inability to examine chronic infections.

*Tupaia belangeri* belongs to the Tupaiidae family, which comprises four genera and 19 extant species (Tsukiyama-Kohara and Kohara, 2014). The evolutionary characterization of 7S RNA-derived short interspersed elements (SINEs) showed that tupaia possess specific chimeric Tu-type II SINEs, and can be grouped with primates (Kriegs et al., 2007). In addition, genomic analysis has suggested that the *Tupaia* genus is more closely related to humans than to rodents (Fan et al., 2013, Kriegs et al., 2007). *T. belangeri* has been previously reported to be susceptible to HBV (Sanada et al., 2016, Walter et al., 1996) and so, can be developed as an immunocompetent animal infection model. However, the molecular basis of HBV pathogenesis has not been fully characterized in the tupaia model because of the lack of characterization tools (such as specific antibodies, quantitative polymerase chain reaction [qPCR] assays, and cDNAs).

In this study, I investigated the susceptibility of tupaia to several strains of HBV and established a qPCR assay for TLRs, cGAS, and cytokines to characterize the innate immune response against HBV infection in tupaia.

## **III.2. Materials and Methods**

### **III.2.1. Animals**

A total of 21 adult and 10 newborn tupaia were used in this study. Adult tupaia were obtained from the Laboratory Animal Center at the Kunming Institute of Zoology, Chinese Academy of Sciences (Kunming, China). This study was carried out in accordance with both the Guidelines for Animal Experimentation of the Japanese Association for Laboratory Animal Science and the Guide for the Care and Use of Laboratory Animals of the National Institute of Health. All

experimental protocols used in this study were approved by the institutional review boards of the regional ethics committees of the Kagoshima University (VM15051, VM13044).

Animals were housed in separate cages and fed a daily regimen of eggs, fruit, water, and dry mouse food; they were handled as humanely as possible in accordance with the guidelines of the Institutional Animal Care and Use Committee for Laboratory Animals.

### **III.2.2. Viruses**

In this study, I used the virus preparation of HBV genotypes A (A2\_JP1, A2\_JP2, A2\_JP4) and C (C\_JPNAT; accession number: AB246345.1) for infecting tupaia, which was used in a previous study (Sanada et al., 2016). Originally, the virus HBV A2\_JP1 was isolated from chronic patient, and HBV A2\_JP2 and A2\_JP4 virus from acute patients and propagated in chimeric mice with humanized liver. The virus preparations used for infecting tupaia were ensured negative for HCV-RNA and HDV-RNA by PCR.

### **III.2.3. Infection**

Before viral infection, all animals used in this study were confirmed negative for HBV by PCR. Six newborn tupaia were infected with HBV genotype A (A2\_JP4) (#336, #337, #338, #339, #N48, and #N93), while four newborn tupaia were infected with HBV genotype C (#59, #60, #340, and #341). The infection was administered subcutaneously and the dose was adjusted to  $10^6$  copies/tupaia. Tupaia #336, #337, #338, and #339 were sacrificed for sampling at 12, 11, 10, and 8 days post-infection (dpi), respectively. Tupaia #340 and #341 were sacrificed at 10 dpi, whereas tupaia #59 and #60 were sacrificed at 12 dpi. For histological analysis, liver tissues were extracted, fixed with paraformaldehyde, and stained with hematoxylin and eosin.

Fifteen adult (1 year-old) tupaia were inoculated with HBV genotype A (A2\_JP1, A2\_JP2, and A2\_JP4). The infection was administered intraperitoneally and the dose was adjusted to  $10^6-7$  copies/tupaia. Nine adults, including three uninfected controls (#N1, #N2, and #N3) and six HBV (A2\_JP1 and A2\_JP4)-infected ones (#17, #32, #36, #22, #43, and #48) were sacrificed

at 28 dpi. Twelve adults, including three uninfected controls (#N4, #N5, and #N6) and nine HBV (A2\_JP1, A2\_JP2, and A2\_JP4)-infected ones (#84, #85, #92, #93, #86, #94, #88, #96, and #97) were sacrificed at 31 weeks post infection (wpi). Liver tissues were extracted from all sacrificed animals. RNA from liver tissues was isolated using the acid guanidium-phenol chloroform extraction method and purified using an RNeasy Mini Kit (Qiagen, Valencia, CA, USA). Before inoculation as well as at determined time points, blood samples were collected by venipuncture; the levels of serum alanine aminotransferase (ALT), hepatitis B surface antigen (HBsAg), and serum HBV-DNA were estimated.

#### **III.2.4. Measurement of ALT and viral load**

The serum ALT level was determined using a Transnase Nissui kit (Nissui Pharmaceutical Co. Ltd., Tokyo, Japan) and standardized; it was represented in IU/liter. HBV-DNA was isolated from the sera samples by using the SMITEST EX-R&D Kits according to the manufacturer's instructions (Medical & Biological Laboratories Co. LTD., Nagano, Japan). The total DNA was extracted from the liver tissues with a homogenizer, treated with proteinase K in a lysis buffer (0.1 M Tris [pH 7.5], 12.5 mM EDTA, 0.15 M NaCl, 1% SDS, and 10 mg/mL proteinase K), purified using the Qiagen QIAamp DNA extraction kit, and finally eluted in 400  $\mu$ L of deionized water. HBV-DNA quantification was performed using qPCR, based on TaqMan chemistry, using the forward primer HB-166-S21 (5'-CACATCAGGATTCCTAGGACC-3'), the reverse primer HB-344-R20 (5'-AGGTTGGTGAGTGATTGGAG-3'), the Taq-Man probe 6-FAM (5'-CAGAGTCTAGACTCGTGGTGGACTTC-TAMRA-3'), and the TaqMan Universal PCR Master Mix (Applied Biosystems, Foster City, CA, USA).

#### **III.2.5. Measurement of HBsAg**

HBsAg levels in the tupaia serum were measured using the two-step sandwich assay principle with a fully automated chemiluminescent enzyme immunoassay system (Lumipulse G 1200, Fujirebio, Tokyo, Japan) (Shinkai et al., 2013).

### **III.2.6. Gene expression analysis by quantitative reverse transcription-PCR (qRT-PCR)**

One-step qRT-PCR was performed in 96-well microplates using a CFX Connect Real-Time PCR Detection System (Bio-Rad, Hercules, CA, USA). Each reaction was performed in triplicate in a 20  $\mu$ L volume with Brilliant III Ultra-Fast SYBR Green QRT-PCR Master Mix (Agilent Technologies, Santa Clara, CA, USA) according to the manufacturer's instructions. Briefly, the cycling conditions comprised reverse transcription at 50 °C for 10 min, initial denaturation at 95 °C for 3 min, and 40 cycles at 95 °C for 5 s and 60 °C for 10 s for all measurements except that of TLR8, sodium-taurocholate cotransporting polypeptide (NTCP), and TNF- $\alpha$ . The annealing/extension temperature used for TLR8 and NTCP was 55 °C, while that for TNF- $\alpha$  was 65 °C, with a 10-s incubation at each step. The specificity of the PCR was confirmed by melt curve analysis and gel electrophoresis of the amplified product. After each run, a melt curve analysis was performed from 65 °C to 95 °C at a heat increment rate of 0.1 °C/s and continuous fluorescence measurement. Each experiment included a no-template control and a standard curve for each gene. Standards were generated from pre-quantified plasmids containing the sequence of the target gene. Tupaia GAPDH or actin was used as endogenous controls for normalizing the results. Primers used for the amplification of the target and reference genes and the lengths of amplified products are shown in Table 2.1.

### **III.2.7. Statistical analysis**

To analyze the statistical significance of differences of HBV-A2 and HBV-C viral replication in tupaia and differences in gene expression of the control and virus-infected animals, unpaired t-tests were performed using the GraphPad software. P values < 0.05 were considered significant. All tests performed were two-sided.

### **III.3. Results**

#### **III.3.1. Infection of tupaia with HBV genotypes A2 and C**

Newborn tupaia were infected with HBV genotypes A (A2\_JP4) and C (C\_JPNAT) and characterized at 8–12 dpi (Figure 2.1). Intrahepatic HBV-A2 replication was significantly higher than that of HBV-C. In HBV-A2 infections I could detect 196.3 (#339), 145.1 (#338), 7.7 (#337), and 481.9 (#336) copies of HBV-DNA at 8–12 dpi, whereas in HBV-C infections I could detect 4.3 (#340) and 13.6 (#341) copies of HBV-DNA at 10 dpi in per microgram of total DNA, respectively. No HBV-DNA was detected in #59 and #60 at 12 dpi (Figure 2.1A). Upon performing histological analysis of liver tissues isolated from HBV A2\_JP4-infected tupaia, I observed abnormal architecture of liver cell cords and mitotic figures at 8 dpi (Figure 2.1B). These results indicated that HBV-A2 could grow in tupaia liver cells more efficiently than HBV-C.

#### **III.3.2. Chronic infection by HBV genotype A2 in tupaia**

I infected newborn tupaia with HBV A2\_JP4 and monitored the serum HBV-DNA and ALT levels (Figure 2.2). In tupaia #N48 and #N93, HBV-DNA was detected from 27 to 43 wpi (Figure 2.2A) and 12–35 wpi (Figure 2.2B), respectively. These results indicated that HBV-A2 could establish chronic infection. With these results, I addressed the effects of HBV-A2 on innate immune response in tupaia.

#### **III.3.3. Effect of HBV genotype A2 in tupaia**

I infected six adult tupaia with HBV genotype A (A2\_JP1 and A2\_JP4), which was originally isolated from hepatitis B patients and propagated in chimeric mice with humanized liver. At 28 dpi, the infected tupaia were sacrificed and intrahepatic HBV-DNA levels and serum ALT levels were estimated (Figure 2.3A, B). HBV-DNA and HBsAg were detected in the liver tissues from all six tupaia (Figure 2.3B, 3C). The level of HBV-DNA was higher in HBV A2\_JP1-infected tupaia (#17, #32, and #36) than in HBV A2\_JP4-infected ones (#22, #43,

and #48), while HBsAg level was higher in HBV A2\_JP4-infected tupaia than in HBV A2\_JP1-infected ones.

### **III.3.4. Expression levels of cytokines and TLRs in liver tissues of HBV-A2-infected tupaia at 28 dpi**

I isolated liver RNA from six HBV-A2-infected tupaia and three uninfected control ones at 28 dpi and measured the levels of cytokine mRNAs (Figure 2.4) and TLR1–9 mRNAs (Figure 2.5). Significant suppression of interferon (IFN)- $\beta$  was observed in tupaia #22, #43, and #48 (A2\_JP4-infected). In tupaia infected with HBV A2\_JP1, no significant change was observed in the level of IFN- $\beta$  (Figure 2.4A), but TNF- $\alpha$  expression was found to be significantly upregulated (Figure 2.4B). At 28 dpi, the expression of IL-6 was significantly increased in tupaia #36, while it was significantly suppressed in tupaia #43 (Figure 2.4C).

Expression of TLR1 was significantly suppressed in HBV A2\_JP4-infected tupaia (#22, #43, #48), and expression of TLR3 and 9 was significantly increased in HBV A2\_JP1-infected tupaia (#17, #32, and #36) (Figure 2.5A, C, and I). A significant increase in TLR8 expression was found in all HBV-A2-infected tupaia (Figure 2.5H).

### **III.3.5. Expression levels of cytokines and TLRs in liver tissues of tupaia chronically infected with HBV-A2 at 31 wpi**

To analyze the immune response in the chronic phase, I infected nine adult tupaia with HBV genotype A (A2\_JP1, A2\_JP2, and A2\_JP4). At 31 wpi, the animals were sacrificed and serum ALT and HBsAg levels were measured (Figure 2.6). HBsAg was detected in all the animals (Figure 2.6B).

I isolated the liver RNA from nine HBV-A2-infected tupaia and three uninfected control tupaia at 31 wpi, and measured the levels of cytokine mRNAs (Figure 2.7) and TLR1–9 mRNAs (Figure 2.8). In all tupaia, IFN- $\beta$  was found to be significantly suppressed (Figure 2.7A). No significant change was observed in the level of TNF- $\alpha$  (Figure 2.7B). Significant

increase in the levels of IL-6 was observed in tupaia #93 (Figure 2.7C). TLR3 was found to be significantly suppressed in tupaia #85, #86, #94, and #97 (Figure 2.8C). Suppression of TLR3 was observed in tupaia #84, #92, and #88, while an increase was observed in tupaia #96 (Figure 2.8C), although these changes were not statistically significant. Expression of TLR9 was suppressed in all tupaia except tupaia #93 (Figure 2.8I).

### **III.3.6. Expression of cGAS in the liver tissues of HBV-A2-infected tupaia**

I measured cGAS mRNA expression in liver tissues of HBV-A2-infected tupaia at 28 dpi and at 31 wpi. At 28 dpi, cGAS expression was found to be significantly upregulated in all tupaia (Figure 2.9A). The highest level of intrahepatic cGAS mRNA was observed in tupaia #32, which showed the highest level of intrahepatic HBV-DNA (Figure 2.9A and Figure 2.3B). At 31 wpi, significant upregulation of cGAS was only observed in four tupaia (#85, #86, #93, and #94) (Figure 2.9B).

### **III.3.7. Changes in the expression of NTCP in the liver tissues of HBV-A2-infected tupaia**

In this study, I investigated the association of NTCP in the liver of HBV-A2-infected tupaia at 28 dpi and 31 wpi. At 28 dpi, NTCP expression was found to be significantly suppressed in three tupaia (#17, #36, and #48) (Figure 2.10A). The intrahepatic NTCP and HBV-DNA levels were found to be highest in tupaia #32 (Figure 2.10A and Figure 2.3B). At 31 wpi, overall suppression of NTCP was observed (Figure 2.10B), and NTCP expression was significantly suppressed in seven tupaia (#84, #92, #93, #86, #94, #88, and #96) (Figure 2.10B).

## **III.4. Discussion**

The mechanism of immune response against HBV is still poorly understood due to lack of suitable small animal models. Due to the narrow host range of HBV that infects humans and chimpanzees, the closely related duck hepatitis B virus provides a useful model for hepadnavirus study and duck model of duck hepatitis B virus contributes towards the

understanding of HBV biology (Seeger and Mason, 2015). In this study, I investigated the suitability of tupaia as a new animal model for studying the immune response against HBV infection. Importantly, I found that tupaia were susceptible to HBV infection and upon HBV infection, significant suppression of IFN- $\beta$  was induced in all tupaia at 31 wpi. HBV develops strategies to disrupt IFN- $\beta$  induction through several mechanisms; for example, inhibition of IFN- $\beta$  induction by disrupting the interaction between I $\kappa$ B kinase- $\epsilon$  and the DEAD box RNA helicase by HBV polymerase (Wang and Ryu, 2010). Furthermore, HBV X protein could impair IFN- $\beta$  promoter activation (Jiang and Tang, 2010). Since the production of IFN- $\beta$  through TLR3-mediated signaling is one of the important mechanisms to inhibit intrahepatic HBV replication, the suppression of IFN- $\beta$  might contribute to the establishment of chronic HBV infection (Zhang and Lu, 2015). A significant reduction in hepatic TLR3 mRNAs has been reported in chronic HBV patients (Huang et al., 2013). A similar reduction was also observed in tupaia #22, #43, #48, #84, #85, #92, #86, #88, #94, and #97, and they showed a significant suppression of IFN- $\beta$  as well. In hepatic nonparenchymal cells, IFN- $\beta$  is known to function as a major antiviral factor in response to TLR3 (Wu et al., 2007). At 28 dpi, I found the level of IFN- $\beta$  to be significantly decreased in HBV A2\_JP4-infected tupaia (#22, #43, and #48); this result was consistent with the low level of TLR3. TLR3 was found to be significantly induced in HBV A2\_JP1-infected tupaia (#17, #32, and #36), but IFN- $\beta$  was not significantly induced. In addition, HBV has also been reported to inhibit downstream signals of TLR3, including TIR-domain-containing adapter-inducing interferon- $\beta$ , TNF receptor associated factor, interferon regulatory factor 3 (IRF-3), and IFN-stimulated response element (Zhang and Lu, 2015).

In tupaia #17, #32, #36, and #93, TNF- $\alpha$  expression was found to be significantly increased and TLR9 was found to be induced. TNF- $\alpha$  is known to contribute to the suppression of HBV replication (Watashi et al., 2013, Xu et al., 2011), and to inhibit TLR9-induced HBV clearance

(Chyuan et al., 2015). Therefore, TNF- $\alpha$ -induced clearance of HBV might be impaired by an unknown mechanism in chronically infected hepatocytes. HBsAg, hepatitis B e antigen, or HBV virions have been reported to suppress TLR-induced antiviral activity in hepatic cells by suppressing the activation of IRF-3, nuclear factor kappa B, and extracellular signal-regulated kinase 1/2 (Wu et al., 2009). Consistent with this observation, I found that the TLR response in tupaia #97 was mostly suppressed, and this resulted in the highest levels of HBsAg in this group at 31 wpi. Induction of TLR3, TLR4, TLR5, TLR7, and TLR9 by specific ligands has been found to inhibit HBV replication in the liver of HBV-transgenic mice (Isogawa et al., 2005). In our study, I found that TLR9 mRNA was suppressed in the liver of HBV-infected tupaia (#22, #43, #48, #84, #85, #92, #86, #94, #88, #96, and #97), and this was found to be consistent with previous a report (Huang et al., 2014). At high titers of HBV, it was observed that HBsAg induced the suppression of TLR9 (Shi et al., 2012), which was also observed in HBV A2\_JP4-infected tupaia (#22, #43, and #48).

cGAS could serve as PRR for sensing cytosolic DNA and induces type I interferons through the production of cGAMP, which binds to and activates the adaptor protein stimulator of interferon genes (STING) (Sun et al., 2013). Inhibition of HBV replication was observed by the activation of the cGAS-STING pathway both *in vitro* and *in vivo* (He et al., 2016). In this study, significant upregulation of cGAS was observed in the livers of all HBV-infected tupaia at 28 dpi and only four tupaia (#85, #86, #93, and #94) showed significant induction of cGAS at 31 wpi, but downstream IFN- $\beta$  production was not induced, which might be due to the interference of STING-mediated IFN- $\beta$  production by HBV viral protein (Liu et al., 2015).

NTCP is known as a receptor for HBV infection (Yan et al., 2012) rather than an immune factor, whereas NTCP plays an important role as an immune regulator in HCV infection (Verrier et al., 2016). In this study, I observed the overall suppression of NTCP expression in

the chronic phase of infection, which indicated that the host antiviral immune response modulated viral infection through undefined mechanisms.

In conclusion, I characterized the innate immune response of tupaia against HBV infection. Though further investigations are required to unravel the precise mechanism of the HBV-activated signaling of TLRs, cGAS, and downstream cytokines, the results of this study should contribute towards the development of the tupaia model to clarify the mechanism for the establishment of chronic HBV infection. The tupaia infection model should be a powerful tool to study the HBV infection.

**Table 2.1. Quantitative reverse transcription-polymerase chain reaction primers sequences**

Gene	Primer sequences (5'-3') Forward (F), Reverse (R)	GenBank Accession number	Product length (bp)
tGAPDH	F: AATTTGGCTACAGCAACAGG R: ATTGATGGTTCGTGACAAGG	KC215182	234
tActin	F: GAGCATCCCTAGAGTTCTGCAA R: TCCTGTAACAATGCGTCTCACA	AF110103	102
tTLR1	F: TGCTGACTGTGACCATGACC R: GCAAGTTCCTTGCTCTGCG	KX438361	105
tTLR2	F: AGCTGCTGTTTTACGCTT R: AGGTA AAACTTGGGGATGTG	KX438362	160
tTLR3	F: AGCCTTCAACGACTGATGCT R: GTTGAGGACGTGGAGGTGAT	KX438363	264
tTLR4	F: TACAGAAGCTGGTGGCTGTG R: CTCCAGGTTGGGCAGGTTAG	KX438364	152
tTLR5	F: GCTGGTCAGTGGACATCACA R: CCAGGCCAGCAAATGTGTTC	KX438365	147
tTLR6	F: GTGGAGGACTGGCCTGATTC R: GATGCAGAGGAGGGTCATGG	KX438366	168
tTLR7	F: AGATGTCCCCACTGTTTTGC R: TAACAACGAGGGCAGTTTCC	KX438367	141
tTLR8	F: AAACCTCTCTAGCACTTC R: CAAGTGTTCCTAAGTAGTCC	KX438368	152
tTLR9	F: TATAACTGCATCGCGCAGAC R: CGGCTGTGGATATTGTTGTG	KX438369	257
tIFN- $\beta$	F: GCAGCAGTTTGGCGTGTAAG R: TTCTGGA ACTGCTGTGGTTCG	KX438370	121
tIL-6	F: ATACCAGAACCCACCTCCAC R: GTGCAACCCTGCACTTGTA A	KX438371	115
tTNF- $\alpha$	F: GCCTAGTCAACCCTCTGACC R: CCCTTGTTTTGGGGGTTTGC	KX438372	100
tNTCP	F: TGTGGGCAAGAGCATCATGT R: CACTGTGCATTGAGGCGAAA	JQ608471	123
tcGAS	F: ACGCAAAGGAAGGAAGTGGT R: TTAAACAATCTTTCCTGCAACA	LC259206	145

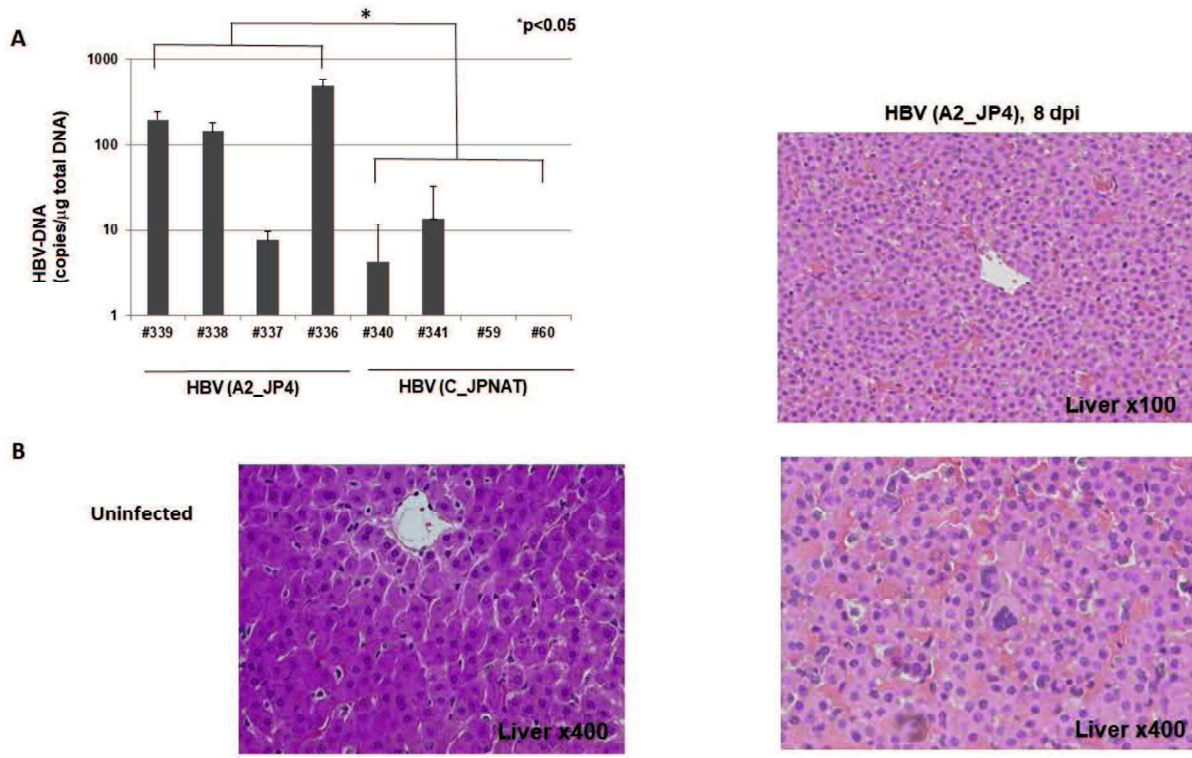


Figure 2.1. HBV genotypes A2 and C infections.

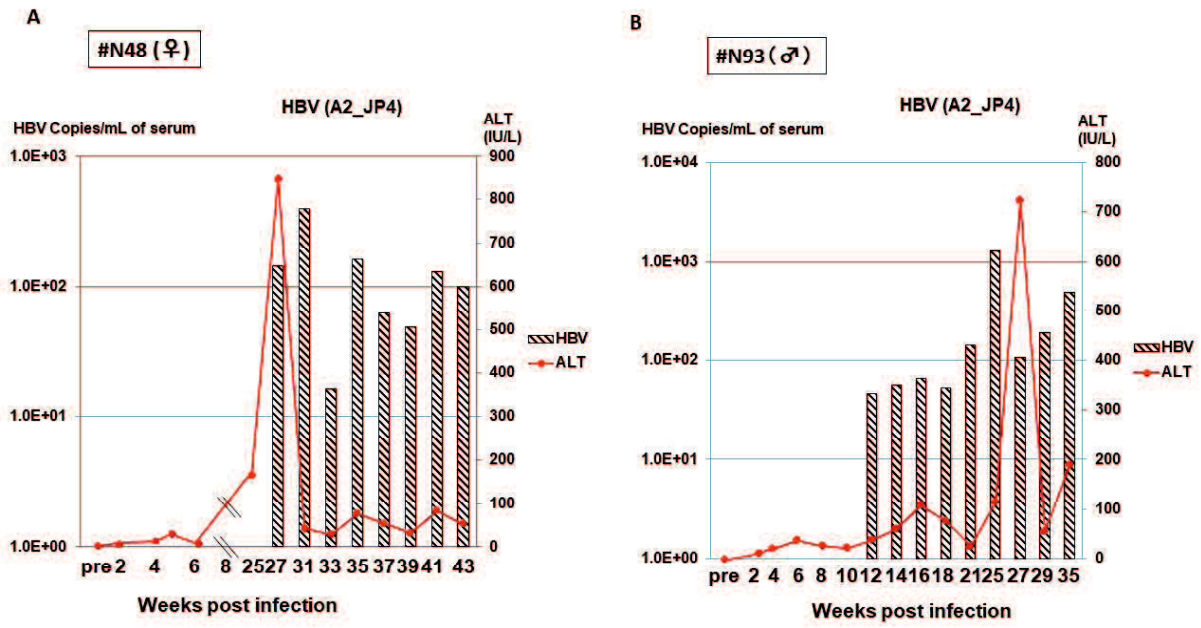


Figure 2.2. HBV-A2 infection in newborn tupaia #N48 and #N93.

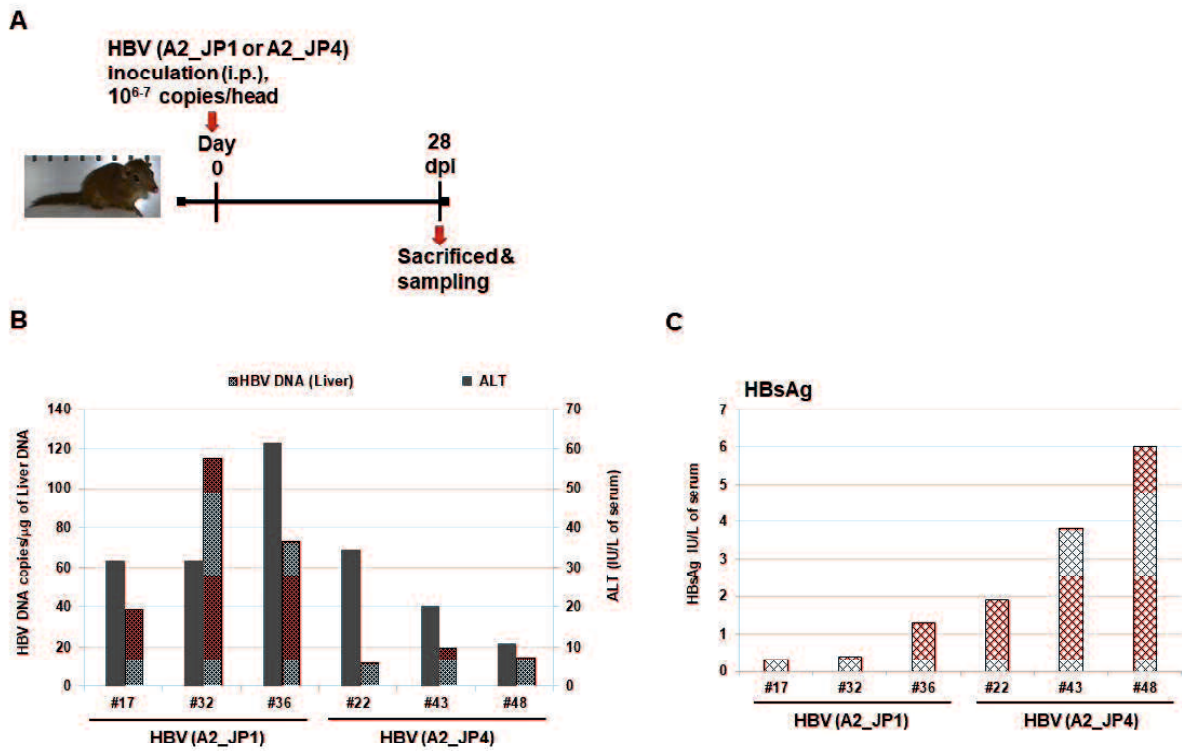


Figure 2.3. HBV-A2 infection in adult tupaia.

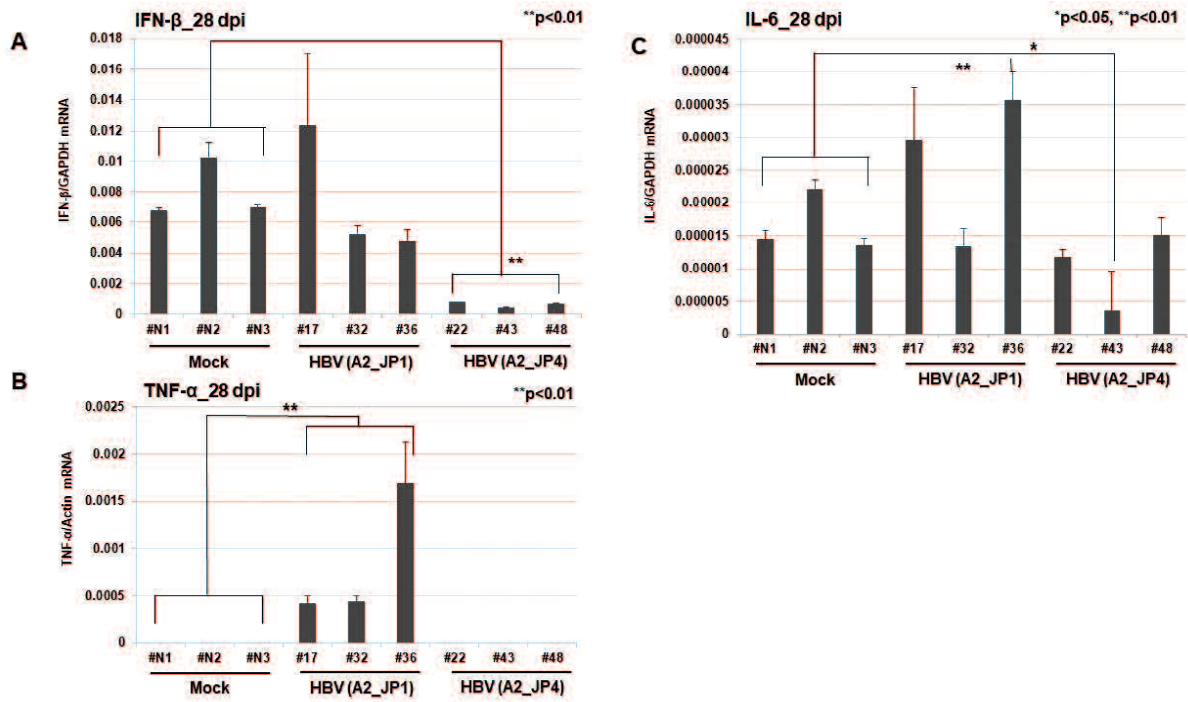
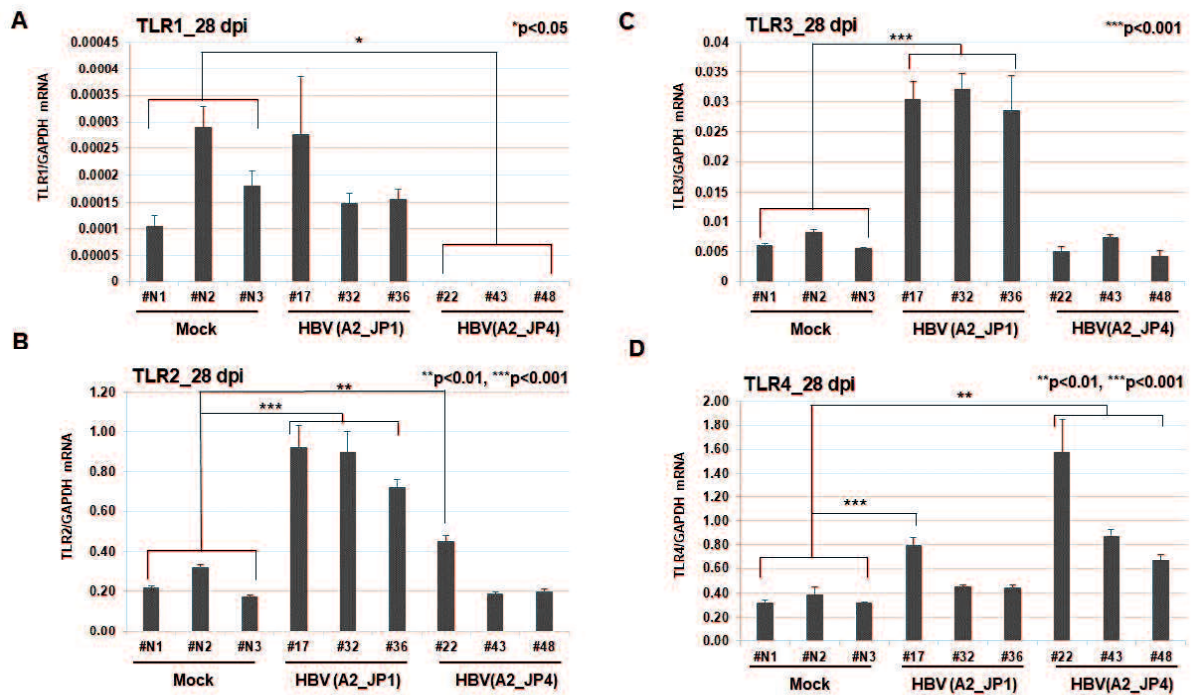


Figure 2.4. Changes in the expression of cytokine levels in HBV-A2-infected tupaia at 28 days post infection.



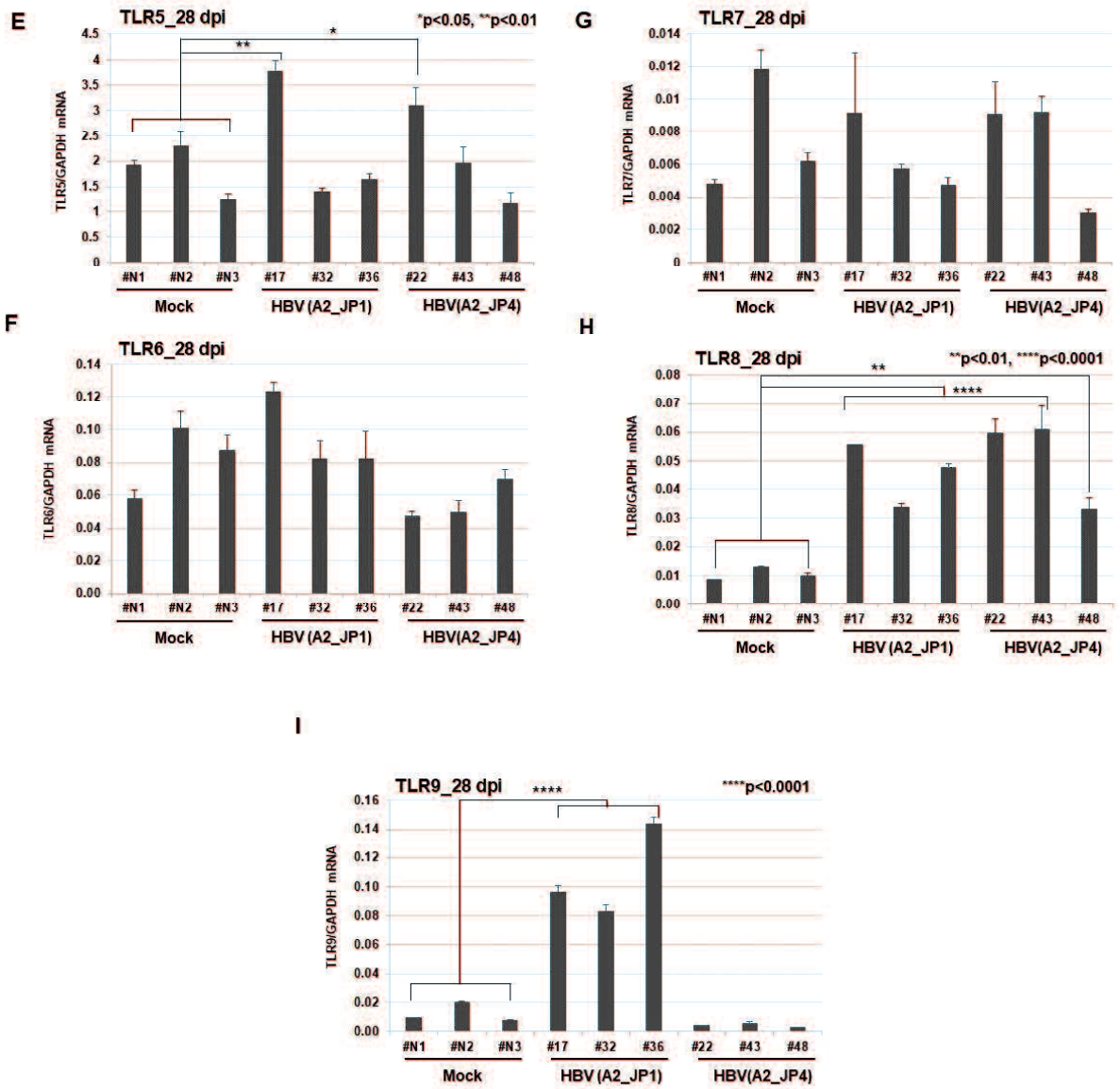


Figure 2.5. Changes in the expression of toll-like receptor mRNAs in HBV-A2-infected tupaias at 28 dpi.

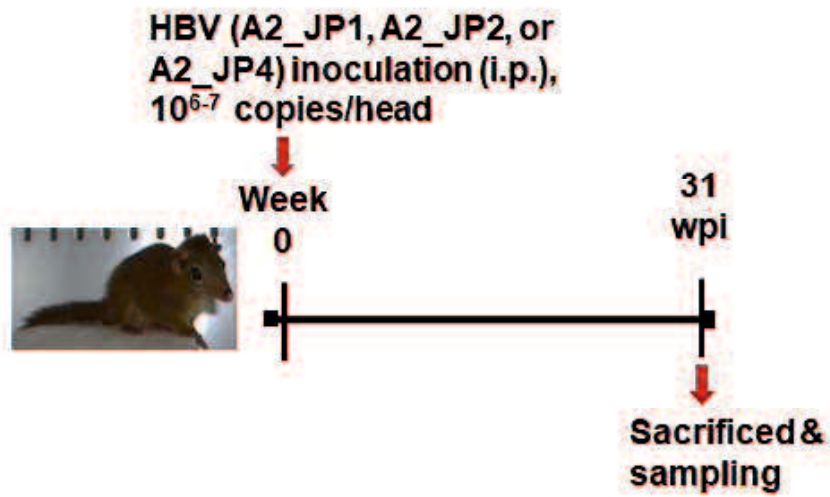
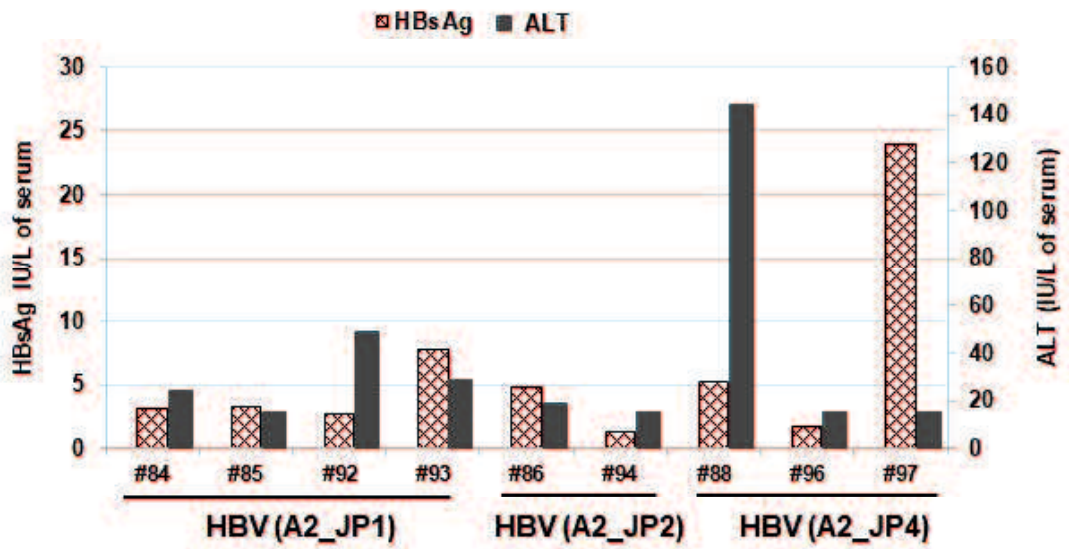
**A****B**

Figure 2.6. HBV-A2 chronic infections in adult tupaia.

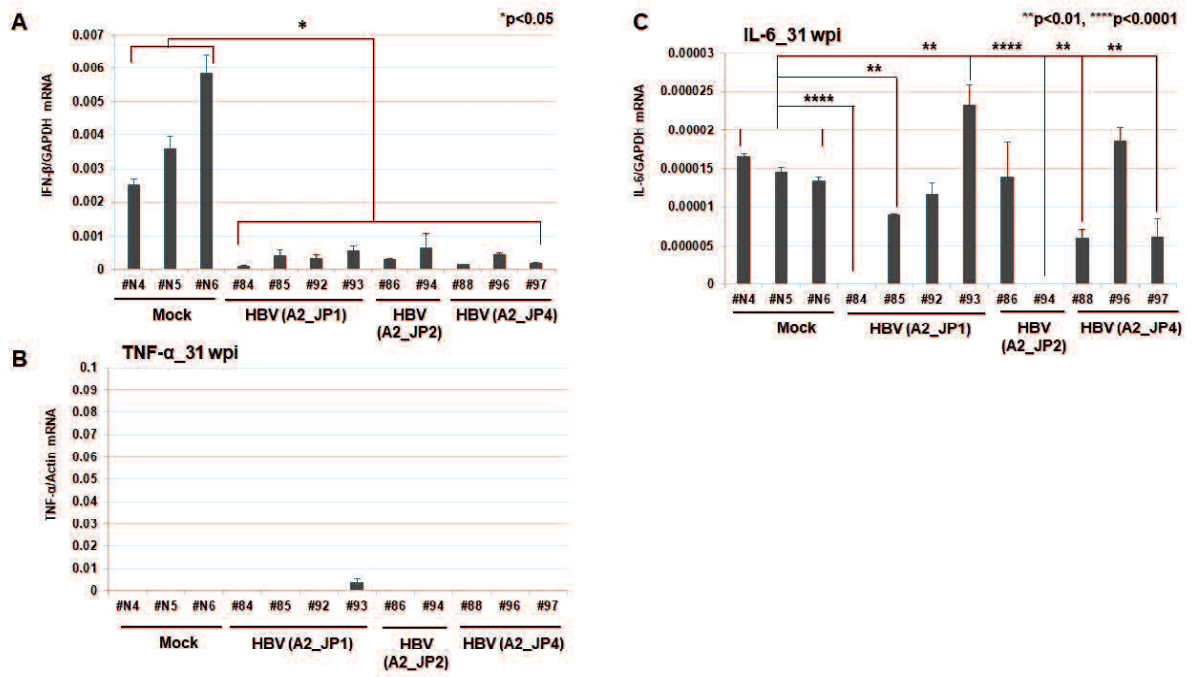
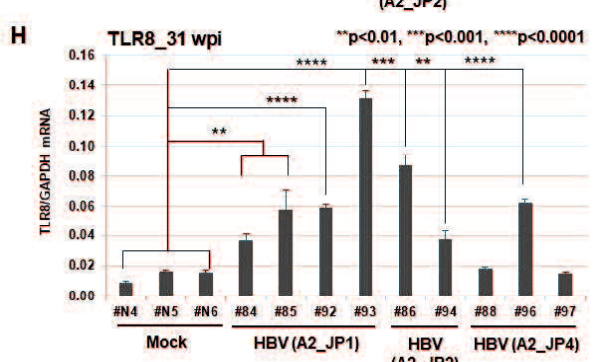
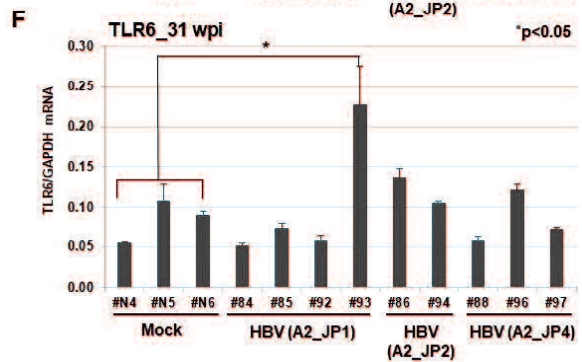
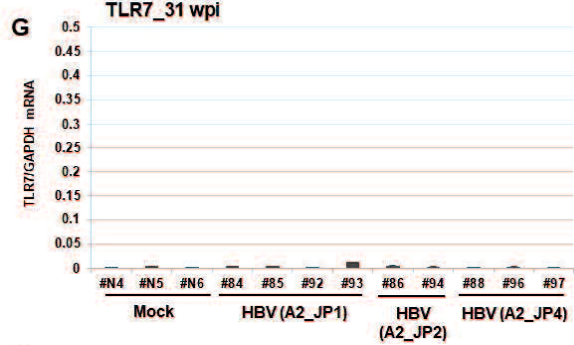
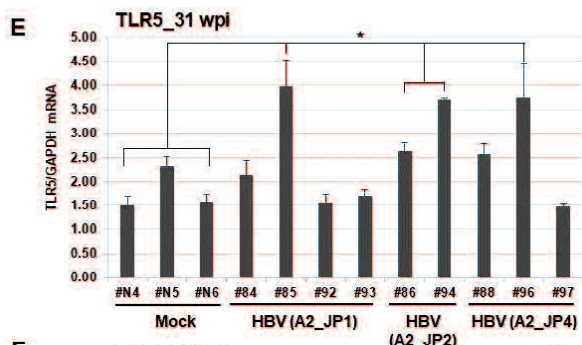
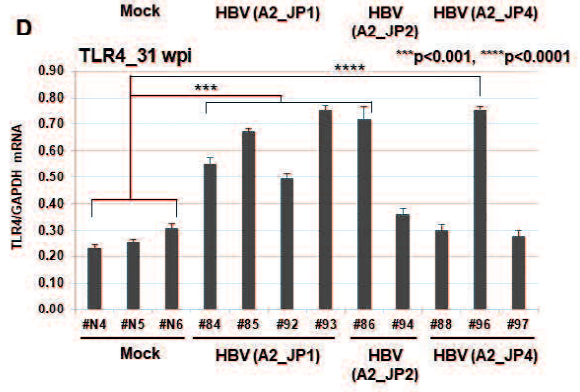
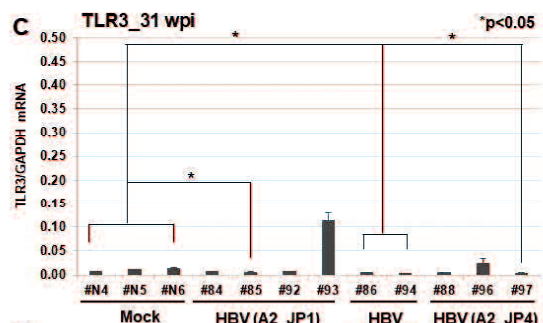
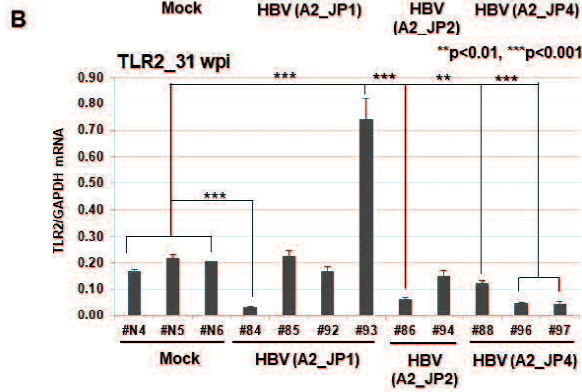
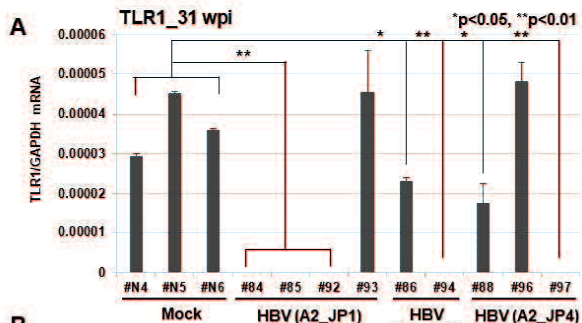


Figure 2.7. Changes in the expression of cytokine mRNAs in HBV-A2-infected tupaia at 31 weeks post infection.



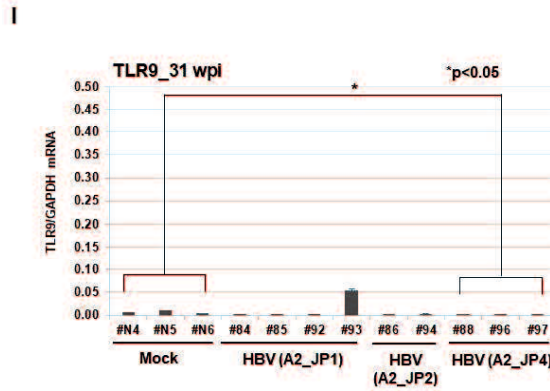


Figure 2.8. Changes in the expression of toll-like receptor mRNAs in HBV-A2-infected tupaia at 31 wpi.

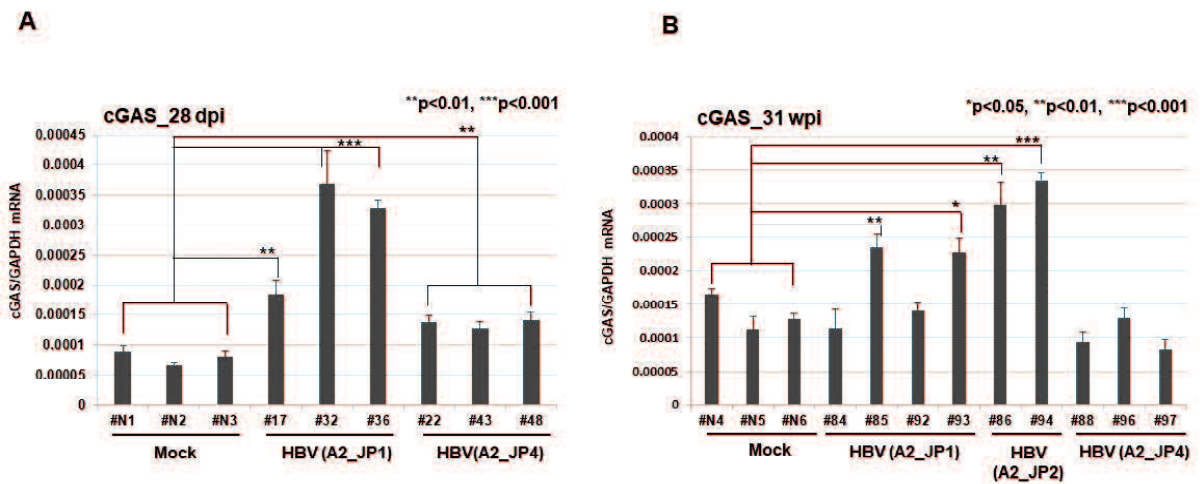


Figure 2.9. Changes in the level of cGAS mRNAs in hepatitis B virus (HBV)-A2-infected tupaia liver tissues.

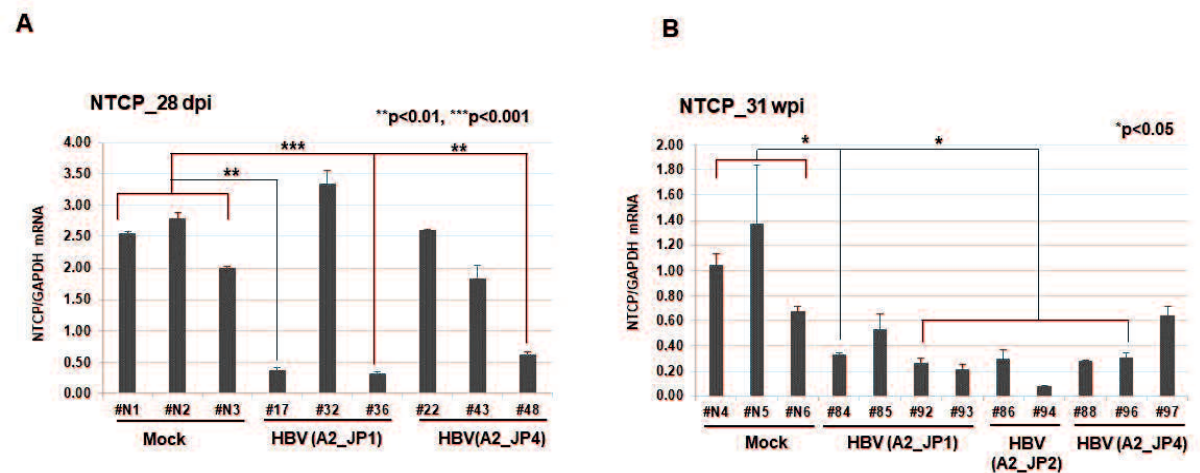


Figure 2.10. Changes in the level of NTCP mRNAs in hepatitis B virus (HBV)-A2-infected tupaia liver tissues.

**Chapter IV: Oxidative stress and immune responses during hepatitis C virus infection  
in *Tupaia belangeri***

## Abstract

Hepatitis C virus (HCV) is a leading cause of chronic liver disease, cirrhosis, and hepatocellular carcinoma. To address the molecular basis of HCV pathogenesis using tupaia (*Tupaia belangeri*), I characterized host responses upon HCV infection. Adult tupaia were infected with HCV genotypes 1a, 1b, 2a, or 4a. Viral RNA, alanine aminotransferase, anti-HCV core and anti-nonstructural protein NS3 antibody titers, reactive oxygen species (ROS), and anti-3 $\beta$ -hydroxysterol- $\Delta$ 24reductase (DHCR24) antibody levels were measured at 2-week intervals from 0 to 41 weeks postinfection. All HCV genotypes established infections and showed intermittent HCV propagation. Moreover, all tupaia produced anti-core and anti-NS3 antibodies. ROS levels in sera and livers were significantly increased, resulting in induction of DHCR24 antibody production. Similarly, lymphocytic infiltration, disturbance of hepatic cords, and initiation of fibrosis were observed in livers from HCV-infected tupaia. Intrahepatic levels of Toll-like receptors 3, 7, and 8 were significantly increased in all HCV-infected tupaia. However, interferon- $\beta$  was only significantly upregulated in HCV1a- and HCV2a-infected tupaia, accompanied by downregulation of sodium taurocholate cotransporting polypeptide. Thus, our findings showed that humoral and innate immune responses to HCV infection, ROS induction, and subsequent increases in DHCR24 auto-antibody production occurred in our tupaia model, providing novel insights into understanding HCV pathogenesis.

#### **IV.1. Introduction**

Hepatitis C virus (HCV) is a major public health problem that infects approximately 130–170 million people worldwide (Lavanchy, 2009; Mohd Hanafiah et al. 2013). HCV causes chronic hepatitis and is a major cause of liver cirrhosis and hepatocellular carcinoma (HCC) (Lavanchy, 2009). The first line of immune defence against HCV relies on cell-intrinsic innate immunity within hepatocytes. The HCV genome is a single-stranded, positive-sense RNA genome. During viral replication, HCV is sensed as non-self by pattern recognition receptors (PRRs) in the host cell, which identify and bind to pathogen-associated molecular patterns (PAMPs) within viral products, leading to activation of innate and adaptive immune responses (Horner & Gale, 2013). Both effective innate and adaptive immune responses are involved in the control of HCV infections (Thimme et al. 2012); however, the role of the humoral immune system in HCV clearance is still unclear (Cashman et al. 2014).

Toll-like receptors (TLRs), an important component of innate immunity, play crucial roles in sensing invaders and initiating innate immune responses, thereby limiting the spreading of infections and modulating adaptive immune responses (Takeuchi & Akira, 2010). Sodium taurocholate cotransporting polypeptide (NTCP), a bile acid transporter expressed at the hepatocyte basolateral membrane (Claro da Silva et al. 2013), can act as a regulator of antiviral immunity in HCV infection (Verrier et al. 2016). HCV infection can induce reactive oxygen species (ROS) production (Korenaga et al. 2005; Tsukiyama-Kohara, 2012) and oxidative stress can lead to the formation of 8-hydroxydeoxyguanosine (8-OHdG), an indicator of oxidative DNA damage (Valavanidis et al. 2009). 3 $\beta$ -Hydroxysterol- $\Delta$ 24reductase (DHCR24), a cholesterol biosynthetic enzyme (Waterham et al. 2001), is an essential host factor that plays a significant role in HCV replication (Takano et al. 2011). Moreover, anti-DHCR24 auto-antibody levels are increased during the progression of HCV infection (Ezzikouri et al. 2015). Indeed, the detection rate of HCC by anti-DHCR24 antibodies is higher (70.6%) than that of

the standard HCC markers, alpha-fetoprotein (54.8%) or protein induced by vitamin K absence or antagonist-II (42.5%) (Ezzikouri et al. 2015).

Recently, HCV can be completely cured by newly approved drugs, direct-acting antivirals (DAAs) (Barth, 2015; Abdelwahab, 2016). However, persistent hepatic inflammation, cirrhosis, and HCC have been reported in patients following viral clearance (Chinchilla-Lopez et al. 2017). To solve these issues and develop an efficient vaccine against HCV, animal models are essential. Lack of small animal models is a great obstacle in the field of HCV research. To date, chimpanzees have been used as infection models for HCV. However, high costs and ethical concerns have restricted the use of chimpanzees in experimental infections. Recently, humanized chimeric mice (Mercer et al. 2001) and genetically humanized mice (Dorner et al. 2011) have been developed for use in HCV infection models (Takano et al. 2011; Mercer et al. 2001). However, the use of mice has some disadvantages, including high cost, immunocompromised animal status, donor-to-donor variability, and inability to examine chronic infections. *Tupaia belangeri* belongs to the Tupaiidae family, which contains four genera and 19 extant species (Tsukiyama-Kohara & Kohara, 2014). The evolutionary characterization of 7S RNA-derived short interspersed elements (SINEs) has shown that tupaia possess specific, chimeric Tu type II SINEs and can be clustered with primates (Kriegs et al. 2007). Thus, genomic analysis suggested that tupaia are more closely related to humans than to rodents (Kriegs et al. 2007; Fan et al. 2013). Tupaia have been reported to be susceptible to several hepatotropic viruses that also infect humans, including hepatitis B virus (Yang et al. 2015; Sanada et al. 2016), HCV (Xu et al. 2007; Amako et al. 2010), and hepatitis E virus (Yu et al. 2016), and can be developed as an immunocompetent animal infection model. However, the molecular basis of HCV pathogenesis has not been fully characterized in the tupaia model due to a lack of characterization tools (e.g., specific antibodies, quantitative polymerase chain reaction [qPCR] assays, and cDNAs).

Therefore, in this study, I evaluated the susceptibility of tupaia to several viral strains of HCV and characterized the effects of HCV infection on ROS generation and its association with anti-DHCR24 antibody levels. I also characterized humoral immune responses to viral proteins and established a qPCR assay to evaluate TLR, NTCP, and cytokine expression to characterize the innate immune response during HCV infection, which may provide significant insight into HCV pathogenesis.

## **IV.2. Materials and Methods**

### **IV.2.1. Animals**

The tupaia used in this study were obtained from the Laboratory Animal Center at the Kunming Institute of Zoology, Chinese Academy of Sciences (Kunming, China). This study was carried out following the Guidelines for Animal Experimentation of the Japanese Association for Laboratory Animal Science and the Guide for the Care and Use of Laboratory Animals of the National Institutes of Health. All experimental protocols were approved by the institutional review boards of the regional ethics committees of Kagoshima University (VM15051 and VM13044).

Animals were individually housed in cages and fed a daily regimen of eggs, fruit, water, and dry mouse food. The animals were humanely handled in accordance with the Institutional Animal Care and Use Committee for Laboratory Animals.

### **IV.2.2. Virus infection**

All animals were found to be negative for HCV by quantitative real-time-PCR before viral infection. Four adult tupaia (#21, #22, #23, and #24) were infected with HCV (genotypes 1a, 1b, 4a, and 2a [JFH1]), as described previously<sup>26</sup>, and three normal tupaia (#3, #5, and #38), which were not infected with HCV, were used as controls. Briefly, tupaia (#21, #22, #23, and #24) were infected at 12 months of age under anaesthesia induced by intramuscular injection

of ketamine hydrochloride and atropine at 50 mg/kg body weight prior to virus inoculation and bleeding. Inocula derived from chimeric mice were introduced twice intraperitoneally at  $1.5 \times 10^8$  copies/mL for genotype 1a, 107 copies/mL for genotypes 1b and 4a, and  $1.2 \times 10^8$  copies/mL for genotype 2a (JFH1) for tupaia #21, #22, #23, and #24, respectively.

The infected animals were bled (0.5 mL) biweekly, and sera were separated, aliquoted, and immediately used or stored at  $-80^\circ\text{C}$  for further analysis. At 41 wpi, infected and control animals were sacrificed, and liver tissues were extracted. RNA from liver tissues was isolated using the acid guanidinium-phenol-chloroform extraction method and purified with an RNeasy Mini Kit (Qiagen, Valencia, CA, USA). For histological analysis, liver tissues were characterized by haematoxylin and eosin (H&E) or silver staining, as described previously (Sekiguchi et al. 2012).

#### **IV.2.3. Measurement of ALT levels and viral load**

Serum ALT level was determined using a Transnase Nissui kit (Nissui Pharmaceutical Co. Ltd., Tokyo, Japan); data were standardized and represented in IU/L. RNA was isolated from sera (50  $\mu\text{L}$ ) using SepaGene RV-R (Sanko Junyaku Co., Ltd., Tokyo, Japan). HCV RNA levels were quantified using qRT-PCR, as reported previously (Takeuchi et al. 1999).

#### **IV.2.4. Gaussia luciferase immunoprecipitation system (GLIPS) assays**

To evaluate antibody levels, GLIPS assays were performed as reported previously<sup>49</sup>, with some modifications, using SureBeads Protein G magnetic beads (Bio-Rad, Hercules, CA, USA). Briefly, the HCV core gene (1b, nucleotides 341–759), HCV NS3 gene (1b, nucleotides 3991–4753), and tupaia DHCR24 gene (nucleotides 31–1599) were subcloned into the Gaussia luciferase vector (pGLIP vector) (Matsuu et al. 2015) and expressed in HEK293 cells with Lipofectamine LTX and Plus Reagent (Invitrogen, Carlsbad, CA, USA) according to the manufacturer's instructions. At 24–48 h after transfection, cells were lysed with Renilla Luciferase Assay Lysis Buffer (1 $\times$ ) and centrifuged at  $20,380 \times g$  for 5 min at  $4^\circ\text{C}$ , and

supernatants were collected and used immediately or stored at  $-80^{\circ}\text{C}$ . The luminescence of the crude extract was measured for 10 s using the Renilla luciferase assay system (Promega, Madison, WI, USA) on the GloMax-Multi + Detection System (Promega).

Immunoprecipitation assays were performed in duplicate in 96-well plates, and 100-fold diluted serum (1  $\mu\text{L}$  equivalent) was used. To prepare beads, 25  $\mu\text{L}$  of the Protein G magnetic bead suspension was added to each well and washed with 200  $\mu\text{L}$  phosphate-buffered saline (PBS) + 0.1% Tween 20 (PBS-T) three times using a DynaMag-96 Side Skirted plate (Invitrogen). Supernatants were removed using an aspirator. Next, 100  $\mu\text{L}$  of diluted serum from HCV-infected or mock-infected tupaia or known antibodies (used as a positive control) of different concentrations (10, 100, or 1000 ng) was added to the beads and incubated for 30 min at room temperature on a rotator. The beads were then washed three times with PBS-T, and lysates containing corresponding antigen or negative control antigens (empty vector) of  $10^7$  light units were added to each well. After 1-h incubation at room temperature on a rotator, beads were washed with PBS-T at least three times. Finally, the beads were transferred with 50  $\mu\text{L}$  of PBS into plates to be read, and 50  $\mu\text{L}$  of Renilla substrate-buffer mixture ( $1\times$ ) was added to each well using an injector system during luminescence measurement, as stated above. The antibody titer was expressed as relative light units (RLU).

#### **IV.2.5. Quantification of ROS levels**

Total free radicals in serum or liver samples from HCV-infected and uninfected control tupaia were measured using an OxiSelect In Vitro ROS/RNS Assay Kit (Cell Biolabs, Inc., San Diego, CA, USA) according to the manufacturer's protocol. Each reaction was performed in duplicate. Different concentrations of  $\text{H}_2\text{O}_2$  were used in each reaction plate as positive controls to confirm the test conditions. Sera were diluted in PBS (1:200), and 50  $\mu\text{L}$  of the diluted samples was collected into each well for the assay. For tissue lysates, 30 mg of liver tissues was homogenised using TissueLyser LT (Qiagen) in 1 mL PBS and centrifuged at  $10,000 \times g$  for 5

min. The supernatant was diluted in PBS (1:100), and 50  $\mu$ L of the diluted samples was used in each well for the assay. The stabilized, highly reactive 2',7'-dichlorodihydrofluorescein (DCFH) form was oxidized by ROS in the samples, and a catalyst was added to accelerate the reaction. The fluorescence of the oxidized DCFH to 2',7'-dichlorofluorescein (DCF) was proportional to the concentration of ROS in the samples. Green fluorescence was monitored at 525 nm excitation/580–640 nm emission using the GloMax-Multi + Detection System (Promega). The ROS level was expressed as relative fluorescence units (RFU).

#### **IV.2.6. Determination of 8-OHdG levels in genomic DNA from liver tissues**

DNA was extracted from frozen liver tissues using the phenol-chloroform extraction method. The level of 8-OHdG in extracted DNA was determined using the OxiSelect Oxidative DNA Damage ELISA Kit (Cell Biolabs, Inc.) according to the manufacturer's protocol with some modifications. Briefly, 100  $\mu$ g DNA was digested with 6 units of nuclease P1 for 2 h at 37 °C in a final concentration of 200 nM sodium acetate (pH 5.5). Then, the DNA reaction mixture was subjected to further digestion with 2 units of alkaline phosphatase for 1 h at 37 °C in a final concentration of 1M Tris (pH 7.5). Finally, the reaction mixture was centrifuged for 5 min at 6,000  $\times$  g and the supernatant was used for 8-OHdG ELISA assay. Each reaction was performed in duplicate. The 8-OHdG content in unknown samples was determined by comparison with predetermined 8-OHdG standard curves.

#### **IV.2.7. Gene expression analysis by qRT-PCR**

Tupaia TLR and cytokine mRNA expression levels were measured by qRT-PCR, as described previously (Kayesh et al. 2017). Primers used to detect tupaia NTCP gene [GenBank accession number: JQ608471] were as follows: forward primer (5'-TGTGGGCAAGAGCATCATGT-3') and reverse primer (5'-CACTGTGCATTGAGGCGAAA-3'), and the reaction conditions were similar to that used for TLR8 (Kayesh et al. 2017). Tupaia GAPDH was used as an endogenous control for normalization of the results.

#### **IV.2.8. Statistical analysis**

To analyse the statistical significance of antibody titers and ROS levels in animals before and after infection and to determine gene expression differences between uninfected controls and virus-infected individuals, unpaired t-tests were conducted using GraphPad software (<http://graphpad.com/quickcalcs/ttest1/>). Differences with P values of less than 0.05 were considered significant. All tests were two-sided.

### **IV.3. Results**

#### **IV.3.1. Alanine aminotransferase (ALT) levels and viral loads in HCV-infected tupaia sera**

Tupaia were infected with HCV genotypes 1a (#21), 1b (#22), 4a (#23), and 2a (#24). The level of ALT fluctuated, and intermittent growth of HCV was observed in all tupaia (Figure 3.1A, 3.2A, 3.3A and 3.4A). The highest ALT level (317.5 IU/L) was observed in tupaia #23 at 29 weeks post-infection (wpi). Virus could be detected in serum at 25 (51 copies/mL) and 31 wpi (43 copies/mL) in tupaia #21; at 13 wpi (21 copies/mL) in tupaia #22; at 7 (4 copies/mL), 29 (13 copies/mL), and 31 wpi (50 copies/mL) in tupaia #23; and at 11 (120 copies/mL), 15 (2 copies/mL), and 23 wpi (75 copies/mL) in tupaia #24 (Figure 3.1A, 3.2A, 3.3A and 3.4A).

#### **IV.3.2. Measurement of anti-core and anti-NS3 antibody titers**

To investigate the course of HCV-specific humoral immune responses in HCV-infected tupaia, I measured the levels of anti-core and anti-NS3 antibody titers in serum samples before infection (0 wpi) and every 2 weeks from 3 wpi to until the tupaia were sacrificed at 41 wpi. Despite fluctuations, significant increases in anti-core antibody levels were observed in all tupaia from 3 to 41 wpi (Figure 3.1B, 3.2B, 3.3B and 3.4B). In tupaia #21, significant increases in anti-NS3 antibody titers were observed at 3 and 25–35 wpi (Figure 3.1B). In tupaia #22,

significant increases in anti-NS3 antibody titers were observed at 3, 15, and 21–41 wpi (Figure 3.2B). Significant increases in anti-NS3 antibodies were observed in tupaia #23 and #24 from 3 to 41 wpi (Figure 3.3B and 3.4B).

At 3 wpi, though virus could not be detected in sera, a significant increase in anti-core and anti-NS3 antibody production was observed in all HCV-infected tupaia. Anti-core antibody production was decreased after the initial increase at 3 wpi, which further increased during or around peak viral propagation and fluctuated (Figure 3.1B, 3.2B, 3.3B and 3.4B). The highest anti-core antibody production was observed in tupaia #22 at 29 wpi (Figure 3.2B). Additionally, anti-NS3 antibody production sharply decreased after 3 wpi and fluctuated. The highest anti-NS3 antibody production was observed in tupaia #23 at 3 wpi (Figure 3.3B). Overall, peak NS3 antibody production was observed during or after peak viral propagation. Anti-core and anti-NS3 antibody titers in uninfected controls and positive controls were measured to ensure the specificity of the assay (data not shown).

#### **IV.3.3. Histological analysis of liver tissues from HCV-infected tupaia**

Histological analysis showed chronic hepatitis including abnormal architecture of liver cell cords, piecemeal necrosis, hepatocyte swelling, and lymphocytic infiltration into liver tissues of HCV-infected tupaia compared with that of normal tupaia liver tissues (Figure 3.5). Silver staining showed increased fibres among hepatocytes (tupaia #21 and #22) (Figure 3.5C, D) and thickened fibres (tupaia #23 and #24) (Figure 3.5E, F), indicating the progression of fibrosis in HCV-infected tupaia livers.

#### **IV.3.4. Measurement of ROS levels and anti-DHCR24 antibody titers**

To investigate the effects of HCV infection on ROS generation, I measured ROS levels in sera from HCV-infected tupaia at 2-week intervals from 0 to 41 wpi. ROS levels were increased in all HCV-infected tupaia compared to ROS levels before infection (Figure 3.1C, 3.2C, 3.3C and 3.4C). ROS levels were also evaluated in mock-infected controls and with different

concentrations of H<sub>2</sub>O<sub>2</sub> as a positive control to ensure the appropriateness of the assay conditions (data not shown).

To investigate whether increased ROS production induced anti-DHCR24 auto-antibody levels in HCV-infected tupaia, I measured the levels of serum anti-DHCR24 antibodies at 2-week intervals from 0 to 41 wpi. High levels of serum anti-DHCR24 antibodies were observed in all HCV-infected tupaia following ROS induction (Figure 3.1 C, 3.2 C, 3.3C and 3.4C). To ensure the specificity of the assay, anti-DHCR24 antibody titers in normal and positive controls were also evaluated (Data not shown).

#### **IV.3.5. Measurement of oxidative stress in the liver**

To determine intrahepatic oxidative stress, I measured ROS levels in liver tissues at 41 wpi in normal and HCV-infected tupaia and found significantly higher ROS levels in HCV-infected tupaia liver tissues compared to normal controls (Figure 3.6A). Additionally, at 41 wpi, I measured 8-OHdG levels in genomic DNA extracted from HCV-infected tupaia liver tissues to evaluate oxidative DNA damage. A significant increase in 8-OHdG levels was observed in all HCV-infected tupaia compared to normal controls (Figure 3.6B).

#### **IV.3.6. Changes in TLR, NTCP, and cytokine expression in liver tissues**

To investigate the mRNA expression patterns of TLRs, NTCP, and cytokines in liver tissues from HCV-infected tupaia, I isolated RNA from the livers of HCV-infected tupaia and measured the level of TLR3, TLR7, TLR8, NTCP, and cytokines (interferon [IFN]- $\beta$  and interleukin [IL]-6) mRNAs at 41 wpi. Upregulation of TLR3, TLR7, and TLR8 was observed in the liver tissues of all HCV-infected tupaia (#21, #22, #23, and #24) compared to uninfected normal tupaia (#3, #5, and #38; Figure 3.7). NTCP was significantly suppressed in tupaia #21 and #24 and significantly upregulated in tupaia #22 and #23 (Figure 3.8A). Moreover, significant upregulation of IFN- $\beta$  was observed in all tupaia, except tupaia #22 (Figure 3.8B). IL-6 levels were significantly increased in tupaia #22 and #24 (Figure 3.8C).

#### **IV.4. Discussion**

In this study, I demonstrated, for the first time, that ROS levels were higher in sera and liver tissues from HCV-infected tupaia than in that from uninfected tupaia. These data were consistent with previous findings of higher ROS levels in sera (De Maria et al. 1996) and liver tissues (Valgimigli et al. 2000; Valgimigli et al. 2002) of HCV-infected patients. I also observed increased 8-OHdG levels in livers from HCV-infected tupaia. These data were consistent with previous findings of higher 8-OHdG levels in livers from patients with chronic HCV infections (Mahmood et al. 2004; Fujita et al. 2004). Previous studies have found that ROS induces the upregulation of DHCR24 (Tsukiyama-Kohara, 2012; Saito et al. 2012). Consistent with these results, I showed that anti-DHCR24 antibody production was increased with ROS generation during the course of HCV infection in tupaia. Thus, the tupaia HCV infection model supported the possibility that anti-DHCR24 antibodies could be a valuable marker to monitor HCV infection in vivo and should be consistent with previous evidence demonstrating that anti-DHCR24 auto-antibodies could be a useful biomarker for hepatitis C progression (Ezzikouri et al. 2015).

In this study, I also characterized humoral and intrahepatic innate immune responses in tupaia infected with different HCV strains. Anti-NS3 and anti-core antibodies have been reported to be predominant in chronic HCV infections (Ishii et al. 1997). In fact, at 3 wpi, I found that all infected tupaia produced anti-core and anti-NS3 antibodies but were negative for serum HCV RNA. In a previous study, HCV RNA was detected only in the liver after 172 wpi (Amako et al. 2010); therefore, HCV may replicate in the liver but not be released into the serum via an unknown mechanism. A longitudinal study in humans, with a median follow-up of 7 years, also reported cases in which core antibody was positive but HCV RNA was negative (Hoare et al. 2008). Additionally, the highest anti-core antibody levels in tupaia #22 were observed at 29 wpi, indicating robust viral replication occurred somewhere in the tupaia body. At 41 wpi, upon

histological analysis of liver tissues of HCV-infected tupaias, lymphocytic infiltration was observed, indicating the occurrence of inflammation in the liver.

TLRs are important initiators of cytokine production, and the TLR signalling pathway serves as a link between innate and acquired immunity (Kawai & Akira, 2010; Akira et al. 2006). TLRs act as PRRs for recognizing HCV PAMPs (Yang & Zhu, 2015). In this study, I found significant increases in TLR3, TLR7, and TLR8 mRNA levels in liver tissues in chronically HCV-infected tupaias with different genotypes. These results highlighted that HCV could trigger innate immune responses in livers of chronically infected tupaias. Thus, these data confirmed previous studies reporting that HCV could be recognized by TLR3, TLR7, and TLR8 in cell cultures (Metz et al. 2013; Lee et al. 2015).

HCV mainly infects hepatocytes, and two PRRs (retinoic acid-inducible genes I [RIG-I] and TLR3) recognize HCV RNA to trigger production of multiple cytokines, including type I IFN. HCV develops strategies to evade these immune responses through several mechanisms; for example, the cleavage or relocalisation of IFN- $\beta$  promoter stimulator 1 by HCV NS3/4 A protease inhibits RIG-I signalling (Foy et al. 2005; Sklan et al. 2009; Li et al. 2005). Furthermore, NS3/4 A disrupts the TLR3 pathway by degradation of TIR-domain-containing adapter-inducing IFN- $\beta$  (Li et al. 2005). HCV core inhibits IFN signalling by interfering with the Janus kinase/signal transducer and activator of transcription pathway (Bode et al. 2003), and HCV NS5A blocks 2'5' oligoadenylate synthetase and induces IL-8 (Polyak et al. 2001; Rehmann, 2009). In livers from HCV-infected tupaias, TLR3 was induced in all four tupaias, whereas downstream IFN- $\beta$  induction was observed in three tupaias (#21, #23, and #24).

Silencing of NTCP could inhibit HCV infection, whereas overexpression of NTCP could enhance HCV infection in cell culture (Verrier et al. 2016). NTCP can act as a regulator of antiviral immune responses in the liver. Moreover, NTCP is associated with the IFN response, and increased NTCP expression could suppress interferon-induced transmembrane protein

(IFITM)-2 and IFITM-3 expression, and vice versa (Verrier et al. 2016). In this study, I found downregulation of NTCP but upregulation of IFN- $\beta$  in tupaia #21 and #24. Significant upregulation of NTCP was observed in tupaia #22 and #23, and upregulation of IFN- $\beta$  was only observed in tupaia #23. Thus, further studies are needed to explore the detailed mechanisms involved in NTCP-IFN interactions in HCV infection.

In conclusion, the tupaia infection model developed in this study was an effective approach to analyse the pathogenesis of HCV infection. ROS generation induced by HCV infection may be a trigger for the generation of anti-DHCR24 antibodies. Production of anti-core and anti-NS3 antibodies and intrahepatic innate immune responses upon HCV infection by alterations of TLR, NTCP, and cytokine expression highlights the potential applications of the tupaia infection model for the evaluation of HCV pathogenesis. Furthermore, tupaia could be a suitable small animal model for the evaluation of vaccines. The findings of this study provide novel insights into HCV pathogenesis and virus-host interactions.

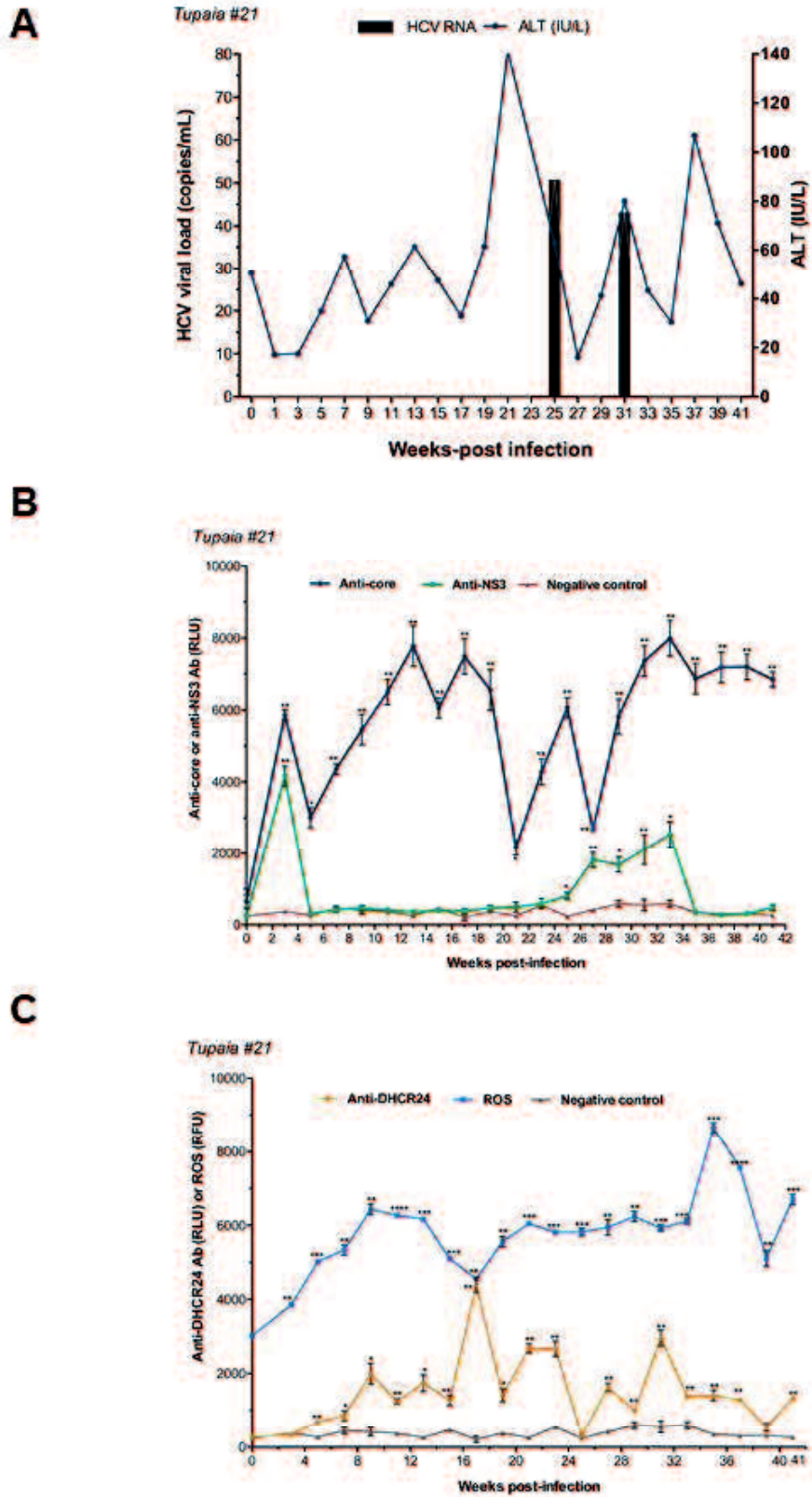


Figure 3.1. Response of tupaia to HCV1a infection.

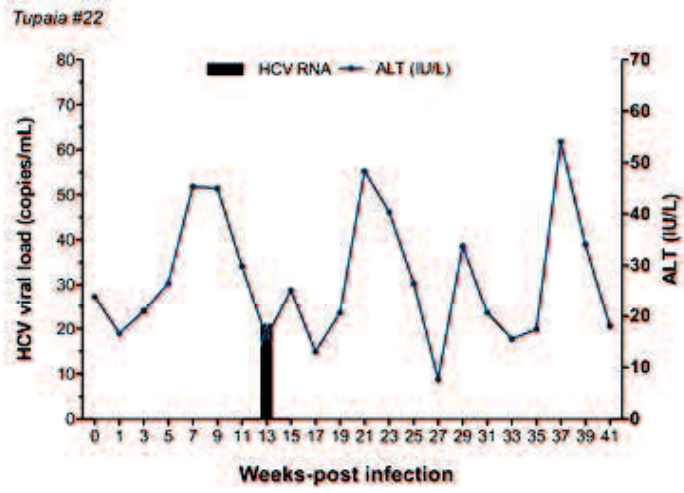
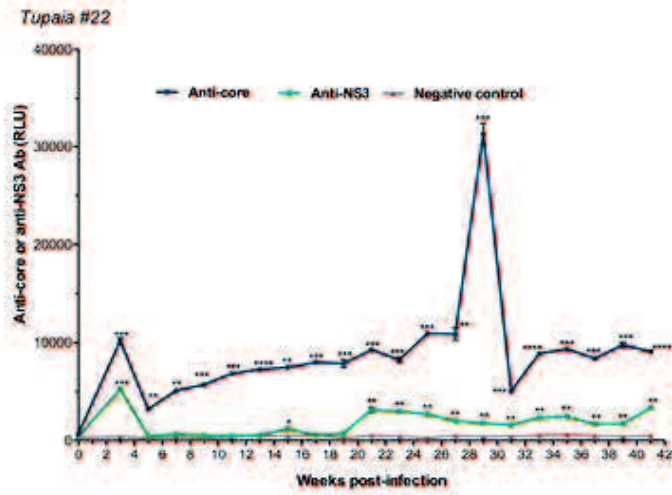
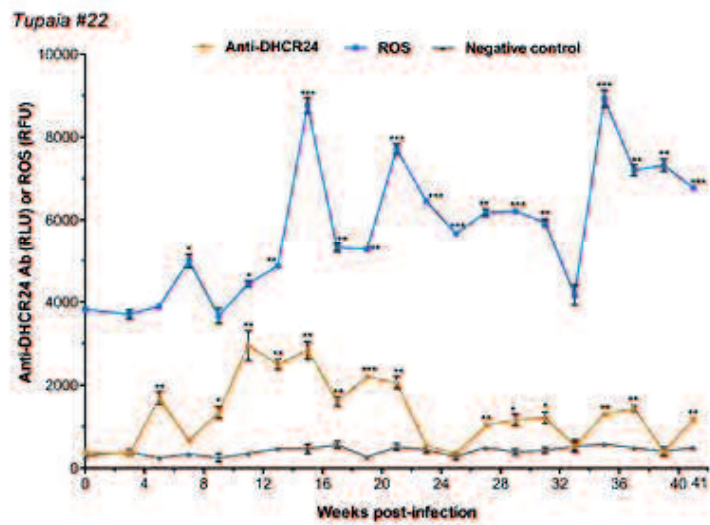
**A****B****C**

Figure 3.2. Response of tupaia to HCV1b infection.

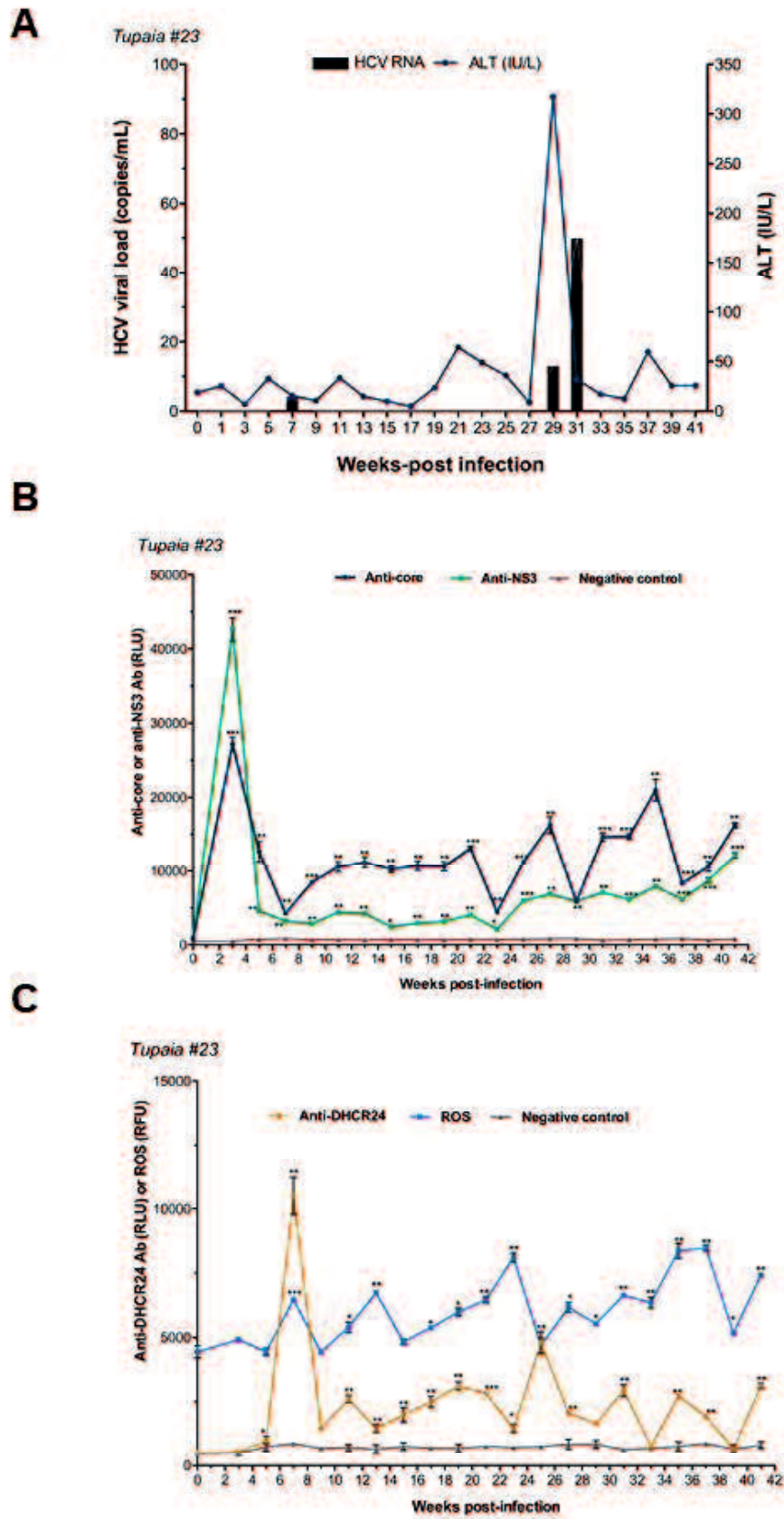


Figure 3.3. Response of tupaia to HCV4a infection.

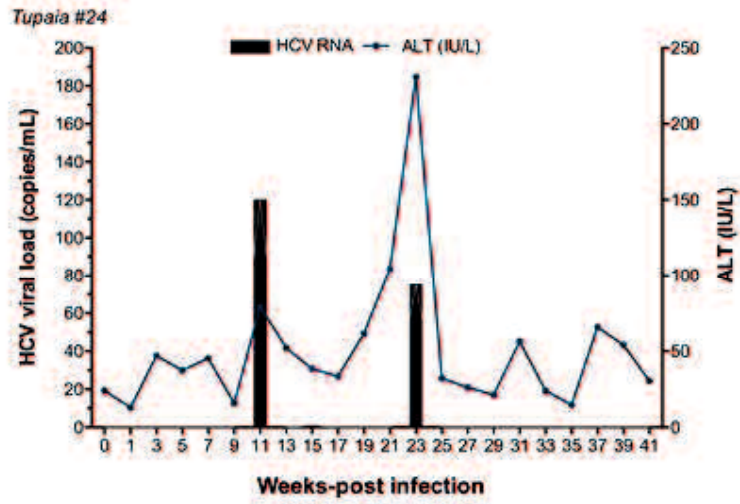
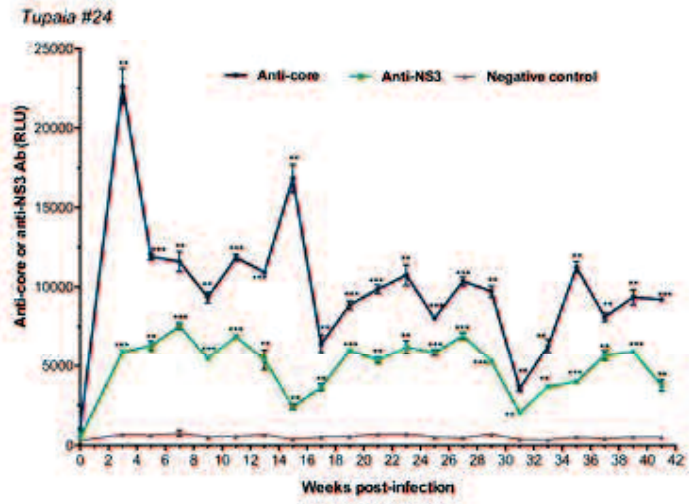
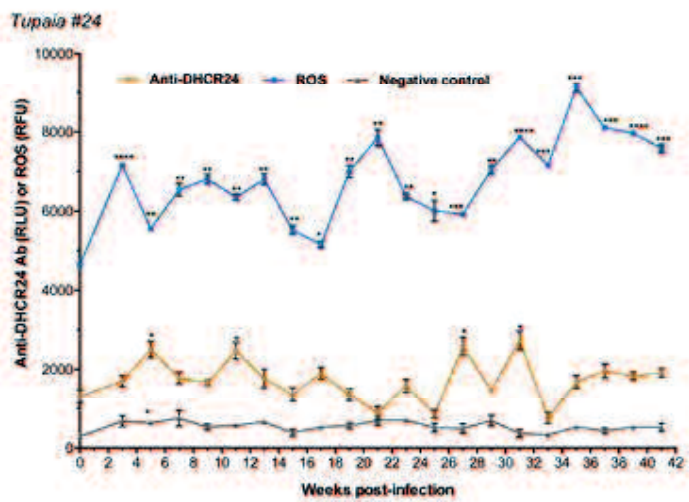
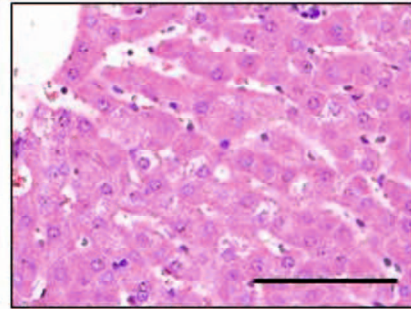
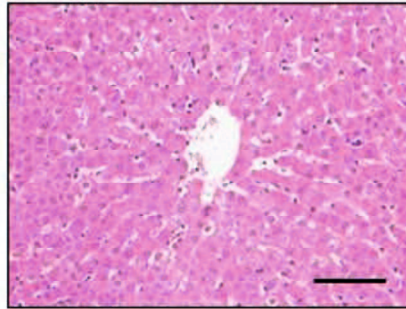
**A****B****C**

Figure 3.4. Response of tupaia to HCV2a infection.

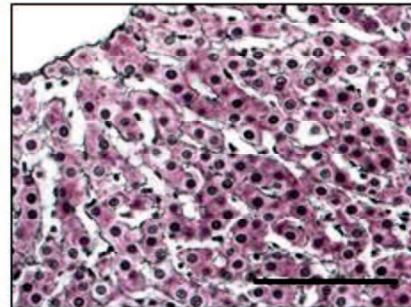
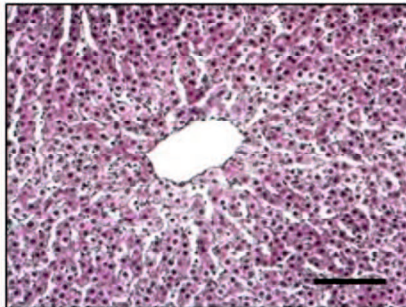
**A**

**Normal tupaia (#5)**

**HE  
staining**



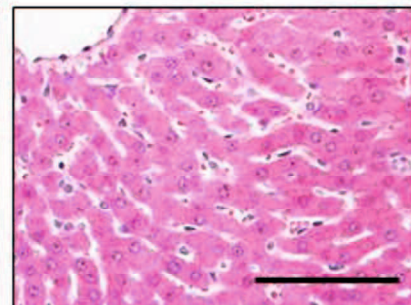
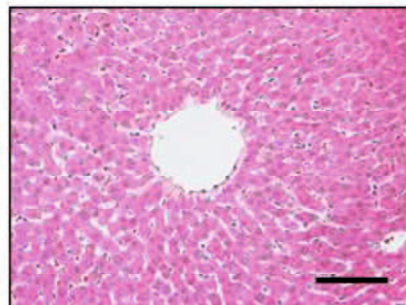
**Silver  
staining**



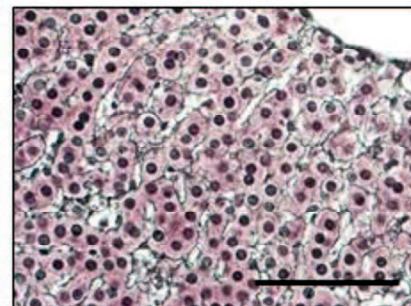
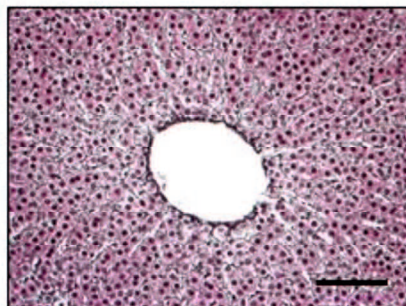
**B**

**Normal tupaia (#38)**

**HE  
staining**



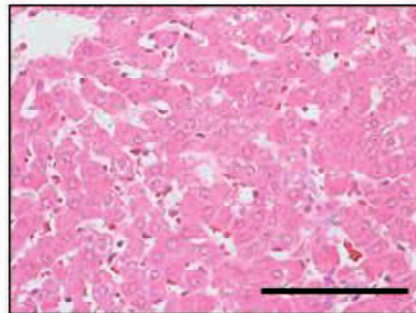
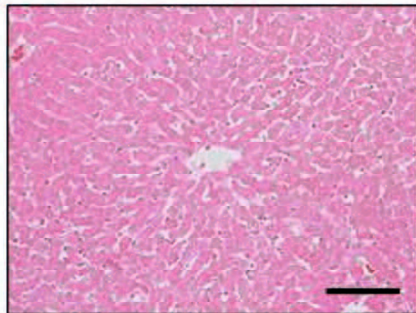
**Silver  
staining**



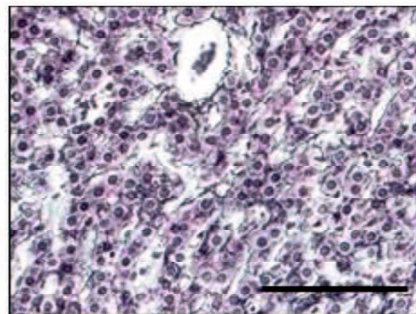
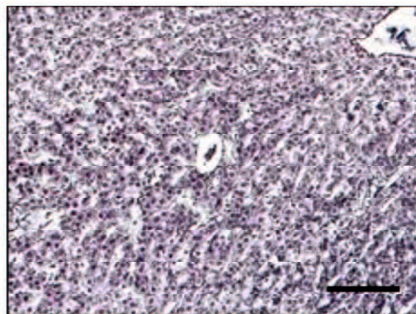
**C**

**HCV infected tupaia (#21)**

**HE  
staining**



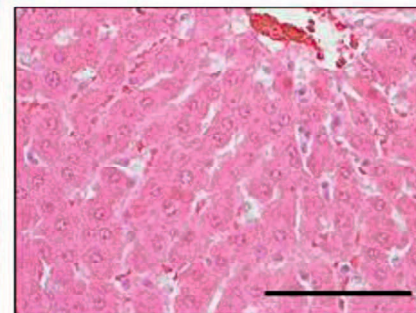
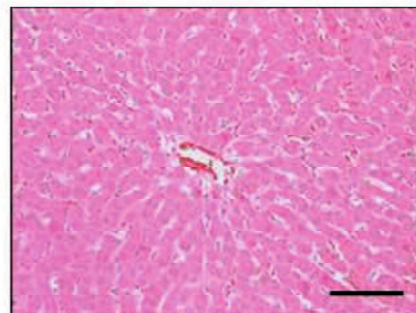
**Silver  
staining**



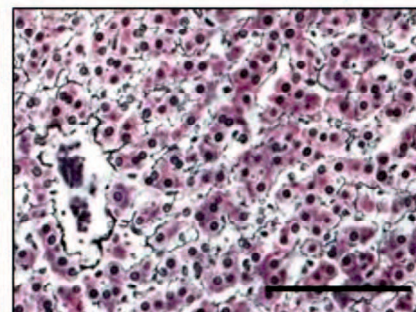
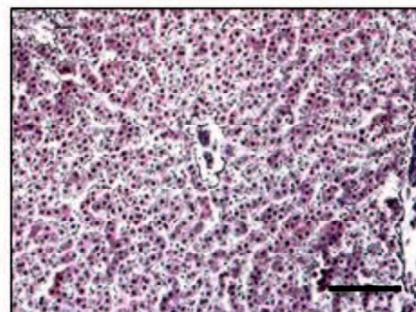
**D**

**HCV infected tupaia (#22)**

**HE  
staining**



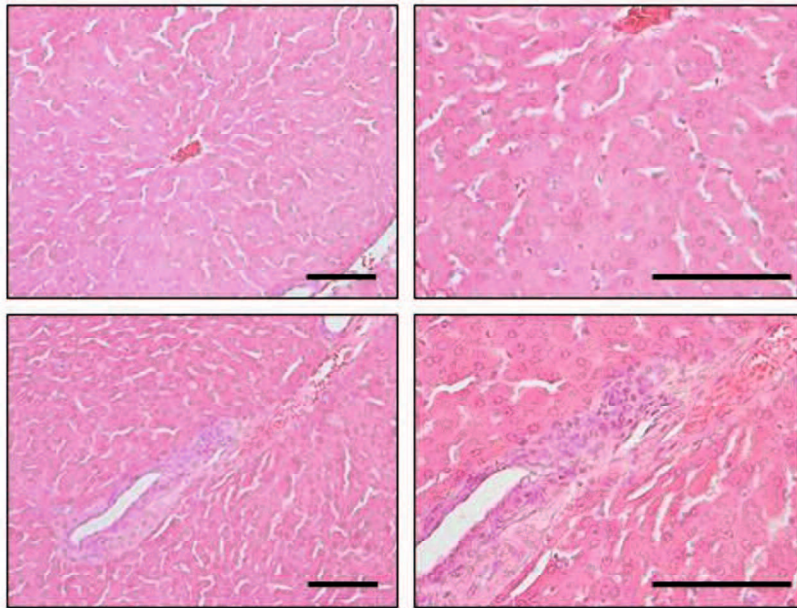
**Silver  
staining**



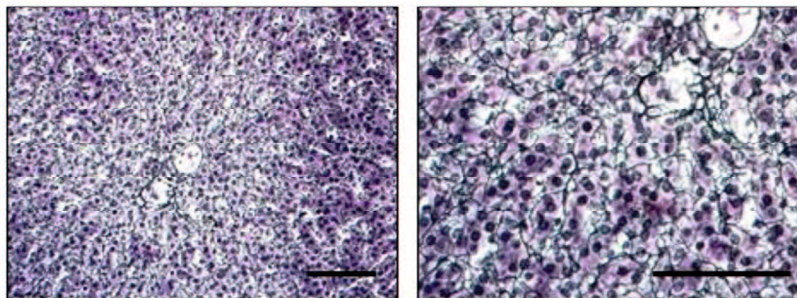
**E**

**HCV infected animal (#23)**

**HE  
staining**



**Silver  
staining**



**F**

**HCV infected animal (#24)**

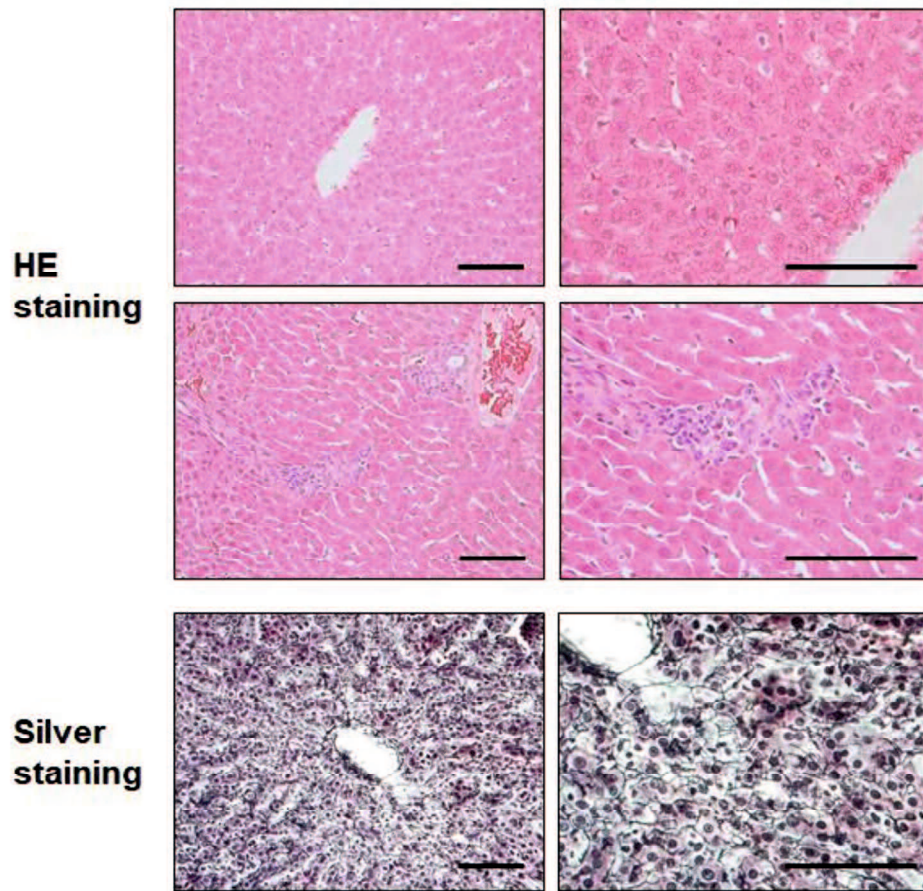


Figure 3.5. Histopathological analysis of liver tissues from normal and HCV-infected tupaia at 41 wpi.

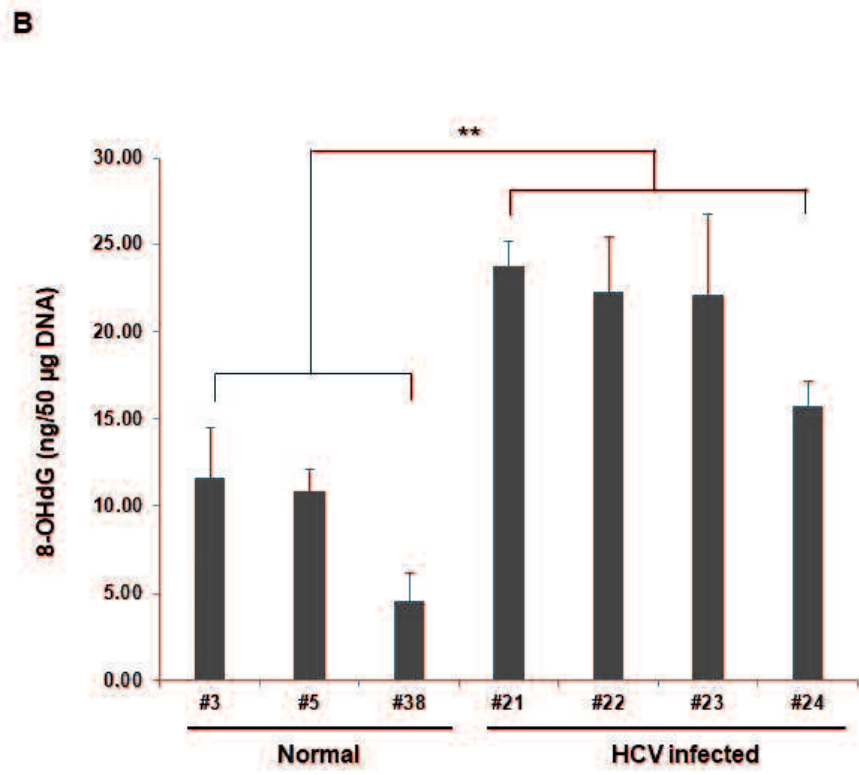
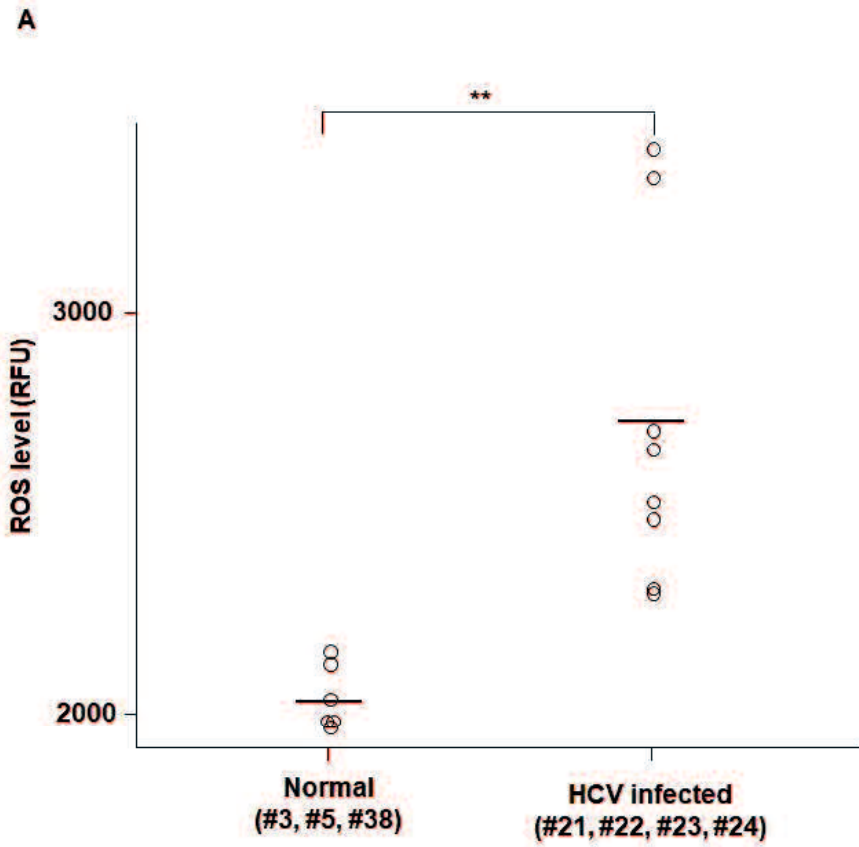


Figure 3.6. Intrahepatic ROS and 8-OHdG levels in normal and HCV-infected tupaia at 41 wpi.

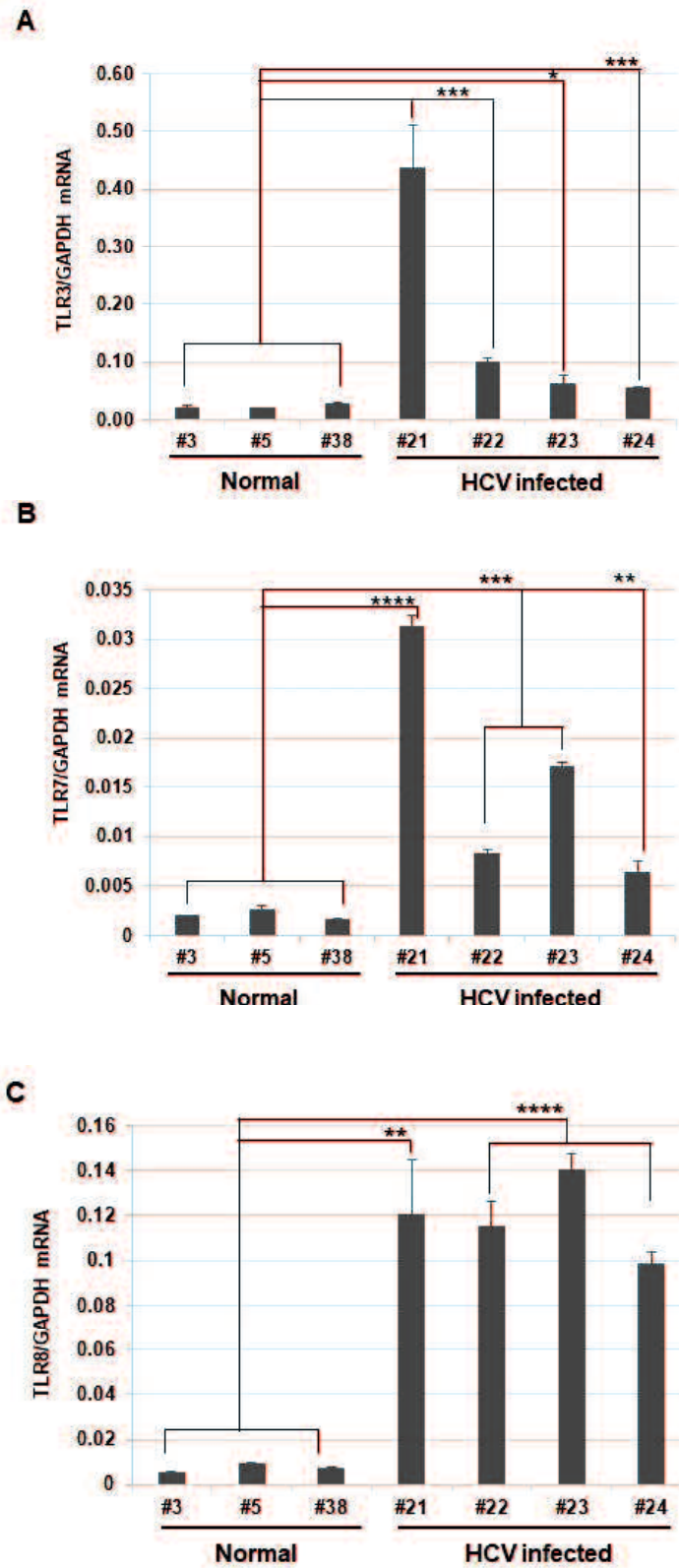


Figure 3.7. Changes in the expression of *TLR* mRNAs in HCV-infected tupaia at 41 wpi.

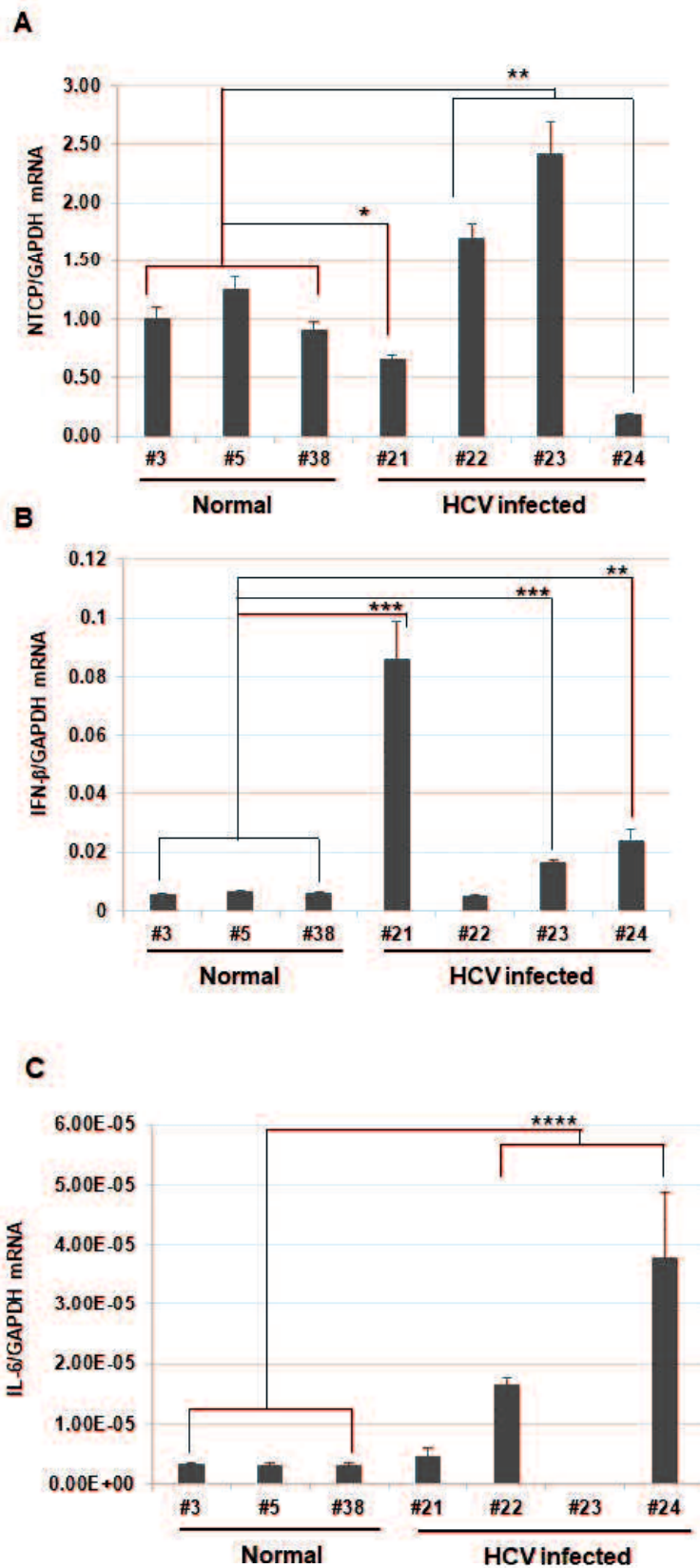


Figure 3.8. Changes in the expression of *NTCP* and cytokine mRNAs in HCV-infected tupaias at 41 wpi.

## **Chapter V: General Discussion**

Suitable small animal model is an invaluable tool for viral pathogenesis study and host response characterization. Lack of suitable small animal model becomes as a major obstacle for investigations of DENV pathogenesis and development of effective therapeutic and preventive interventions. Similarly, HBV and HCV pathogenesis study is also hampered by the lack of suitable animal model. So far, chimpanzee has been used as the natural infection model for HBV and HCV, but it is almost impossible to use chimpanzee in experimental infection due to strict ethical and animal welfare issues, and extreme expenses. So, alternative animal model is imperative for improving the understanding of viral pathogenesis and virus-host interactions.

In the present study, I demonstrated that tupaia cells are susceptible to dengue virus infection with four different serotypes and characterized host innate immune response upon dengue virus infection, which will pave the way to utilize tupaia as an animal model for dengue virus infection study.

In HBV infection in tupaia, I demonstrated that IFN- $\beta$  may play an important role in establishing the chronic infection in tupaia model. So, the understanding of the mechanisms of how IFN- $\beta$  gets suppressed and its association with chronicity of the infection is very important to investigate.

In HCV infection in tupaia, I demonstrated that HCV could induce ROS generation, which may also induce the generation of DHCR24 auto antibody. I also characterized humoral and intrahepatic innate immune responses in tupaia infected with different HCV strains, and the findings of this study should provide novel insights into HCV pathogenesis and virus-host interactions.

Because of the genetic similarity to primates, tupaia could be developed as a appropriate small animal model for viral pathogenesis study. However, unavailability of commercial specific antibodies and other tools hamper its easy and extended use in experiments.

## References

- Abdelwahab, S.F., 2016. Cellular immune response to hepatitis-C-virus in subjects without viremia or seroconversion: is it important? *Infect. Agent. Cancer* 11, 23.
- Akira, S., Uematsu, S., Takeuchi, O., 2006. Pathogen recognition and innate immunity. *Cell* 124, 783–801.
- Amako, Y., Tsukiyama-Kohara, K., Katsume, A., Hirata, Y., Sekiguchi, S., Tobita, Y., Hayashi, Y., Hishima, T., Funata, N., Yonekawa, H., Kohara, M., 2010. Pathogenesis of hepatitis C virus infection in *Tupaia belangeri*. *J. Virol.* 84, 303–311.
- Aoki, C., Hidari, K.I.P.J., Itonori, S., Yamada, A., Takahashi, N., Kasama, T., Hasebe, F., Islam, M. A., Hatano, K., Matsuoka, K., Taki, T., Guo, C. T., Takahashi, T., Sakano, Y., Suzuki, T., Miyamoto, D., Sugita, M., Terunuma, D., Morita, K., Suzuki, Y., 2006. Identification and characterization of carbohydrate molecules in mammalian cells recognized by dengue virus type 2. *J. Biochem.* 139, 607–614.
- Balsitis, S.J., Coloma, J., Castro, G., Alava, A., Flores, D., McKerrow, J.H., Beatty, P.R., Harris, E., 2009. Tropism of dengue virus in mice and humans defined by viral nonstructural protein 3-specific immunostaining. *Am. J. Trop. Med. Hyg.* 80, 416–424.
- Barnes, P.J., Karin, M., 1997. Nuclear factor-kappa B - a pivotal transcription factor in chronic inflammatory diseases. *N. Engl. J. Med.* 336, 1066–1071.
- Barth, H., 2015. Hepatitis C virus: Is it time to say goodbye yet? Perspectives and challenges for the next decade. *World J. Hepatol.* 7, 725–737.
- Bhatt, S., Gething, P.W., Brady, O.J., Messina, J.P., Farlow, A.W., Moyes, C.L., Drake, J.M., Brownstein, J.S., Hoen, A.G., Sankoh, O., Myers, M.F., George, D.B., Jaenisch, T., Wint, G. R., Simmons, C.P., Scott, T.W., Farrar, J.J., Hay, S.I., 2013. The global distribution and burden of dengue. *Nature.* 496(7446), 504–507.

- Blasius, A.L., Beutler, B., 2010. Intracellular Toll-like receptors. *Immunity*. 32(3), 305–315.
- Bode, J.G., Ludwig, S., Ehrhardt, C., Albrecht, U., Erhardt, A., Schaper, F., Heinrich, P.C., Häussinger, D., 2003. IFN-alpha antagonistic activity of HCV core protein involves induction of suppressor of cytokine signaling-3. *FASEB J.* 17, 488–490.
- Bonner, S.M., O’Sullivan, M.A., 1998. Endothelial cell monolayers as a model system to investigate dengue shock syndrome. *J. Virol. Methods*. 71, 159–167.
- Brown, J., Wang, H., Hajishengallis, G.N., Martin, M., 2011. TLR-signaling networks: an integration of adaptor molecules, kinases, and cross-talk. *J. Dent. Res.* 90, 417–427.
- Bustos-Arriaga, J., García-Machorro, J., León-Juárez, M., García-Cordero, J., Santos-Argumedo, L., Flores-Romo, L., Méndez-Cruz, A.R., Juárez-Delgado, F.J., Cedillo-Barrón, L., 2011. Activation of the innate immune response against DENV in normal non-transformed human fibroblasts. *PLoS Negl. Trop. Dis.* 5, e1420.
- Carter, A. B., Monick, M.M., Hunninghake, G.W., 1999. Both Erk and p38 kinases are necessary for cytokine gene transcription. *Am. J. Respir. Cell Mol. Biol.* 20(4), 751–758.
- Cashman, S.B., Marsden, B.D., Dustin, L.B., 2014. The Humoral Immune Response to HCV: Understanding is Key to Vaccine Development. *Front. Immunol.* 5, 550.
- Chan, K.W.K., Watanabe, S., Kavishna, R., Alonso, S., Vasudevan, S.G., 2015. Animal models for studying dengue pathogenesis and therapy. *Antiviral Res.* 123, 5–14.
- Chinchilla-Lopez, P., Qi, X., Yoshida, E.M., Mendez-Sanchez, N., 2017. The Direct-Acting Antivirals for Hepatitis C Virus and the Risk for Hepatocellular Carcinoma. *Ann. Hepatol.* 16, 328–330.

- Chyuan, I.T., Tsai, H.F., Tzeng, H.T., Sung, C.C., Wu, C.S., Chen, P.J., Hsu, P.N., 2015. Tumor necrosis factor-alpha blockage therapy impairs hepatitis B viral clearance and enhances T-cell exhaustion in a mouse model. *Cell. Mol. Immunol.* 12, 317–325.
- Civril, F., Deimling, T., de Oliveira Mann, C.C., Ablasser, A., Moldt, M., Witte, G., Hornung, V., Hopfner, K.P., 2013. Structural mechanism of cytosolic DNA sensing by cGAS. *Nature.* 498, 332–337.
- Claro da Silva, T., Polli, J.E., Swaan, P.W., 2013. The solute carrier family 10 (SLC10): beyond bile acid transport. *Mol. Aspects Med.* 34, 252–269.
- Conceição, T.M., El-Bacha, T., Villas-Bôas, C.S.A., Coello, G., Ramírez, J., Montero-Lomeli, M., Da Poian, A.T., 2010. Gene expression analysis during dengue virus infection in HepG2 cells reveals virus control of innate immune response. *J. Infect.* 60(1), 65-75.
- Costa, V.V., Fagundes, C.T., Souza, D.G., Teixeira, M.M., 2013. Inflammatory and innate immune responses in dengue infection: Protection versus disease induction. *Am. J. Pathol.* 182(6), 1950–1961.
- De Maria, N., Colantoni, A., Faggioli, S., Liu, G.J., Rogers, B.K., Farinati, F., Van Thiel, D.H., Floyd, R.A., 1996. Association between reactive oxygen species and disease activity in chronic hepatitis C. *Free Radic. Biol. Med.* 21, 291–295.
- Diamond, M.S., Edgil, D., Roberts, T.G., Lu, B., Harris, E., 2000. Infection of human cells by dengue virus is modulated by different cell types and viral strains. *J. Virol.* 74(17), 7814–7823.
- Dorner, M., Horwitz, J.A., Robbins, J.B., Barry, W.T., Feng, Q., Mu, K., Jones, C.T., Schoggins, J.W., Catanese, M.T., Burton, D.R., Law, M., Rice, C.M., Ploss, A., 2011. A genetically humanized mouse model for hepatitis C virus infection. *Nature* 474, 208–211.

- Eliot, O., 1971. Bibliography of the tree shrews. *Primates* 12, 323–414.
- Ezzikouri, S., Kimura, K., Sunagozaka, H., Kaneko, S., Inoue, K., Nishimura, T., Hishima, T., Kohara, M., Tsukiyama-Kohara, K., 2015. Serum DHCR24 Auto-antibody as a new Biomarker for Progression of Hepatitis C. *EBioMedicine* 2, 604–612.
- Fan, Y., Huang, Z.Y., Cao, C.C., Chen, C.S., Chen, Y.X., Fan, D.D., He, J., Hou, H.L., Hu, L., Hu, X.T., Jiang, X.T., Lai, R., Lang, Y.S., Liang, B., Liao, S.G., Mu, D., Ma, Y.Y., Niu, Y.Y., Sun, X.Q., Xia, J.Q., Xiao, J., Xiong, Z.Q., Xu, L., Yang, L., Zhang, Y., Zhao, W., Zhao, X. D., Zheng, Y.T., Zhou, J.M., Zhu, Y.B., Zhang, G.J., Wang, J., Yao, Y.G., 2013. Genome of the Chinese tree shrew. *Nat. Commun.* 4, 1426.
- Foy, E., Li, K., Sumpter, R.Jr., Loo, Y.M., Johnson, C.L., Wang, C., Fish, P.M., Yoneyama, M., Fujita, T., Lemon, S.M., Gale, M.Jr., 2005. Control of antiviral defenses through hepatitis C virus disruption of retinoic acid-inducible gene-I signaling. *Proc. Natl. Acad. Sci. U S A* 102, 2986–2991.
- Fujita, N., Kaito, M., Tanaka, H., Horiike, S., Adachi, Y., 2004. Reduction of serum HCV RNA titer by bezafibrate therapy in patients with chronic hepatitis C. *Am. J. Gastroenterol.* 99, 2280.
- Ganem, D., Prince, A.M., 2004. Hepatitis B virus infection--natural history and clinical consequences. *N. Engl. J. Med.* 350, 1118–1129.
- Gao, P., Ascano, M., Zillinger, T., Wang, W., Dai, P., Serganov, A.A., Gaffney, B.L., Shuman, S., Jones, R.A., Deng, L., Hartmann, G., Barchet, W., Tuschl, T., Patel, D.J., 2013. Structure-function analysis of STING activation by c[G(2',5')pA(3',5')p] and targeting by antiviral DMXAA. *Cell.* 154, 748–762.

- He, J., Hao, R., Liu, D., Liu, X., Wu, S., Guo, S., Wang, Y., Tien, P., Guo, D., 2016. Inhibition of hepatitis B virus replication by activation of the cGAS-STING pathway. *J. Gen. Virol.* 97, 3368–3378.
- Hoare, M., Gelson, W.T., Rushbrook, S.M., Curran, M.D., Woodall, T., Coleman, N., Davies, S.E., Alexander, G.J., 2008. Histological changes in HCV antibody-positive, HCV RNA-negative subjects suggest persistent virus infection. *Hepatology* 48, 1737–1745.
- Horner, S.M., Gale, M., Jr., 2013. Regulation of hepatic innate immunity by hepatitis C virus. *Nat. Med.* 19, 879–888.
- Huang, Y.W., Hsu, C.K., Lin, S.C., Wei, S.C., Hu, J.T., Chang, H.Y., Liang, C.W., Chen, D.S., Chen, P.J., Hsu, P.N., Yang, S.S., Kao, J.H., 2014. Reduced toll-like receptor 9 expression on peripheral CD14<sup>+</sup> monocytes of chronic hepatitis B patients and its restoration by effective therapy. *Antivir. Ther.* 19, 637–643.
- Huang, Y.W., Lin, S.C., Wei, S.C., Hu, J.T., Chang, H.Y., Huang, S.H., Chen, D.S., Chen, P.J., Hsu, P.N., Yang, S.S., Kao, J.H., 2013. Reduced toll-like receptor 3 expression in chronic hepatitis B patients and its restoration by interferon therapy. *Antivir. Ther.* 18, 877–884.
- Ishii, K., Ishibashi, M., Ohtake, T., Kano, S., Saito, H., Watanabe, K., 1997. Characterization of antibodies against core, NS3, NS4, NS5 region of hepatitis C virus in patients with hepatitis C. *Rinsho Byori.* 45, 1156–1162.
- Isogawa, M., Robek, M.D., Furuichi, Y., Chisari, F.V., 2005. Toll-like receptor signaling inhibits hepatitis B virus replication in vivo. *J. Virol.* 79, 7269–7272.
- Jiang, J., Tang, H., 2010. Mechanism of inhibiting type I interferon induction by hepatitis B virus X protein. *Protein Cell* 1, 1106–1117.

- Kawai, T., Akira, S., 2010. The role of pattern-recognition receptors in innate immunity: update on Toll-like receptors. *Nat. Immunol.* 11, 373–384.
- Kawai, T., Akira, S., 2011. Toll-like receptors and their crosstalk with other innate receptors in infection and immunity. *Immunity* 34, 637–650.
- Kayesh, M.E.H., Kitab, B., Sanada, T., Hayasaka, D., Morita, K., Kohara, M., Tsukiyama-Kohara, K., 2017. Susceptibility and initial immune response of *Tupaia belangeri* cells to dengue virus infection. *Infect. Genet. Evol.* 51, 203–210.
- Keating, G.M., Noble, S., 2003. Recombinant hepatitis B vaccine (Engerix-B): a review of its immunogenicity and protective efficacy against hepatitis B. *Drugs* 63, 1021–1051.
- Korenaga, M., Wang, T., Li, Y., Showalter, L.A., Chan, T., Sun, J., Weinman, S.A., 2005. Hepatitis C virus core protein inhibits mitochondrial electron transport and increases reactive oxygen species (ROS) production. *J. Biol. Chem.* 280, 37481–37488.
- Kriegs, J.O., Churakov, G., Jurka, J., Brosius, J., Schmitz, J., 2007. Evolutionary history of 7SL RNA-derived SINEs in Supraprimates. *Trends Genet.* 23, 158–161.
- Kumar, S., Stecher, G., Tamura, K., 2016. MEGA7: Molecular Evolutionary Genetics Analysis version 7.0 for bigger datasets. *Mol. Biol. Evol.* 33, 1870–1874.
- Kurane, I., Janus, J., Ennis, F.A., 1992. Dengue virus infection of human skin fibroblasts in vitro production of IFN-beta, IL-6 and GM-CSF. *Arch. Virol.* 124(1), 21–30.
- Kurane, I., Kontny, U., Janus, J., Ennis, F.A., 1990. Dengue-2 virus infection of human mononuclear cell lines and establishment of persistent infections. *Arch. Virol.* 110(1), 91–101.
- Lavanchy, D., 2009. The global burden of hepatitis C. *Liver Int.* 29 Suppl 1, 74–81.

- Lee, J., Tian, Y., Chan, S.T., Kim, J.Y., Cho, C., Ou, J.H., 2015. TNF-alpha Induced by Hepatitis C Virus via TLR7 and TLR8 in Hepatocytes Supports Interferon Signaling via an Autocrine Mechanism. *PLoS Pathog.* 11, e1004937.
- Lee, W.M., 1997. Hepatitis B virus infection. *N. Engl. J. Med.* 337, 1733–1745.
- Li, K., Foy, E., Ferreon, J.C., Nakamura, M., Ferreon, A.C., Ikeda, M., Ray, S.C., Gale, M.Jr., Lemon, S.M., 2005. Immune evasion by hepatitis C virus NS3/4A protease-mediated cleavage of the Toll-like receptor 3 adaptor protein TRIF. *Proc. Natl. Acad. Sci. U S A* 102, 2992–2997.
- Li, L., Li, Z., Wang, E., Yang, R., Xiao, Y., Han, H., Lang, F., Li, X., Xia, Y., Gao, F., Li, Q., Fraser, N. W., Zhou, J., 2016. Herpes simplex virus 1 infection of tree shrews differs from that of mice in the severity of acute infection and viral transcription in the peripheral nervous system. *J. Virol.* 90(2), 790–804.
- Liang, Z., Wu, S., Li, Y., He, L., Wu, M., Jiang, L., Feng, L., Zhang, P., Huang, X., 2011. Activation of Toll-like receptor 3 impairs the dengue virus serotype 2 replication through induction of IFN- $\beta$  in cultured hepatoma cells. *PLoS One*, 6(8), 2–9.
- Lin, C.L., Kao, J.H., 2015. Hepatitis B virus genotypes and variants. *Cold Spring Harb. Perspect. Med.* 5, a021436.
- Liu, Y., Li, J., Chen, J., Li, Y., Wang, W., Du, X., Song, W., Zhang, W., Lin, L., Yuan, Z., 2015. Hepatitis B virus polymerase disrupts K63-linked ubiquitination of STING to block innate cytosolic DNA-sensing pathways. *J. Virol.* 89, 2287–2300.
- Machida, K., Tsukiyama-Kohara, K., Seike, E., Toné, S., Shibasaki, F., Shimizu, M., Takahashi, H., Hayashi, Y., Funata, N., Taya, C., Yonekawa, H., Kohara, M., 2001. Inhibition of cytochrome c release in Fas-mediated signaling pathway in transgenic mice induced to express hepatitis C viral proteins. *J. Biol. Chem.* 276, 12140–12146.

- Mahmood, S., Kawanaka, M., Kamei, A., Izumi, A., Nakata, K., Niiyama, G., Ikeda, H., Hanano, S., Suehiro, M., Togawa, K., Yamada, G., 2004. Immunohistochemical evaluation of oxidative stress markers in chronic hepatitis C. *Antioxid. Redox Signal.* 6, 19–24.
- Marianneau, P., Mégret, F., Olivier, R., Morens, D. M., Deubel, V., 1996. Dengue 1 virus binding to human hepatoma HepG2 and simian Vero cell surfaces differs. *J. Gen. Virol.* 77(10), 2547–2554.
- Matsuu, A., Hobo, S., Ando, K., Sanekata, T., Sato, F., Endo, Y., Amaya, T., Osaki, T., Horie, M., Masatani, T., Ozawa, M., Tsukiyama-Kohara, K., 2015. Genetic and serological surveillance for non-primate hepacivirus in horses in Japan. *Vet. Microbiol.* 179, 219–227.
- Mercer, D.F., Schiller, D.E., Elliott, J.F., Douglas, D.N., Hao, C., Rinfret, A., Addison, W.R., Fischer, K.P., Churchill, T.A., Lakey, J.R., Tyrrell, D.L., Kneteman, N.M., 2001. Hepatitis C virus replication in mice with chimeric human livers. *Nat. Med.* 7, 927–933.
- Metz, P., Reuter, A., Bender, S., Bartenschlager, R. 2013. Interferon-stimulated genes and their role in controlling hepatitis C virus. *J. Hepatol.* 59, 1331–1341.
- Mohd Hanafiah, K., Groeger, J., Flaxman, A.D., Wiersma, S.T., 2013. Global epidemiology of hepatitis C virus infection: new estimates of age-specific antibody to HCV seroprevalence. *Hepatology* 57, 1333–1342.
- Nakagawa, S., Hirata, Y., Kameyama, T., Tokunaga, Y., Nishito, Y., Hirabayashi, K., Yano, J., Ochiya, T., Tateno, C., Tanaka, Y., Mizokami, M., Tsukiyama-Kohara, K., Inoue, K., Yoshida, M., Takaoka, A., Kohara, M., 2013. Targeted induction of interferon-

- lambda in humanized chimeric mouse liver abrogates hepatotropic virus infection. *PLoS One* 8, e59611.
- Nei, M., Kumar, S., 2000. *Molecular Evolution and Phylogenetics*. Oxford University Press, New York.
- Payne, A.F., Binduga-Gajewska, I., Kauffman, E.B., Kramer, L.D., 2006. Quantitation of flaviviruses by fluorescent focus assay. *J. Virol. Methods*. 134, 183–189.
- Polyak, S.J., Khabar, K.S., Paschal, D.M., Ezelle, H.J., Duverlie, G., Barber, G.N., Levy, D.E., Mukaida, N., Gretch, D.R., 2001. Hepatitis C virus nonstructural 5A protein induces interleukin-8, leading to partial inhibition of the interferon-induced antiviral response. *J. Virol.* 75, 6095–6106.
- Rehermann, B., 2009. Hepatitis C virus versus innate and adaptive immune responses: a tale of coevolution and coexistence. *J. Clin. Invest.* 119, 1745–1754.
- Saito, M., Kohara, M., Tsukiyama-Kohara, K., 2012. Hepatitis C virus promotes expression of the 3beta-hydroxysterol delta24-reductase through Sp1. *J. Med. Virol.* 84, 733–746.
- Saitou, N., Nei, M., 1987. The neighbor-joining method: A new method for reconstructing phylogenetic trees. *Mol. Biol. Evol.* 4, 406–425.
- Sanada, T., Tsukiyama-Kohara, K., Yamamoto, N., Ezzikouri, S., Benjelloun, S., Murakami, S., Tanaka, Y., Tateno, C., Kohara, M., 2016. Property of hepatitis B virus replication in *Tupaia belangeri* hepatocytes. *Biochem. Biophys. Res. Commun.* 469(2), 229–235.
- Sariol, C.A., Martínez, M.I., Rivera, F., van Rodríguez, I., Pantoja, P., Abel, K., Arana, T., Giavedoni, L., Hodara, V., White, L.J., Angleró, Y.I., Montaner, L.J., Kraiselburd, E.N., 2011. Decreased dengue replication and an increased anti-viral humoral response with the use of combined Toll-like receptor 3 and 7/8 agonists in macaques. *PLoS One*, 6(4), e19323.

- Schweitzer, A., Horn, J., Mikolajczyk, R.T., Krause, G., Ott, J.J., 2015. Estimations of worldwide prevalence of chronic hepatitis B virus infection: a systematic review of data published between 1965 and 2013. *Lancet* 386, 1546–1555.
- Seeger, C., Mason, W.S., 2015. Molecular biology of hepatitis B virus infection. *Virology* 479–480, 672–686.
- Sekiguchi, S., Kimura, K., Chiyo, T., Ohtsuki, T., Tobita, Y., Tokunaga, Y., Yasui, F., Tsukiyama-Kohara, K., Wakita, T., Tanaka, T., Miyasaka, M., Mizuno, K., Hayashi, Y., Hishima, T., Matsushima, K., Kohara, M., 2012. Immunization with a recombinant vaccinia virus that encodes nonstructural proteins of the hepatitis C virus suppresses viral protein levels in mouse liver. *PloS One* 7, e51656.
- Shi, B., Ren, G., Hu, Y., Wang, S., Zhang, Z., Yuan, Z., 2012. HBsAg inhibits IFN-alpha production in plasmacytoid dendritic cells through TNF-alpha and IL-10 induction in monocytes. *PloS One* 7, e44900.
- Shi, Y.J., Jiang, Z.Y., Zeng, K., 2006. Effect of IL-6 and TNF-alpha on dengue virus infection of human dendritic cells. *Xi Bao Yu Fen Zi Mian Yi Xue Za Zhi*, 22, 469–471.
- Shinkai, N., Matsuura, K., Sugauchi, F., Watanabe, T., Murakami, S., Iio, E., Ogawa, S., Nojiri, S., Joh, T., Tanaka, Y., 2013. Application of a newly developed high-sensitivity HBsAg chemiluminescent enzyme immunoassay for hepatitis B patients with HBsAg seroclearance. *J. Clin. Microbiol.* 51, 3484–3491.
- Simmons, C.P., Farrar, J.J., van Vinh Chau, N., Wills, B., 2012. Dengue. *N. Engl. J. Med.* 366, 1423–1432.
- Sklan, E.H., Charuworn, P., Pang, P.S., Glenn, J.S., 2009. Mechanisms of HCV survival in the host. *Nat. Rev. Gastroenterol. Hepatol.* 6, 217–227.

- Suksanpaisan, L., Cabrera-Hernandez, A., Smith, D.R., 2007. Infection of human primary hepatocytes with dengue virus serotype 2. *J. Med. Virol.* 79(3), 300–307.
- Sun, L., Wu, J., Du, F., Chen, X., Chen, Z.J., 2013. Cyclic GMP-AMP synthase is a cytosolic DNA sensor that activates the type I interferon pathway. *Science* 339, 786–791.
- Sun, P., Fernandez, S., Marovich, M.A., Palmer, D.R., Celluzzi, C.M., Boonnak, K., Liang, Z., Subramanian, H., Porter, K.R., Sun, W., Burgess, T.H., 2009. Functional characterization of ex vivo blood myeloid and plasmacytoid dendritic cells after infection with dengue virus. *Virology*, 383(2), 207–215.
- Suwanwong, Y., Mounkote, T., Wiwanitkit, V., Soogarun, S., 2010. Detection of dengue virus by simple RT-PCR using universal degenerate primers observations from a preliminary study. *Arch. Hellenic Medicine*, 27(5), 818–821.
- Takano, T., Tsukiyama-Kohara, K., Hayashi, M., Hirata, Y., Satoh, M., Tokunaga, Y., Tateno, C., Hayashi, Y., Hishima, T., Funata, N., Sudoh, M., Kohara, M., 2011. Augmentation of DHCR24 expression by hepatitis C virus infection facilitates viral replication in hepatocytes. *J. Hepatol.* 55, 512–521.
- Taketomi, M., Nishi, Y., Ohkawa, Y., Inui, N., 1986. Establishment of lung fibroblastic cell lines from non-human primate *Tupaia belangeri* and their use in a forward gene mutation assay at the hypoxanthine-guanine phosphoribosyl transferase locus. *Mutagenesis*, 1(5), 359-365.
- Takeuchi, O., Akira, S., 2010. Pattern recognition receptors and inflammation. *Cell* 140, 805–820.
- Takeuchi, T., Katsume, A., Tanaka, T., Abe, A., Inoue, K., Tsukiyama-Kohara, K., Kawaguchi, R., Tanaka, S., Kohara, M., 1999. Real-time detection system for quantification of hepatitis C virus genome. *Gastroenterology* 116, 636–642.

- Thimme, R., Binder, M., Bartenschlager, R., 2012. Failure of innate and adaptive immune responses in controlling hepatitis C virus infection. *FEMS Microbiol. Rev.* 36, 663–683.
- Tsai, Y.T., Chang, S.Y., Lee, C.N., Kao, C.L., 2009. Human TLR3 recognizes dengue virus and modulates viral replication in vitro. *Cell. Microbiol.* 11(4), 604–615.
- Tsukiyama-Kohara, K., 2012. Role of oxidative stress in hepatocarcinogenesis induced by hepatitis C virus. *Int. J. Mol. Sci.* 13, 15271–15278.
- Tsukiyama-Kohara, K., Kohara, M., 2014. *Tupaia belangeri* as an experimental animal model for viral infection. *Exp. Anim.* 63(4), 367–374.
- Valavanidis, A., Vlachogianni, T., Fiotakis, C., 2009. 8-hydroxy-2'-deoxyguanosine (8-OHdG): A critical biomarker of oxidative stress and carcinogenesis. *J. Environ. Sci. Health. C Environ. Carcinog. Ecotoxicol. Rev.* 27, 120–139.
- Valgimigli, L., Valgimigli, M., Gaiani, S., Pedulli, G. F., Bolondi, L., 2000. Measurement of oxidative stress in human liver by EPR spin-probe technique. *Free Radic. Res.* 33, 167–178.
- Valgimigli, M., Valgimigli, L., Trerè, D., Gaiani, S., Pedulli, G.F., Gramantieri, L., Bolondi, L., 2002. Oxidative stress EPR measurement in human liver by radical-probe technique. Correlation with etiology, histology and cell proliferation. *Free Radic. Res.* 36, 939–948.
- Vaughn, D.W., Green, S., Kalayanarooj, S., Innis, B.L., Nimmannitya, S., Suntayakorn, S., Endy, T.P., Raengsakulrach, B., Rothman, A.L., Ennis, F.A., Nisalak, A., 2000. Dengue viremia titer, antibody response pattern, and virus serotype correlate with disease severity. *J. Infect. Dis.* 181, 2–9.

- Verrier, E.R., Colpitts, C.C., Bach, C., Heydmann, L., Zona, L., Xiao, F., Thumann, C., Crouchet, E., Gaudin, R., Sureau, C., Cosset, F.L., McKeating, J.A., Pessaux, P., Hoshida, Y., Schuster, C., Zeisel, M.B., Baumert, T.F., 2016. Solute carrier NTCP regulates innate antiviral immune responses targeting hepatitis C virus infection of hepatocytes. *Cell. Rep.* 17, 1357–1368.
- Vicente, C.R., Herbinger, K.H., Fröschl, G., Malta Romano, C., de Souza Areias Cabidelle, A., Cerutti Junior, C., 2016. Serotype influences on dengue severity: a cross-sectional study on 485 confirmed dengue cases in Vitória, Brazil. *BMC Infect. Dis.* 16, 320.
- Walter, E., Keist, R., Niederost, B., Pult, I., Blum, H.E., 1996. Hepatitis B virus infection of tupaia hepatocytes in vitro and in vivo. *Hepatology* 24, 1–5.
- Wang, H., Ryu, W.S., 2010. Hepatitis B virus polymerase blocks pattern recognition receptor signaling via interaction with DDX3: implications for immune evasion. *PLoS Pathog.* 6, e1000986.
- Watashi, K., Liang, G., Iwamoto, M., Marusawa, H., Uchida, N., Daito, T., Kitamura, K., Muramatsu, M., Ohashi, H., Kiyohara, T., Suzuki, R., Li, J., Tong, S., Tanaka, Y., Murata, K., Aizaki, H., Wakita, T., 2013. Interleukin-1 and tumor necrosis factor- $\alpha$  trigger restriction of hepatitis B virus infection via a cytidine deaminase activation-induced cytidine deaminase (AID). *J. Biol. Chem.* 288, 31715–31727.
- Waterham, H.R., Koster, J., Romeijn, G.J., Hennekam, R.C., Vreken, P., Andersson, H.C., FitzPatrick, D.R., Kelley, R.I., Wanders, R.J., 2001. Mutations in the 3 $\beta$ -hydroxysterol Delta24-reductase gene cause desmosterolosis, an autosomal recessive disorder of cholesterol biosynthesis. *Am. J. Hum. Genet.* 69, 685–694.

- Wu, J., Lu, M., Meng, Z., Trippler, M., Broering, R., Szczeponek, A., Krux, F., Dittmer, U., Roggendorf, M., Gerken, G., Schlaak, J.F., 2007. Toll-like receptor-mediated control of HBV replication by nonparenchymal liver cells in mice. *Hepatology* 46, 1769–1778.
- Wu, J., Meng, Z., Jiang, M., Pei, R., Trippler, M., Broering, R., Bucchi, A., Sowa, J.P., Dittmer, U., Yang, D., Roggendorf, M., Gerken, G., Lu, M., Schlaak, J.F., 2009. Hepatitis B virus suppresses toll-like receptor-mediated innate immune responses in murine parenchymal and nonparenchymal liver cells. *Hepatology* 49, 1132–1140.
- Xu, L., Yu, D., Fan, Y., Peng, L., Wu, Y., Yao, Y.G., 2016. Loss of RIG-I leads to a functional replacement with MDA5 in the Chinese tree shrew. *Proc. Natl. Acad. Sci. U S A.* 113(39), 10950–10955.
- Xu, L., Yu, D., Peng, L., Fan, Y., Chen, J., Zheng, Y.T., Wang, C., Yao, Y.G., 2015. Characterization of a MAVS ortholog from the Chinese tree shrew (*Tupaia belangeri chinensis*). *Dev. Comp. Immunol.* 52(1), 58–68.
- Xu, X., Chen, H., Cao, X., Ben, K., 2007. Efficient infection of tree shrew (*Tupaia belangeri*) with hepatitis C virus grown in cell culture or from patient plasma. *J. Gen. Virol.* 88(9), 2504–2512.
- Xu, Y., Kock, J., Lu, Y., Yang, D., Lu, M., Zhao, X., 2011. Suppression of hepatitis B virus replication in *Tupaia* hepatocytes by tumor necrosis factor alpha of *Tupaia belangeri*. *Comp. Immunol. Microbiol. Infect. Dis.* 34, 361–368.
- Yacoub, S., Mongkolsapaya, J., Screaton, G., 2013. The pathogenesis of dengue. *Curr. Opin. Infect. Dis.* 26, 284–289.
- Yan, H., Zhong, G., Xu, G., He, W., Jing, Z., Gao, Z., Huang, Y., Qi, Y., Peng, B., Wang, H., Fu, L., Song, M., Chen, P., Gao, W., Ren, B., Sun, Y., Cai, T., Feng, X., Sui, J., Li, W.,

2012. Sodium taurocholate cotransporting polypeptide is a functional receptor for human hepatitis B and D virus. *eLife* 1, e00049.
- Yang, C., Ruan, P., Ou, C., Su, J., Cao, J., Luo, C., Tang, Y., Wang, Q., Qin, H., Sun, W., Li, Y., 2015. Chronic hepatitis B virus infection and occurrence of hepatocellular carcinoma in tree shrews (*Tupaia belangeri chinensis*). *Viol. J.* 12(1), 26.
- Yang, D.R., Zhu, H.Z., 2015. Hepatitis C virus and antiviral innate immunity: who wins at tug-of-war? *World J. Gastroenterol.* 21, 3786–3800.
- Yohan, B., Kendarsari, R.I., Mutia, K., Bowolaksono, A., Harahap, A.R., Sasmono, R.T., 2014. Growth characteristics and cytokine/chemokine induction profiles of dengue viruses in various cell lines. *Acta Virol.* 58, 20–27.
- Yu, D., Wu, Y., Xu, L., Fan, Y., Peng L., Xu, M., Yao, Y.-G., 2016b. Identification and characterization of Toll-like receptors (TLRs) in the Chinese tree shrew (*Tupaia belangeri chinensis*). *Dev. Comp. Immunol.* 60, 127–138.
- Yu, W., Yang, C., Bi, Y., Long, F., Li, Y., Wang, J., Huang, F., 2016a. Characterization of hepatitis E virus infection in tree shrew (*Tupaia belangeri chinensis*). *BMC Infect. Dis.* 16(1), 80.
- Zhang, E., Lu, M., 2015. Toll-like receptor (TLR)-mediated innate immune responses in the control of hepatitis B virus (HBV) infection. *Med. Microbiol. Immunol.* 204, 11–20.
- Zuniga, E.I., Macal, M., Lewis, G.M., Harker, J.A., 2015. Innate and adaptive immune regulation during chronic viral infections. *Annu. Rev. Virol.* 2, 573–597.